Kyoto FDEPS lectures 4-7 xi 2007
Dynamics of oceans and atmospheres
P.B. Rhines
University of Washington

- 1. rotating, stratified fluids: oceans and atmospheres
  - vorticity: a vector-tracer in classical homogeneous fluids
- geostrophic adjustment, thermal wind
- 2. wave dynamics: fundamentals, group velocity, energetics, ray theory
- potential vorticity (PV)
  - vortex stretching, Prandtl's ratio, geography of PV
- 3. Rossby waves
- 4. instability => geostrophic turbulence; subtropical gyres: dynamics, jets and gyres
- 5. meridional overturning circulations and the thermohaline circulation
- 6. Seminar: subpolar climate dynamics observed from above and below: altimetry and Seagliders

Texture

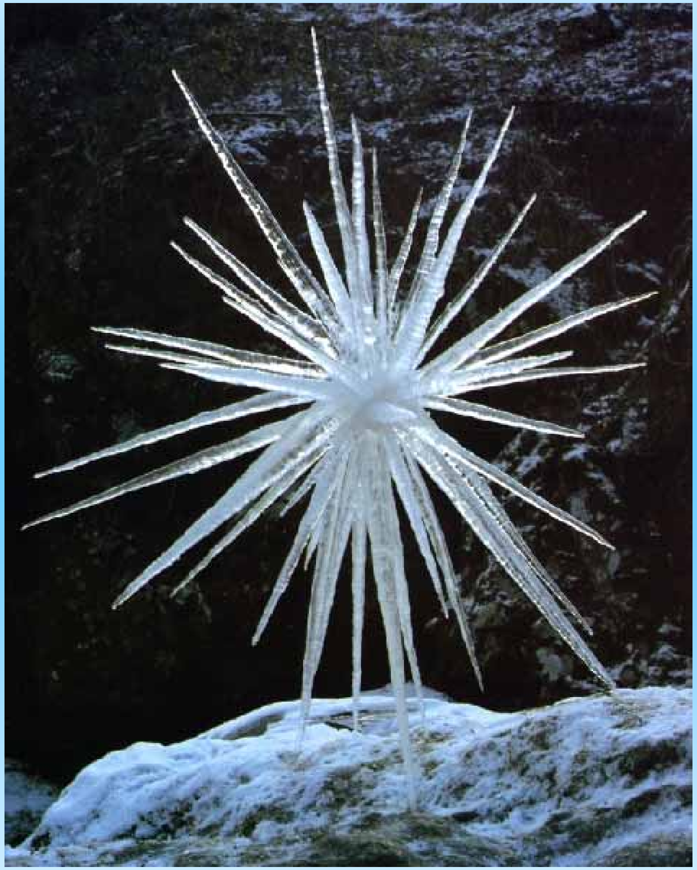

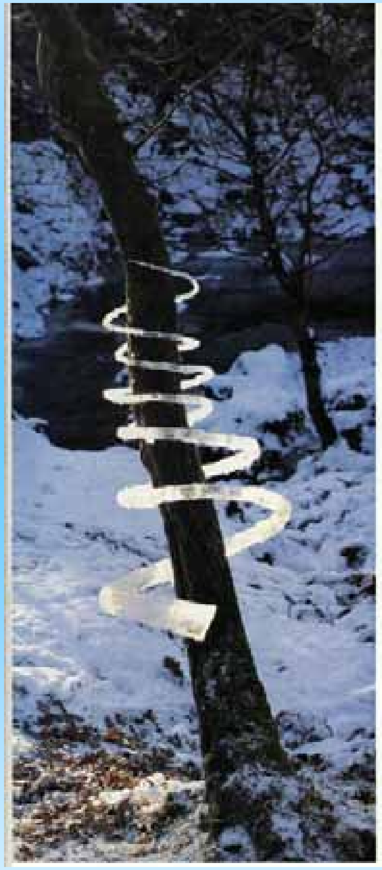

Andy Goldsworthy

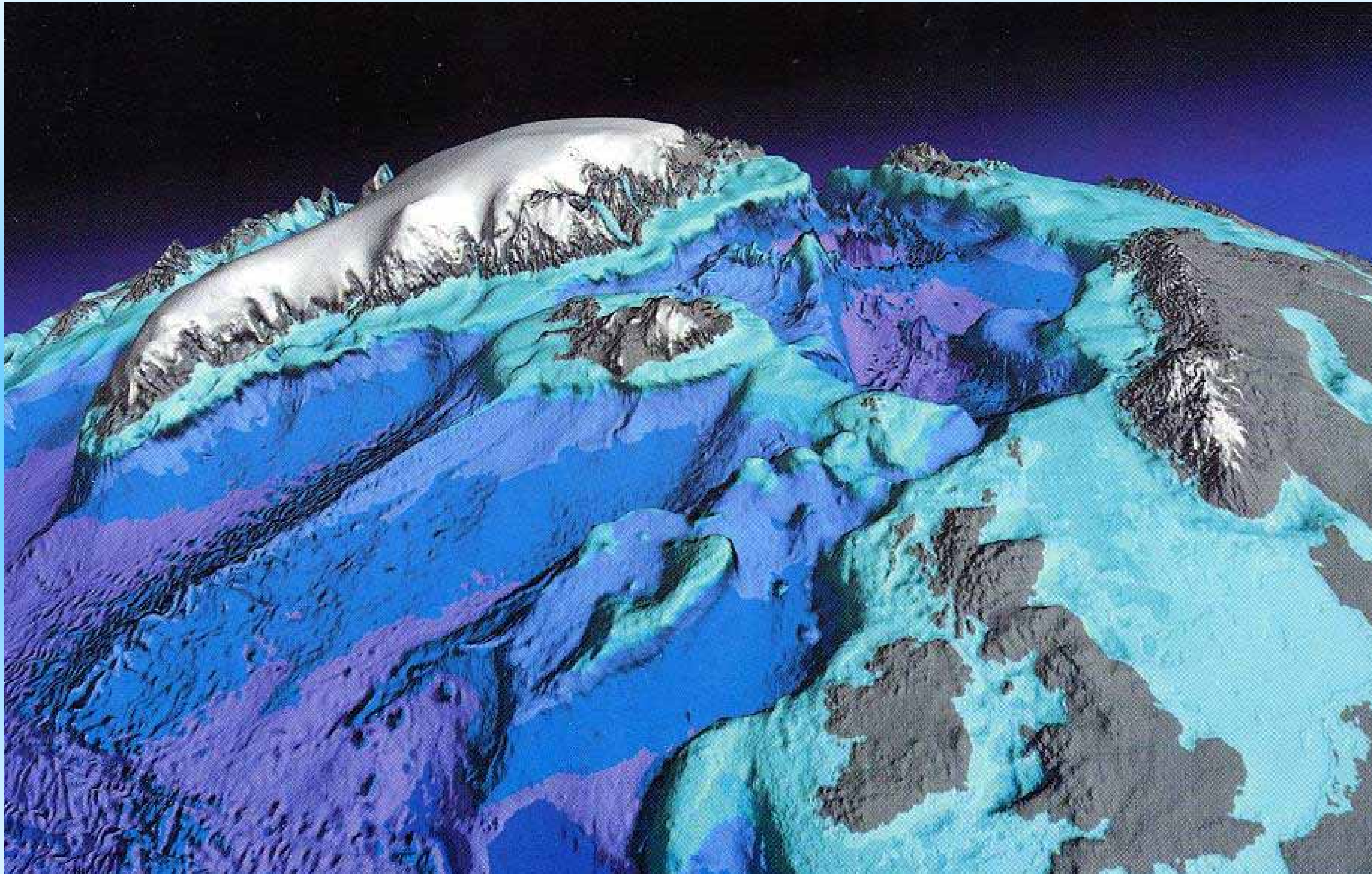

AGU, 2003

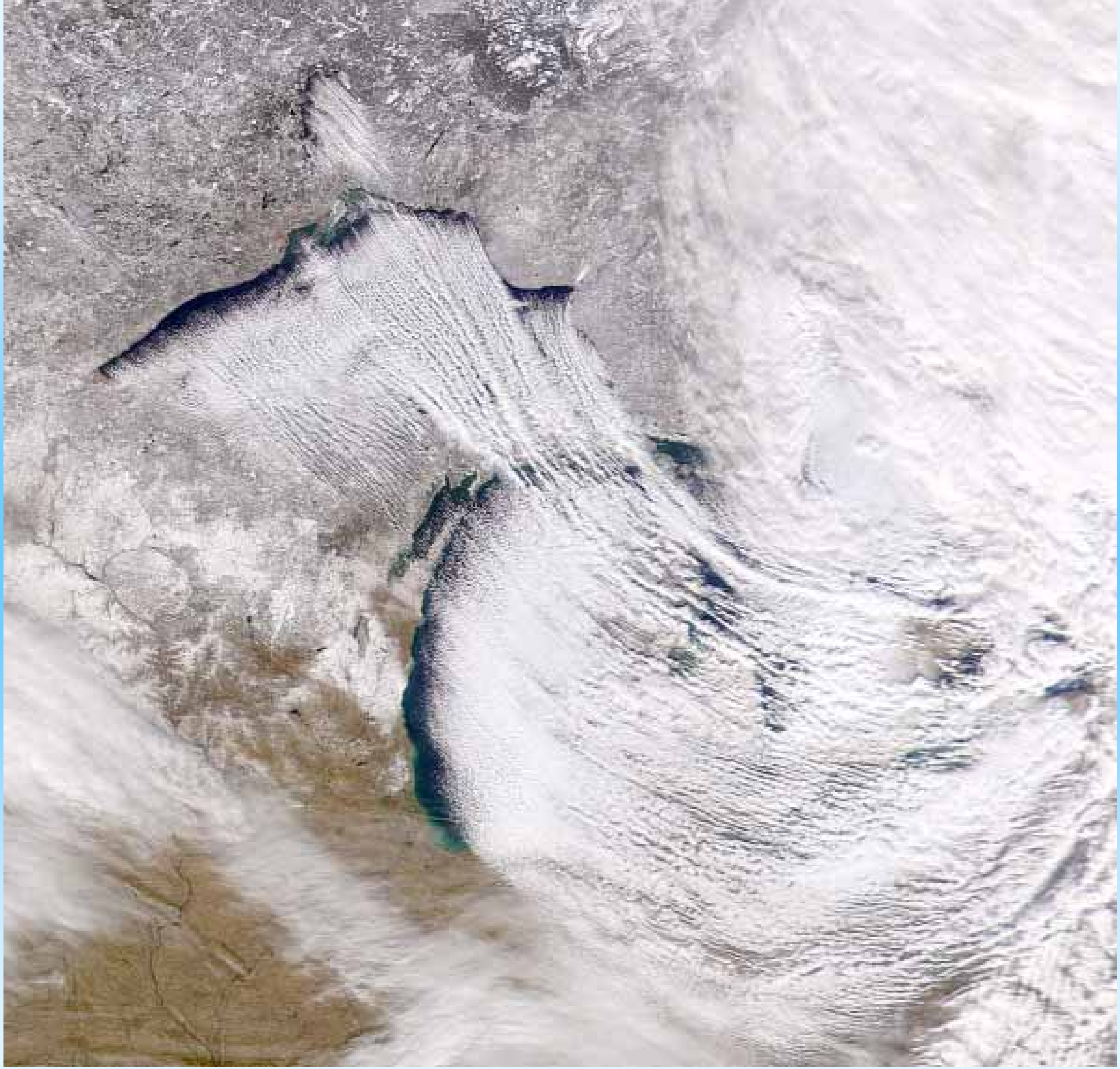

water evaporates from the Great Lakes when cold north winds blow over them. It soon condenses back into water, as cloud droplets which then rain or snow out…The lake water has become cloud, and then the cloud piles up as deep snow, downwind of the lakes. This is called ‘lake-effect snow’.

SeaWiFS Chlorophyll-a Concentration (OC4 algorithm)
16-30 April 2003 Composite

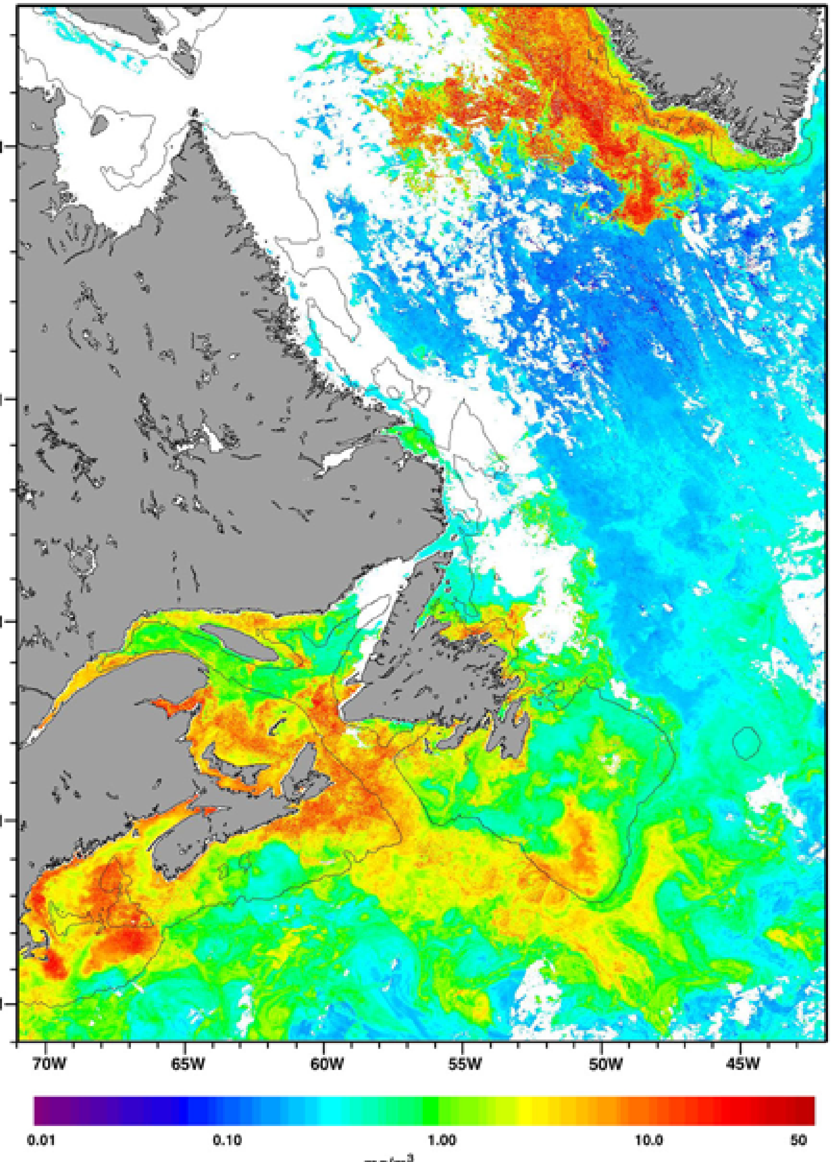

Sea Surface Temperature
16-30 April 2003 Composite

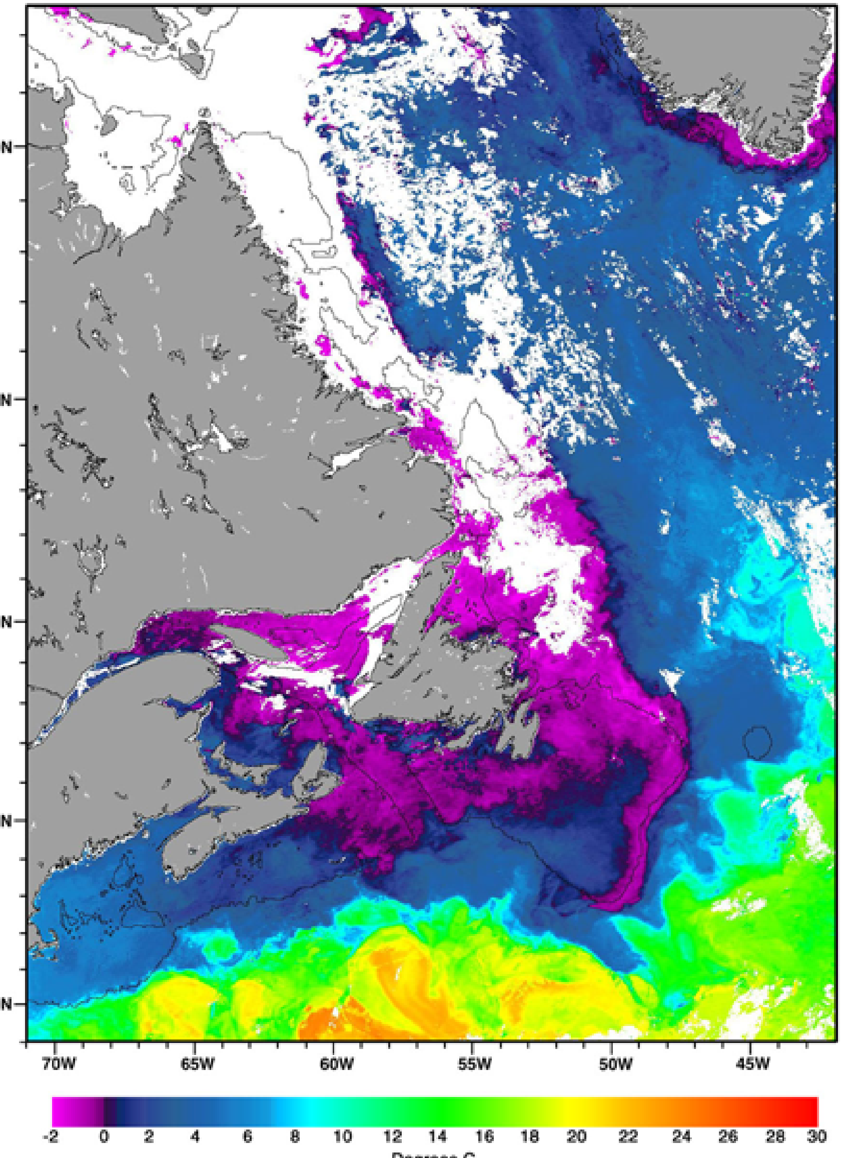

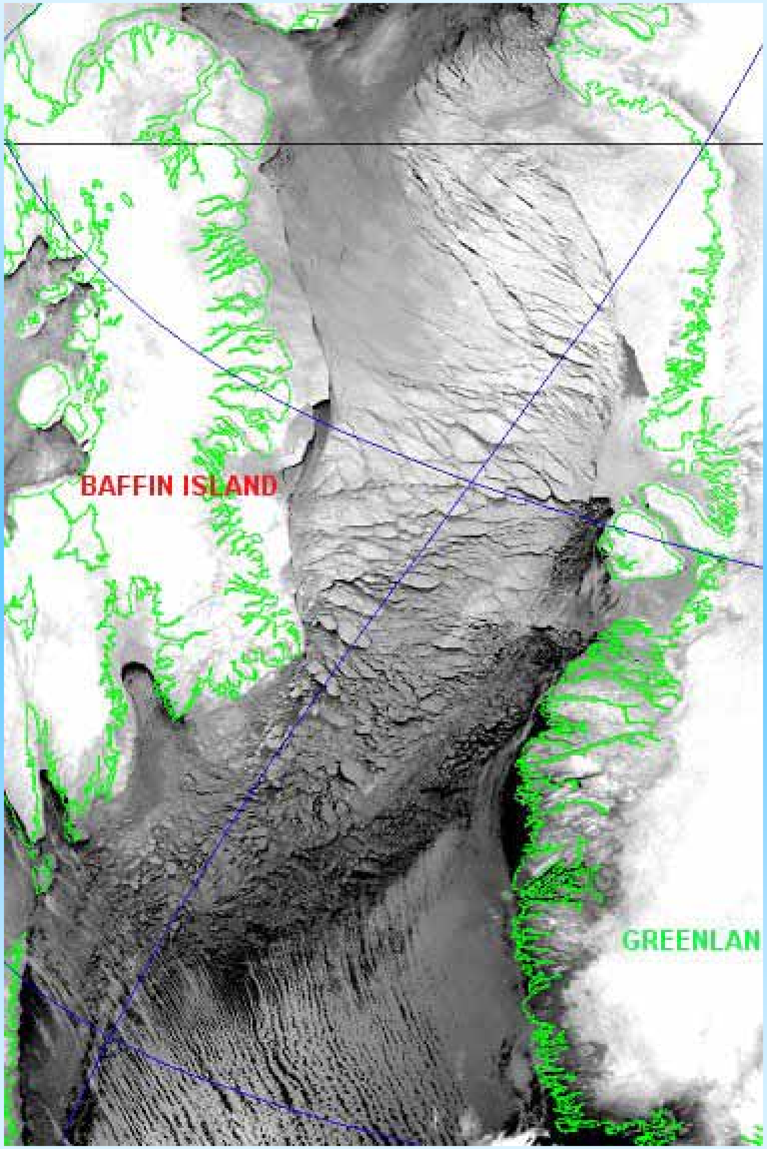
BAFFIN ISLAND
GREENLAN

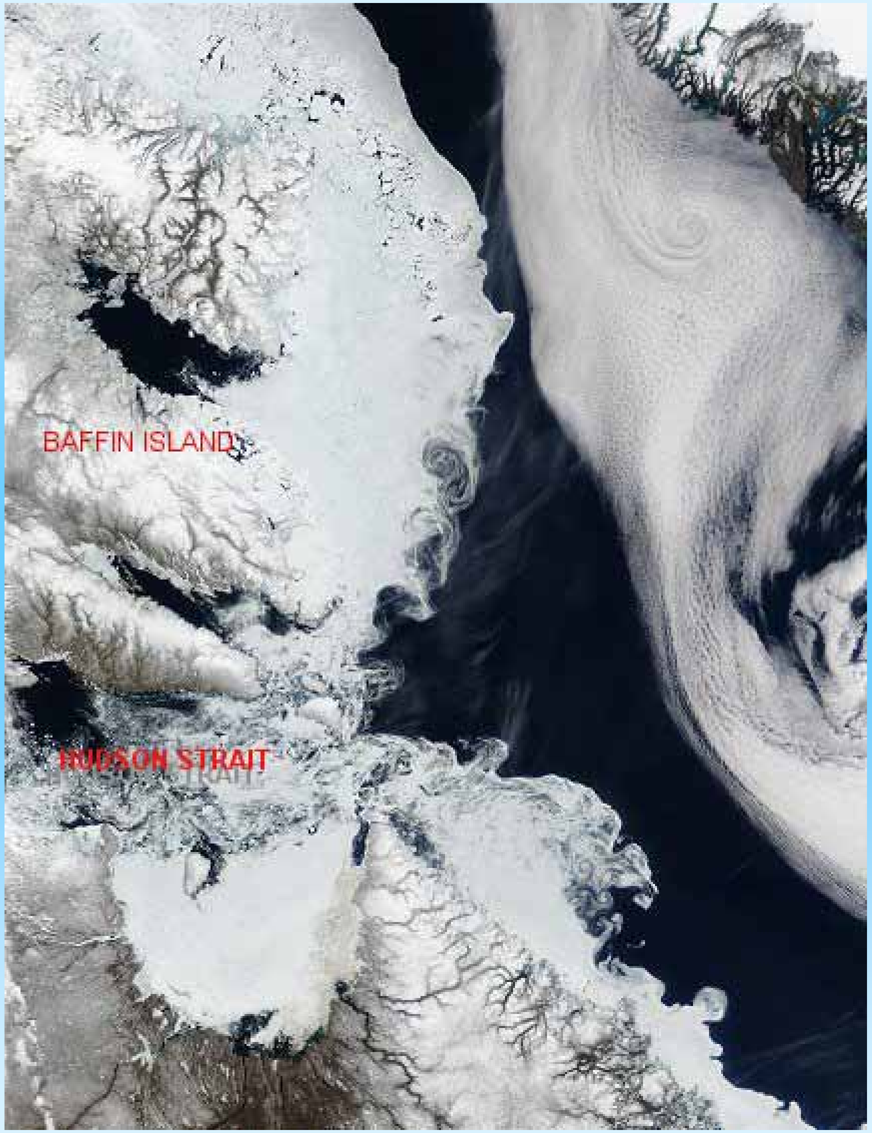
BAFFIN ISLAND
HUDSON STRAIT

Erika Dan temperature section, 60^0N

Labrador-Greenland-Rockall-Ireland

Worthington+Wright, 1970

warm, saline water moving north from the subtropics

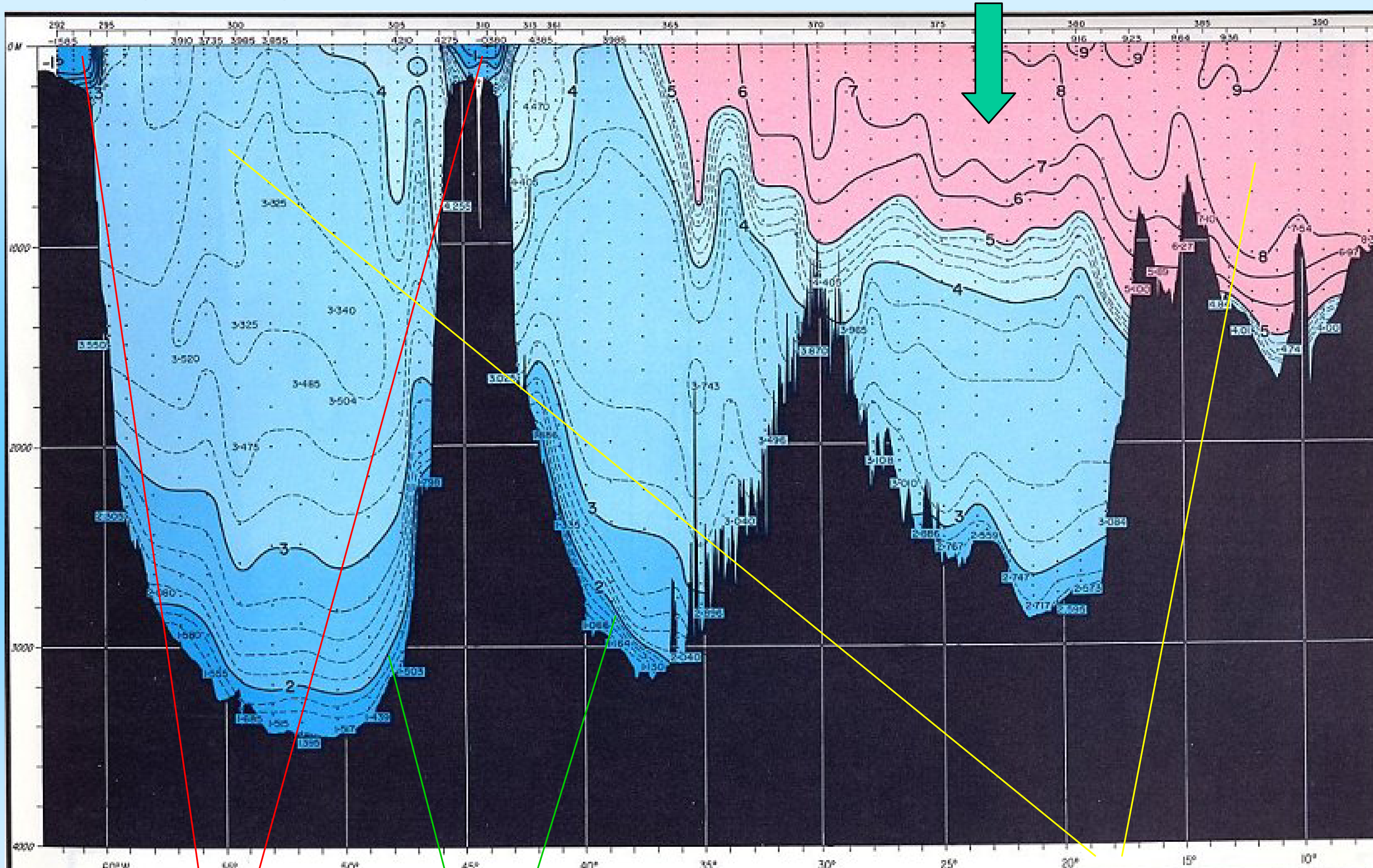

shallow continental shelf circulation (unresolved in CCMs)

deep overflows from Denmark Strait/I.S. Ridge

deep winter mixing, sensitive to upper ocean low-salinity waters

Five Davis Strait Seaglider temperature sections showing Arctic cold water entering the Labrador Sea, have unprecedented spatial resolution Eriksen & *Rhines UW*

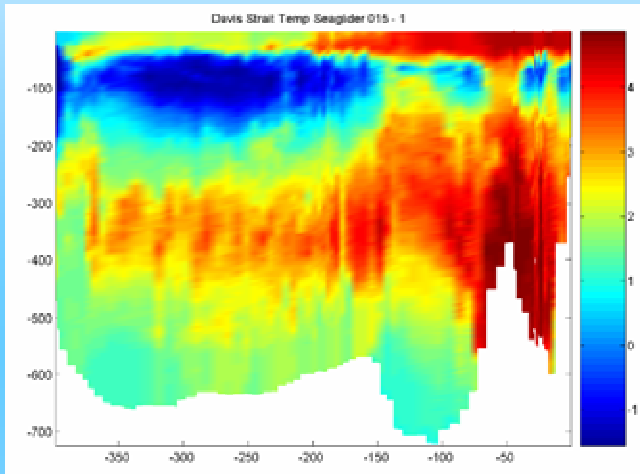

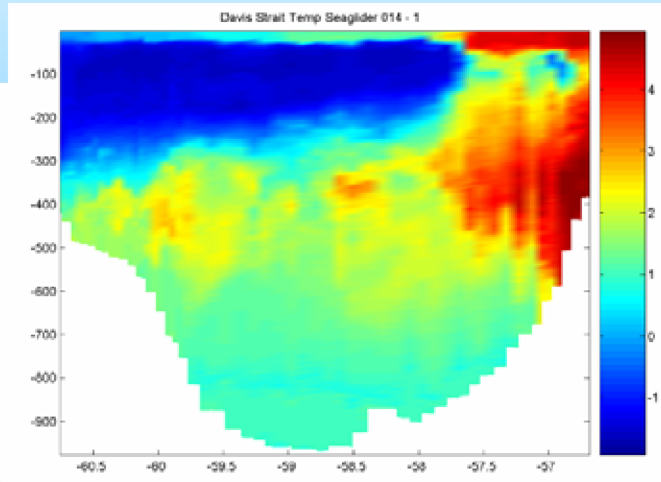

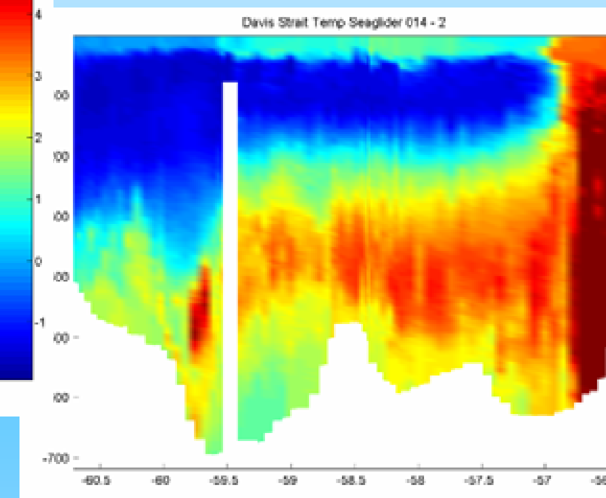

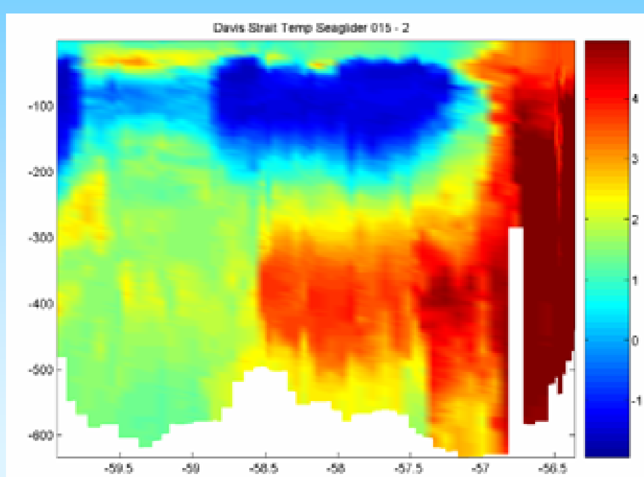

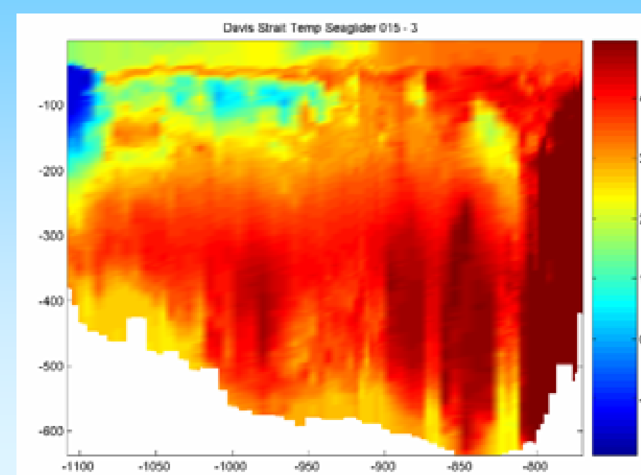

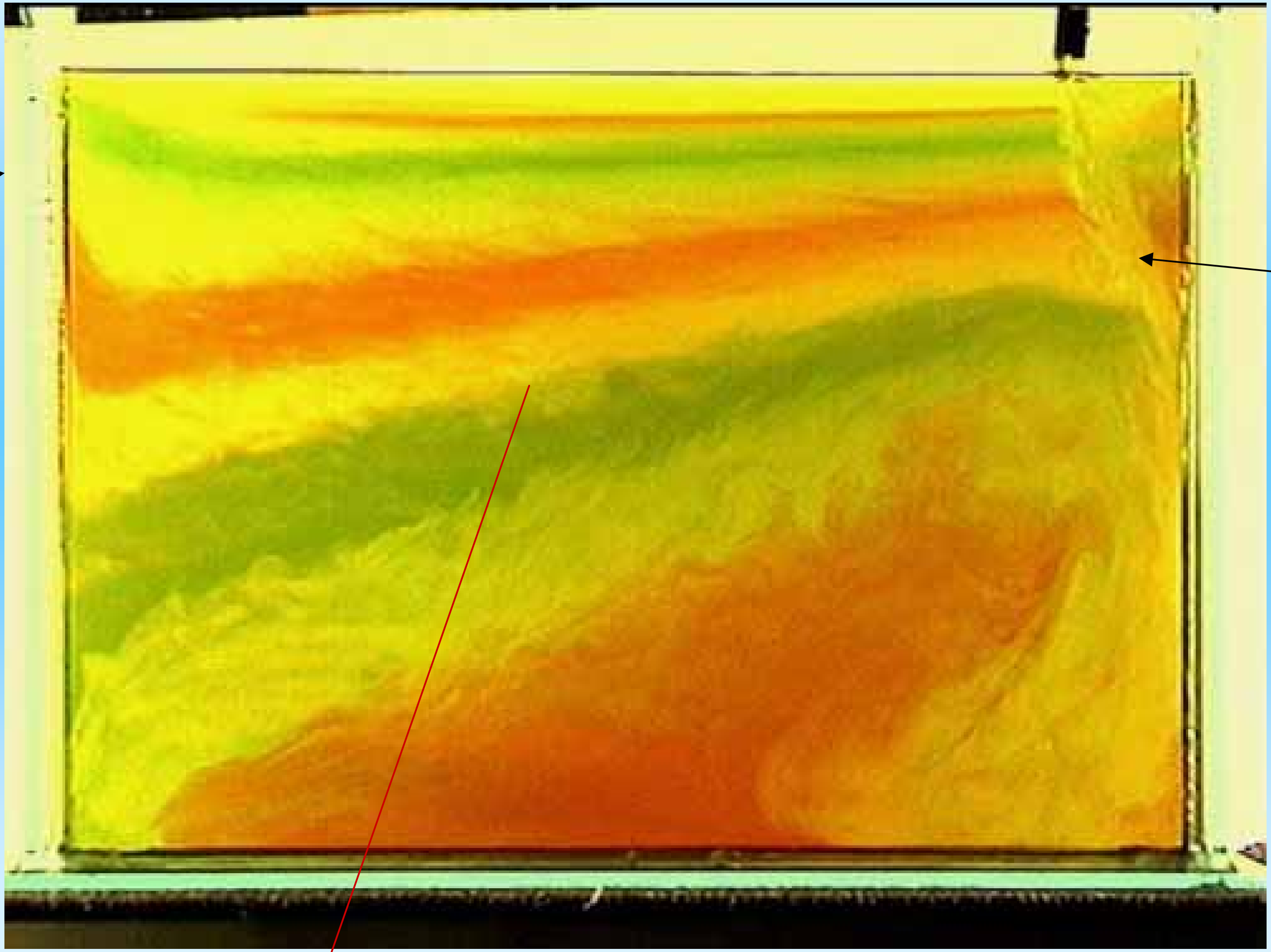
boundary
mixing/
upwelling
entrainment
broad upwelling, yet much of it recirculates below the mixed layer

Jets occur in rotating fluids for many reasons, here driven by thermal convection in a bowl-shaped basin. The jets in the lefthand image occur due to the very strong topographic PV gradient, at high rotation (low Rossby number). Condie & Rhines 'Topographic Hadley Cells JFM 1994; Rhines 'Jets', CHAOS 1994.

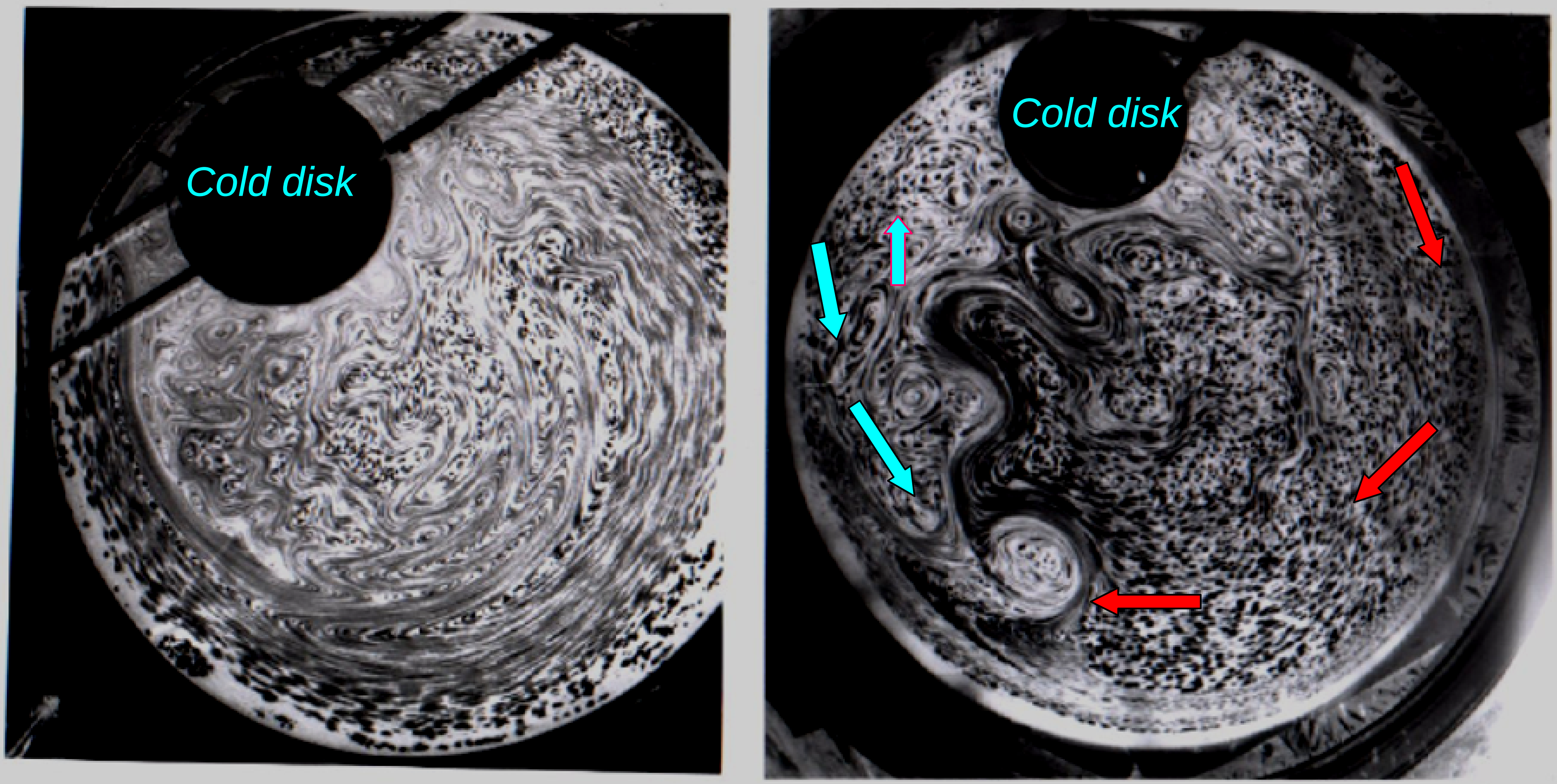

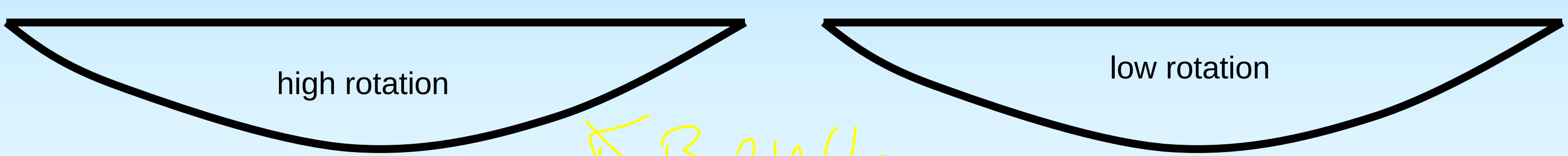

BOWL GEOMETRY

spatially homogeneous, density stratified rotating convection viewed from the side:

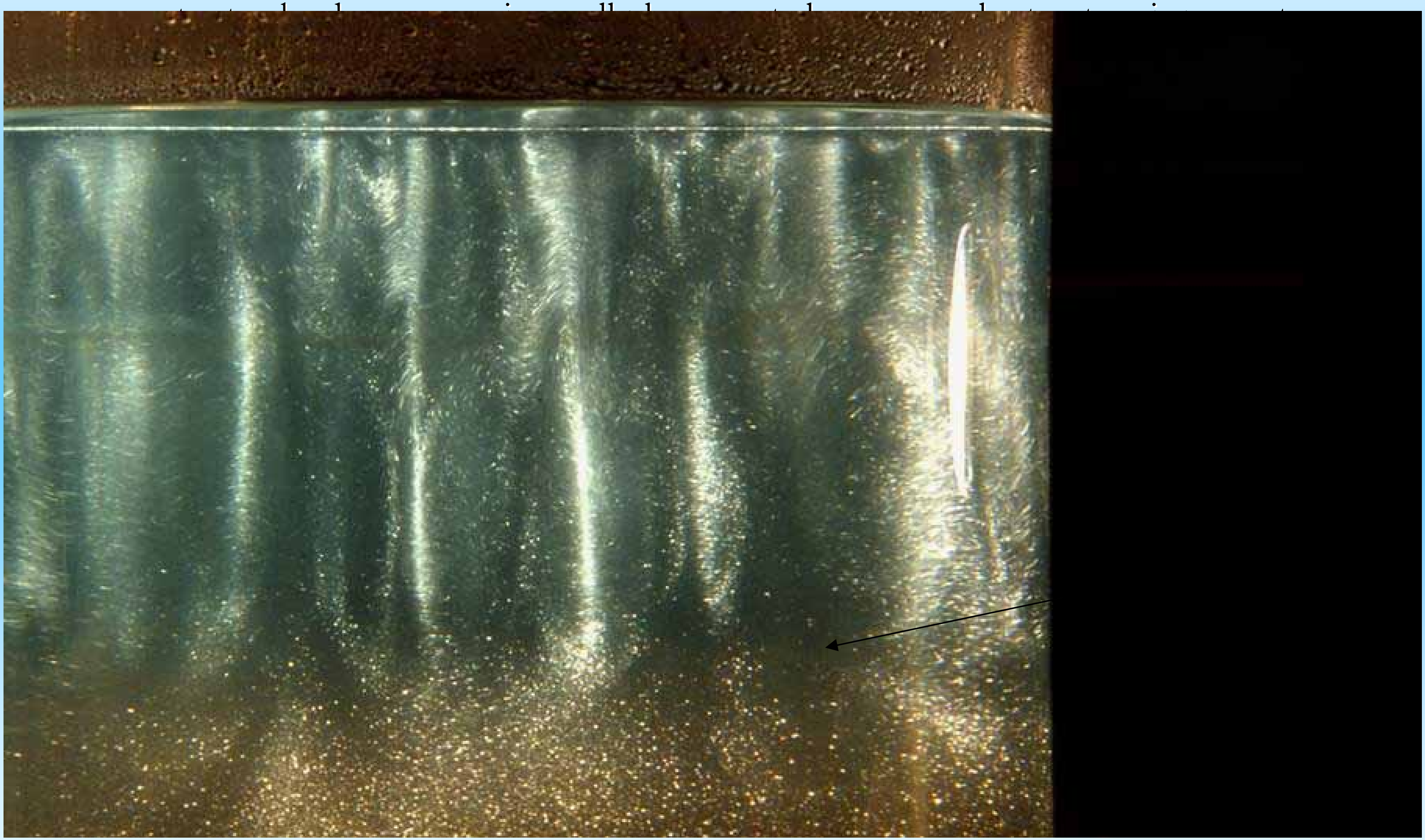

GFD lab Univ of Washington

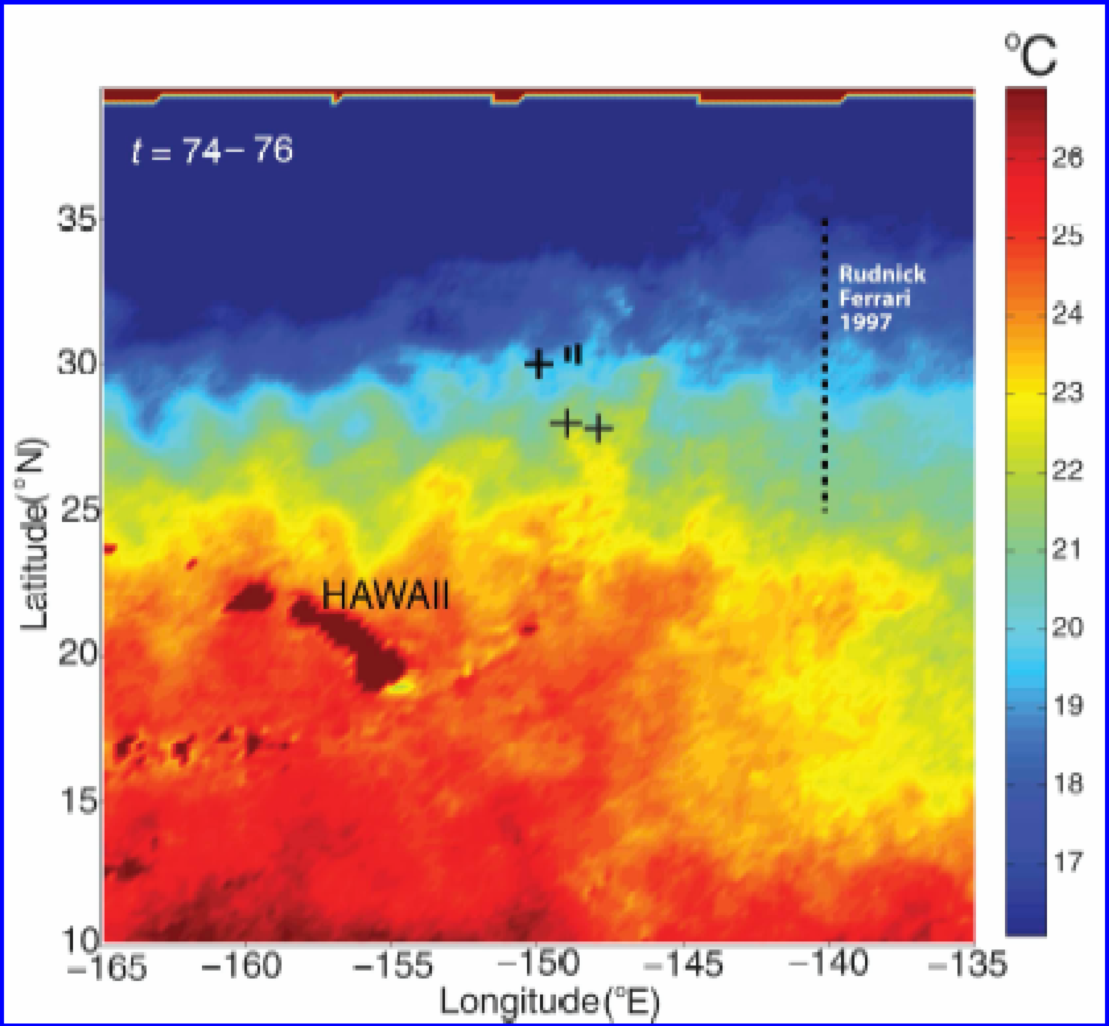

- SST during March 2004
- The subtropical front is a zone of several fronts.
- Density effects of T and S mostly compensate near 30^o N, much less so near 28^o N
- +s mark two 100-km-long surveys at beginning and end of restratification study following a drogued float

Hosegood, Gregg, Alford (2007)

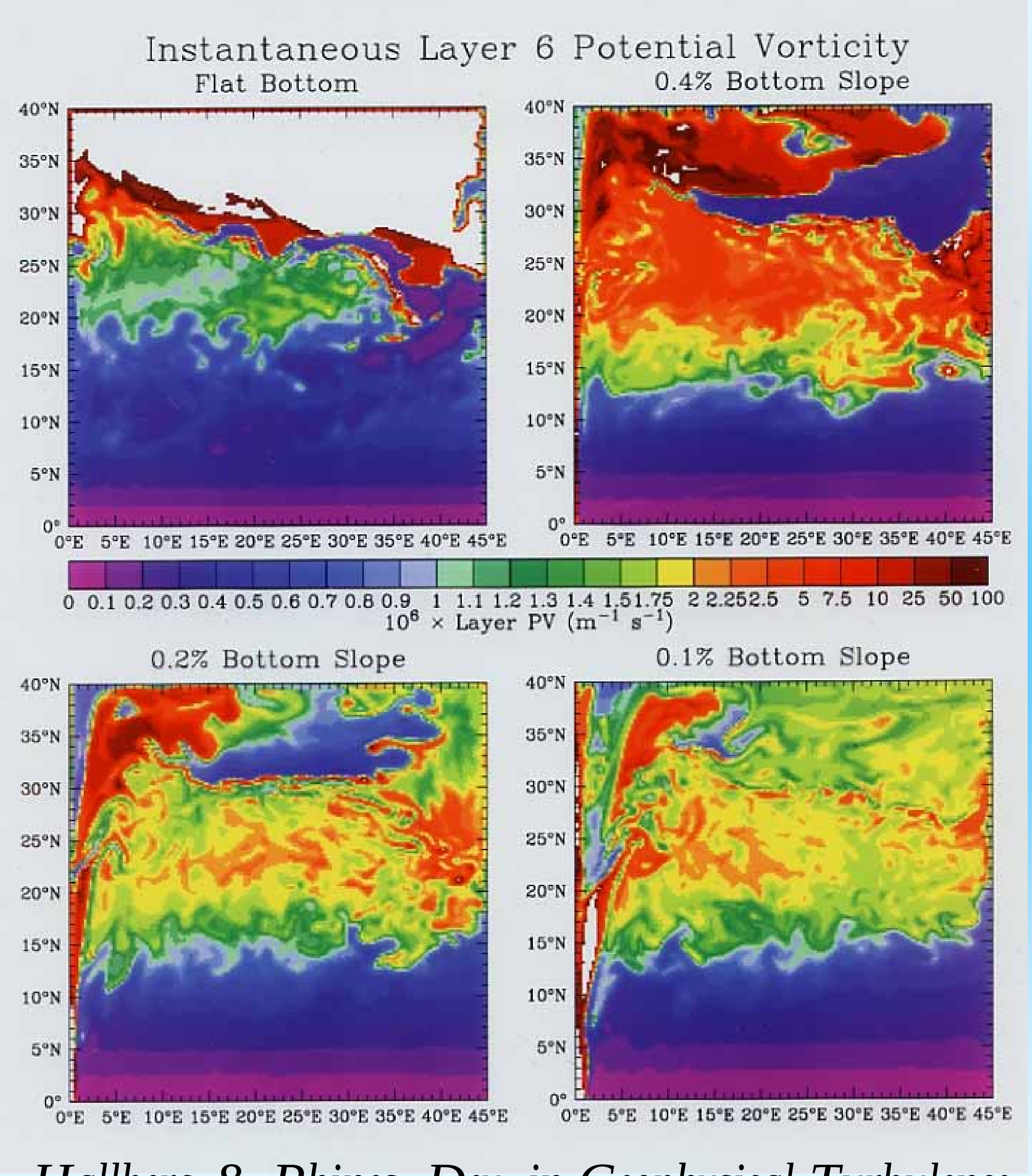

potential vorticity and buoyancy are the fundamental field variables for circulation

(here in 4 box-ocean wind-driven simulations)

Hallberg & Rhines Dev. in Geophysical Turbulence, R. Kerr Ed., 2000

Theta-S diagram for Atlantic ocean (Southern Ocean to subpolar North Atlantic)

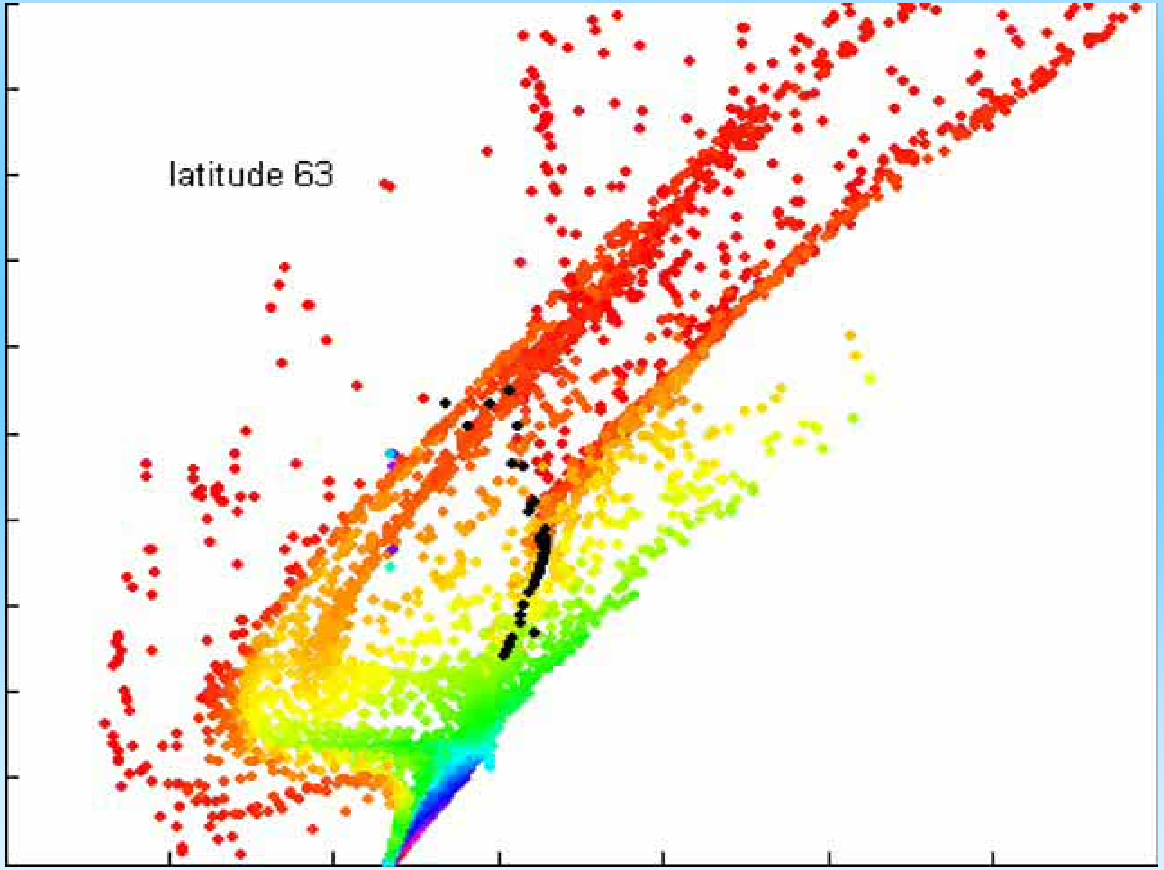

cylinder wake in a soap film

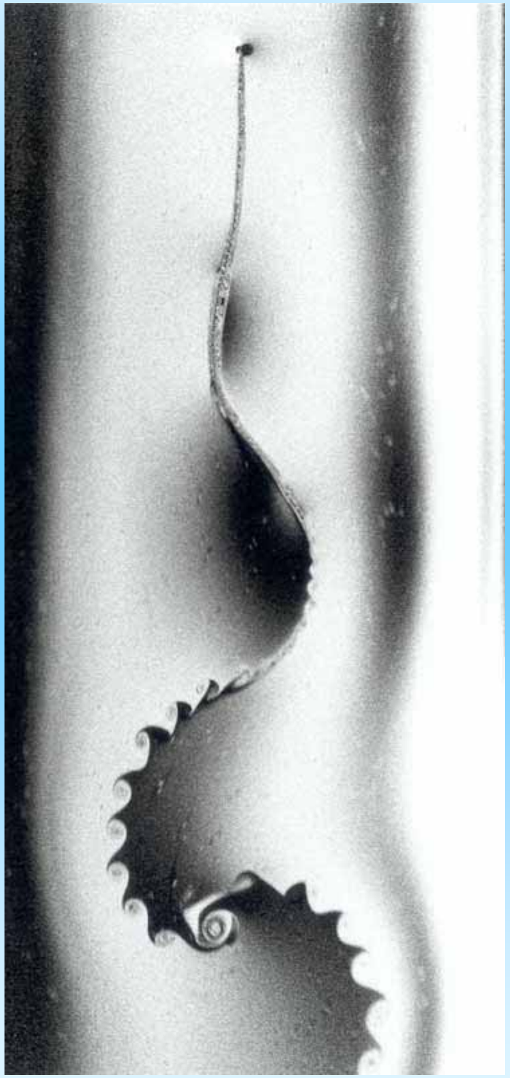

Marvin Rutger

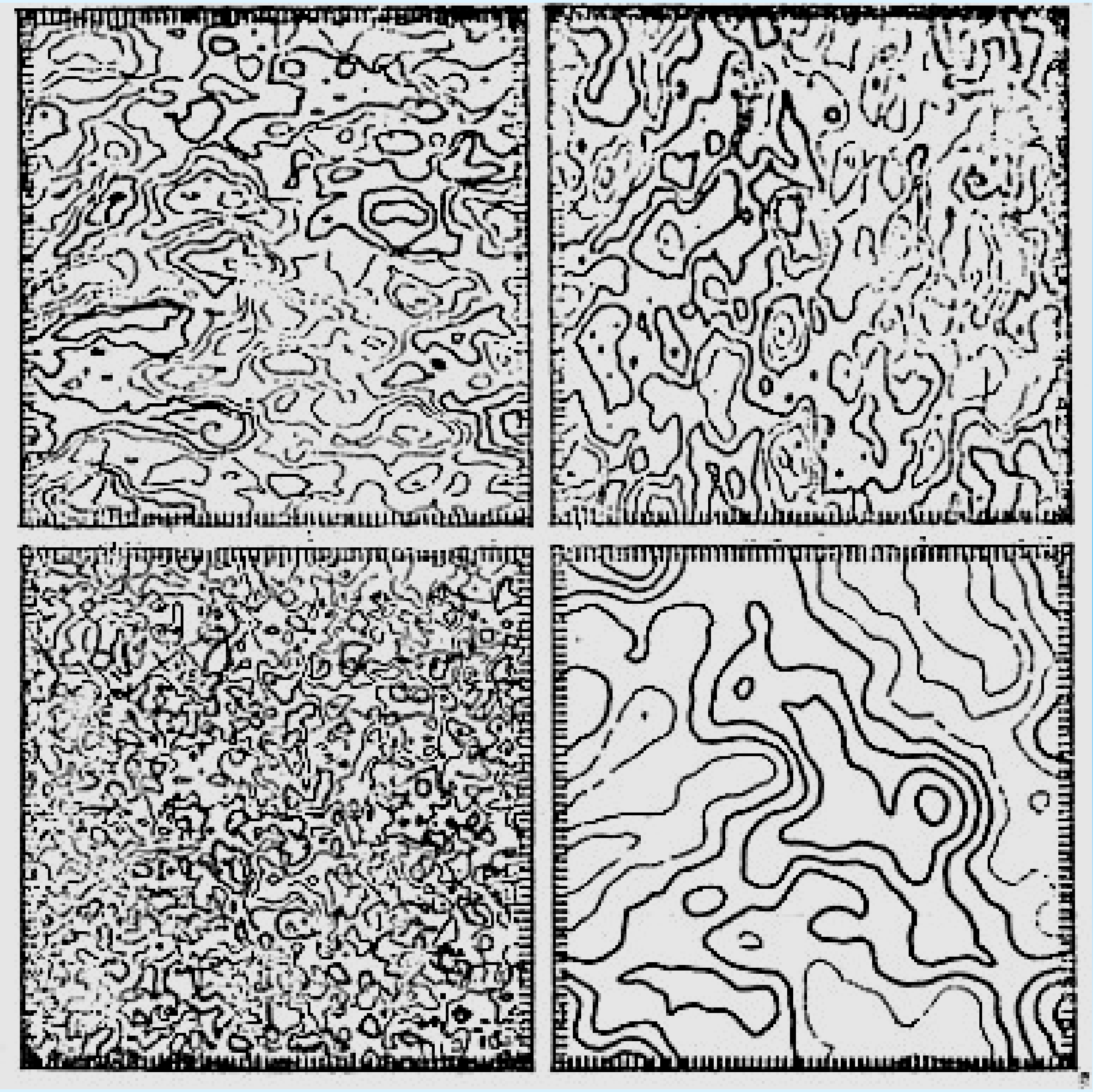

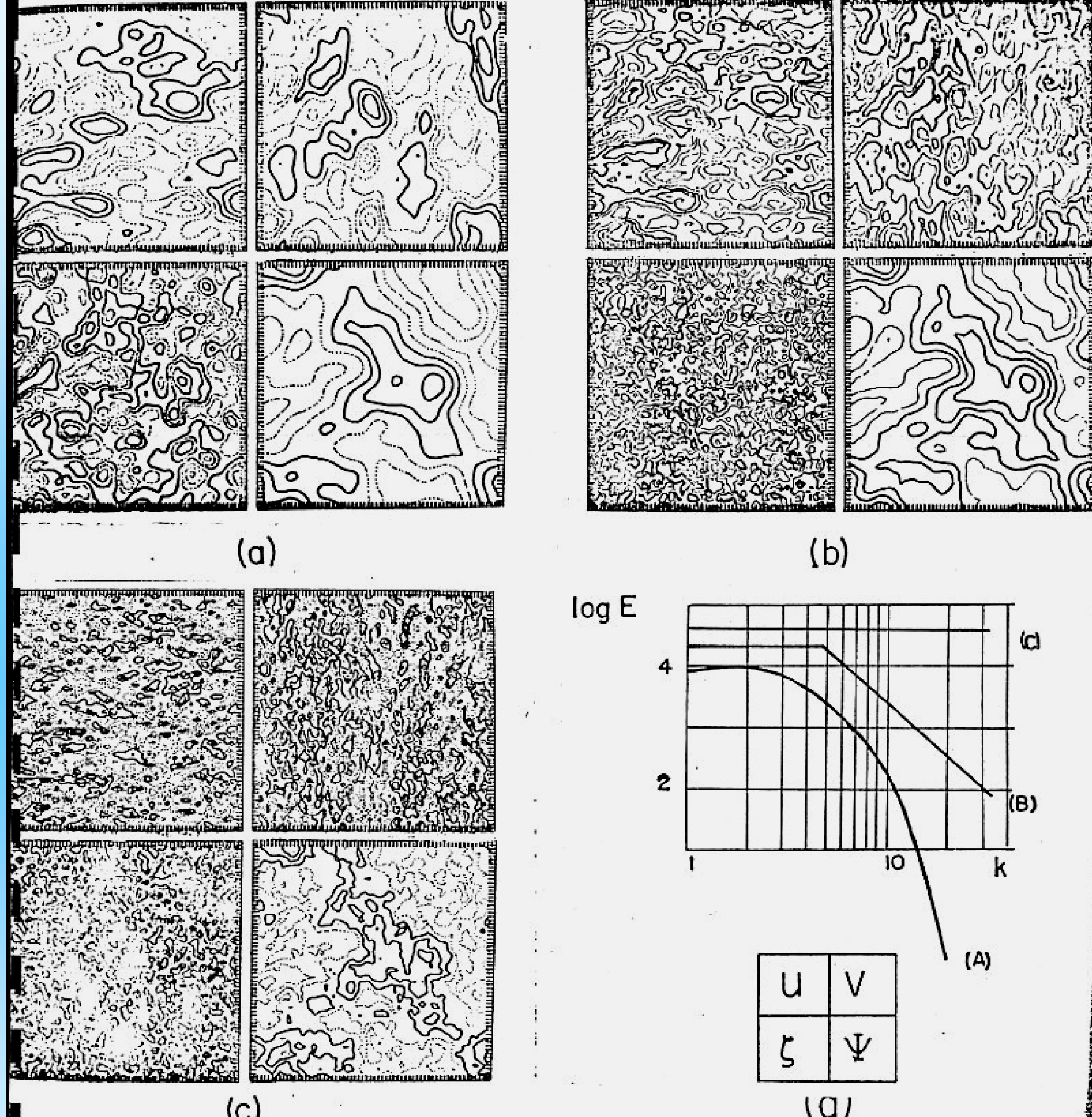

Figure 2.1 Artificially generated fields of ψ (or pressure), velocity components u, v and vorticity ζ. The azimuthal wavenumber dependence is fixed. (a), for scalar-wavenumber spectrum $E = ke^{-2/3k}$; (b), for $E = 1.0$ $(k < 5)$, $E = (k/5)^{-3}$ $(k > 5)$; (c) for $E =$ const. The discrimination between associated fields ψ, u, v, ζ increase with spectral bandwidth.

textures of different dynamical variables

Vorticity in a ‘classic’ non-rotating fluid

Vortex lines move with the (ideal) fluid….A famous billboard in Times Square, New York, 1950s. Note the size of the vortex rings, which are real.

Broadway's Billboard Creator Dies

Douglas Leigh, who helped turn Broadway into the Great White Way with spectacular billboards like the Camel sign that emitted real smoke rings, died on Tuesday. He was 92. Mr. Leigh also bathed the tops of many of Manhattan's skyscrapers, including the Empire State Building, in light. Page C32.

vortex lines are ‘vector tracers’ that move with the fluid

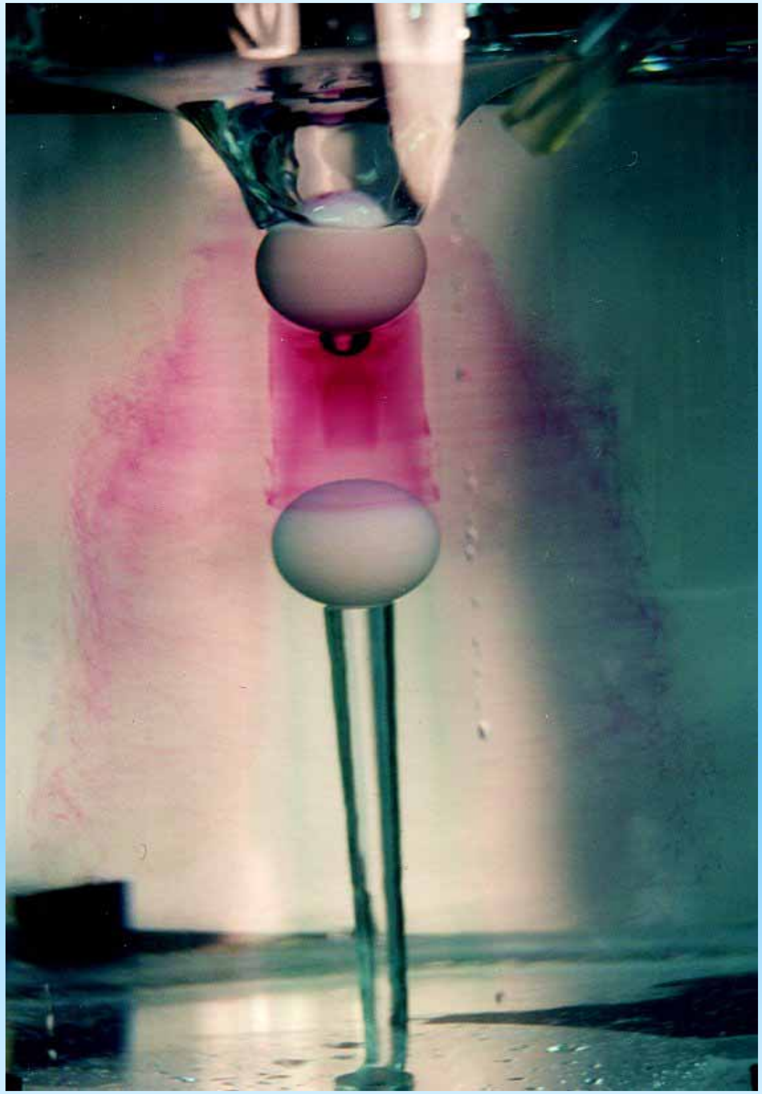

vorticity: teaching tornados

'Levitated' balls with strong vertical and horizontal shear layers contain radial/vertical viscous overturning

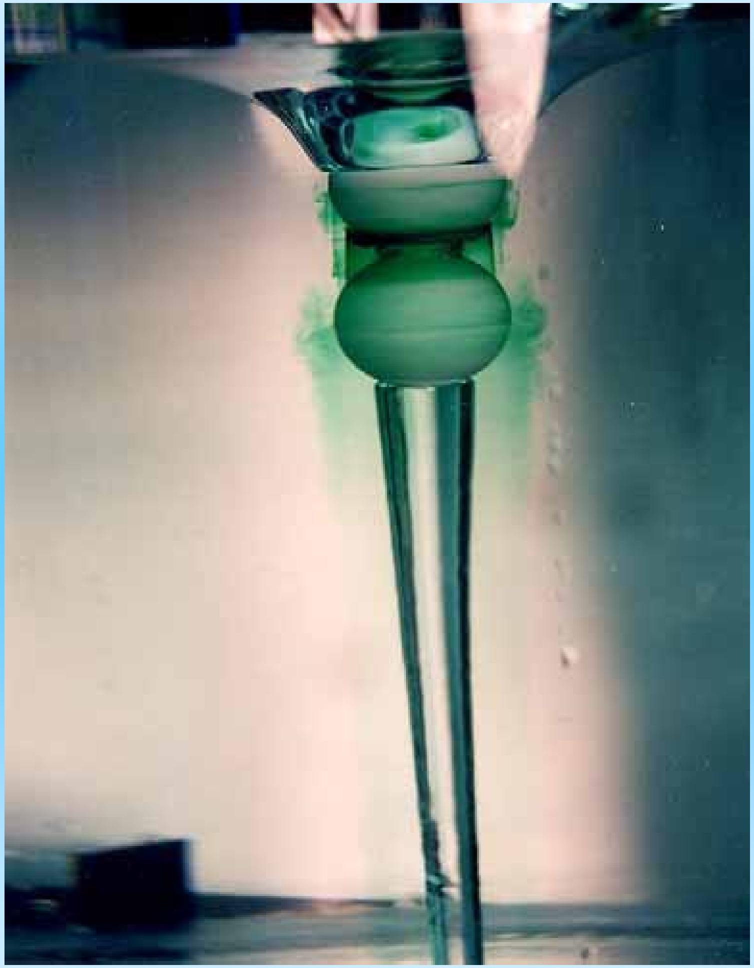

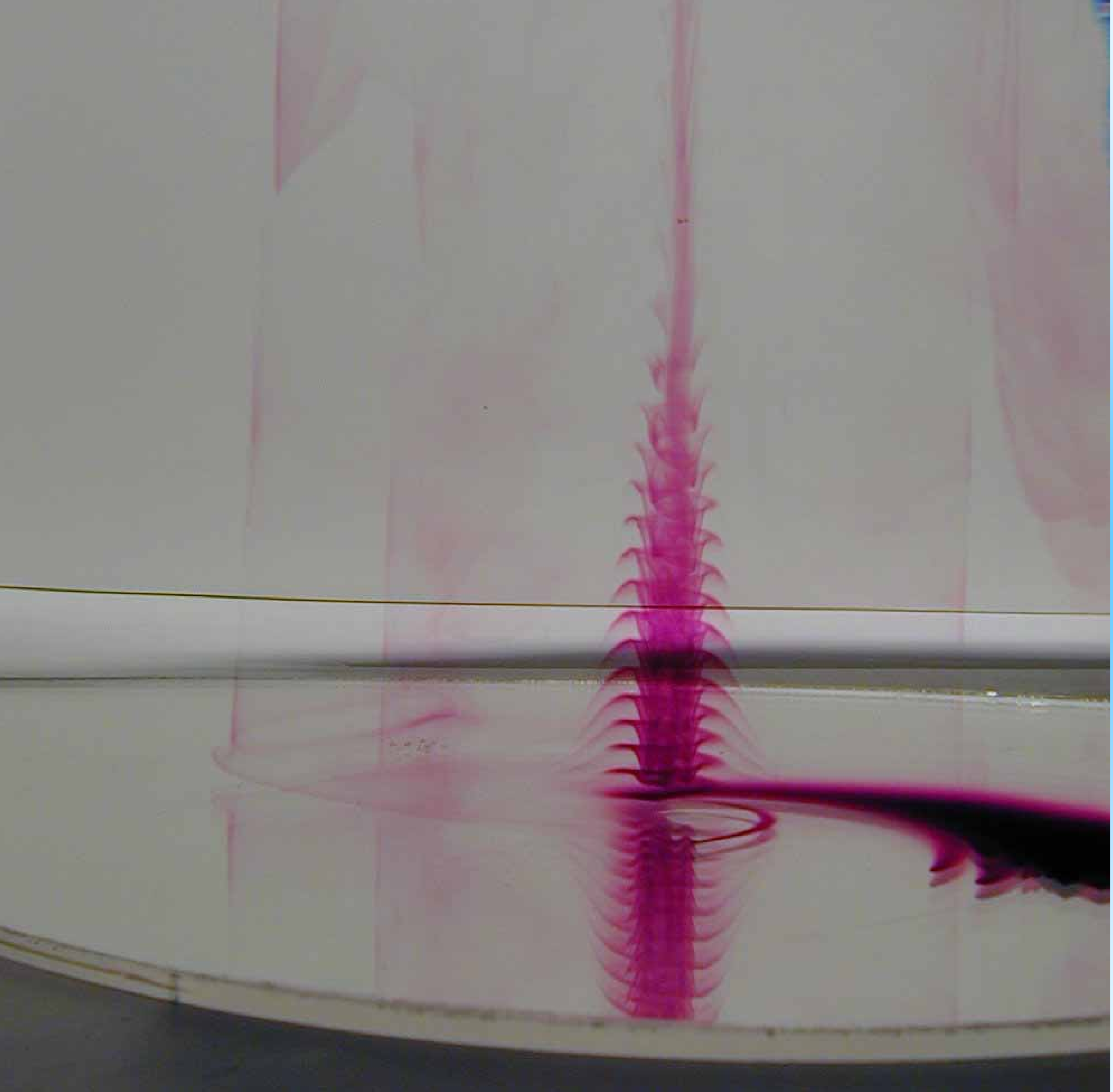

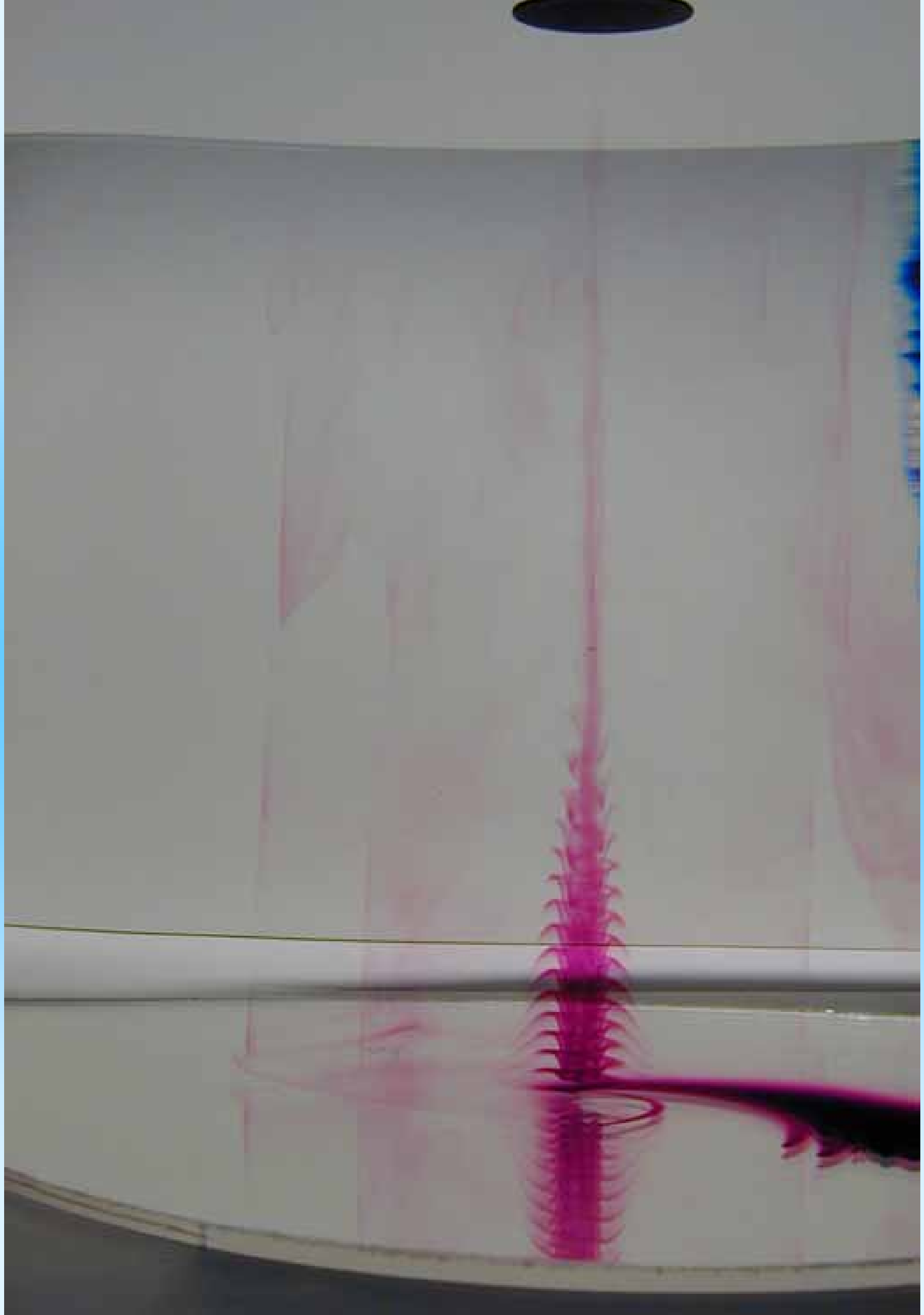

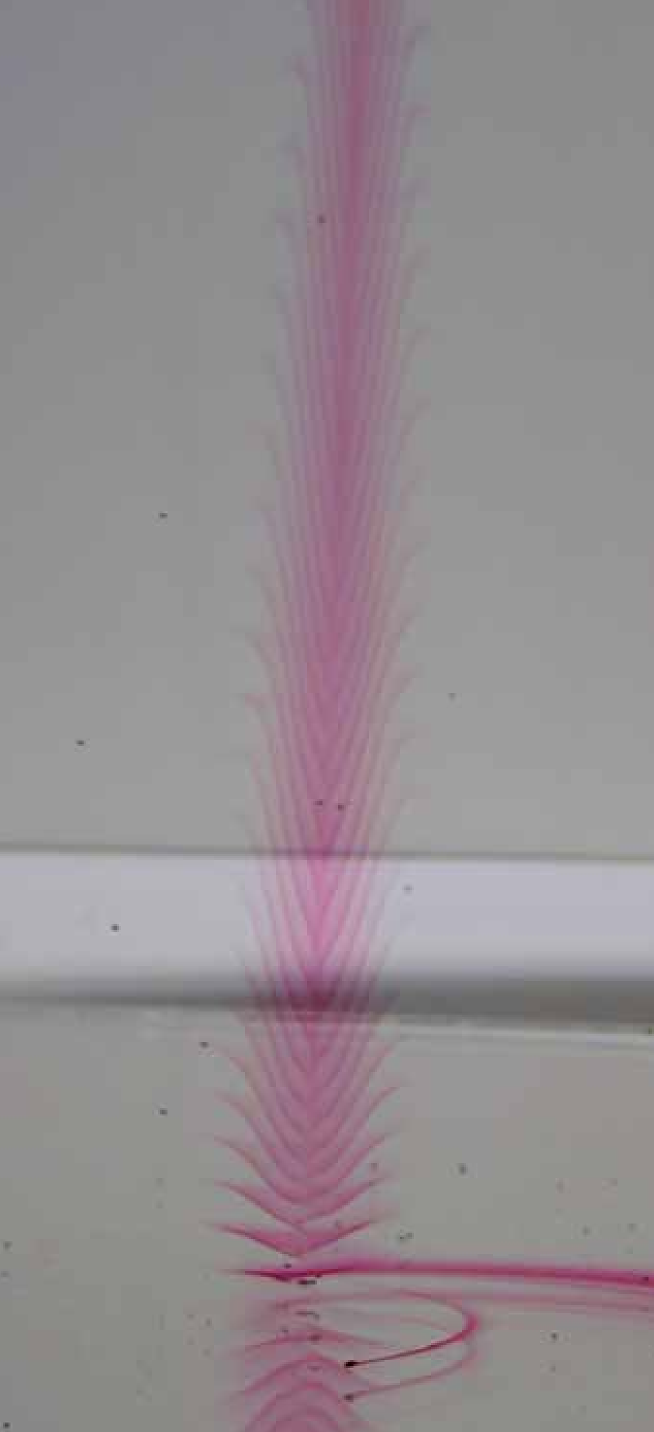
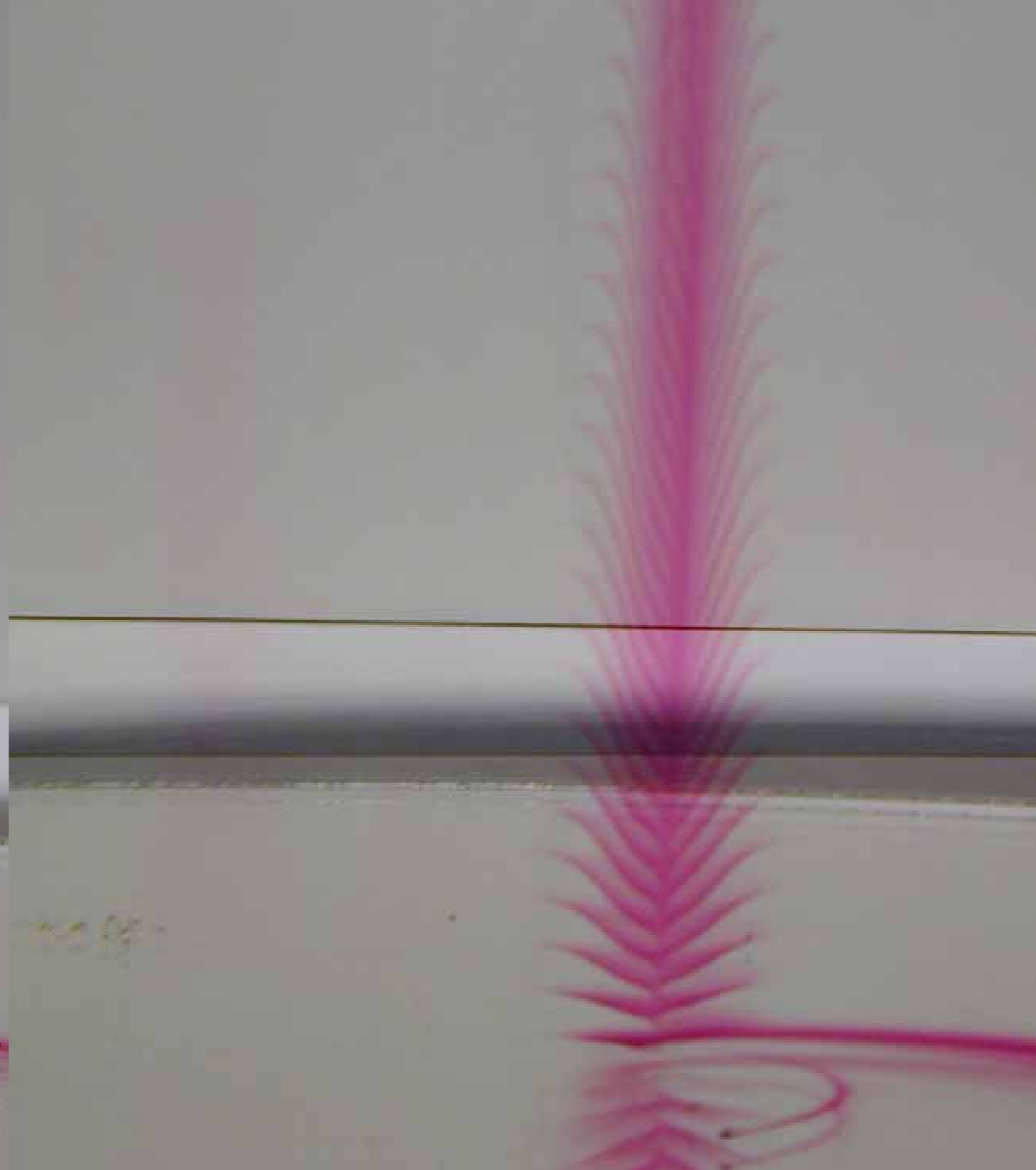

Vorticity and forces:

$$I = \tfrac{1}{2} \int \omega \times r \, dV$$

or one-half the dipole moment of the vorticity field is equal to the 'impulse', or time-integrated force exerted on a fluid…2/3 of which appears as momentum change of the fluid in 3D (the actual number depends uncomfortably on the shape of the control volume, as it recedes to infinity).

(in 2D the expression for impulse, '½' is absent, yet the momentum change in a 2D fluid is still ½ I, that is ½ $\int \omega \times r \, dV$) r=position vector, ω=vorticity vector *Saffman, Vortex Dynamics, CUP*

the rest of the impulse exerts a pressure force on the fluid at a great distance; this confusion is resolved if the fluid is slightly compressible in which case all the impulse appears as momentum.

dipole wakes in the wake of the *Aleutian Islands express the force exerted on the mountain slopes*

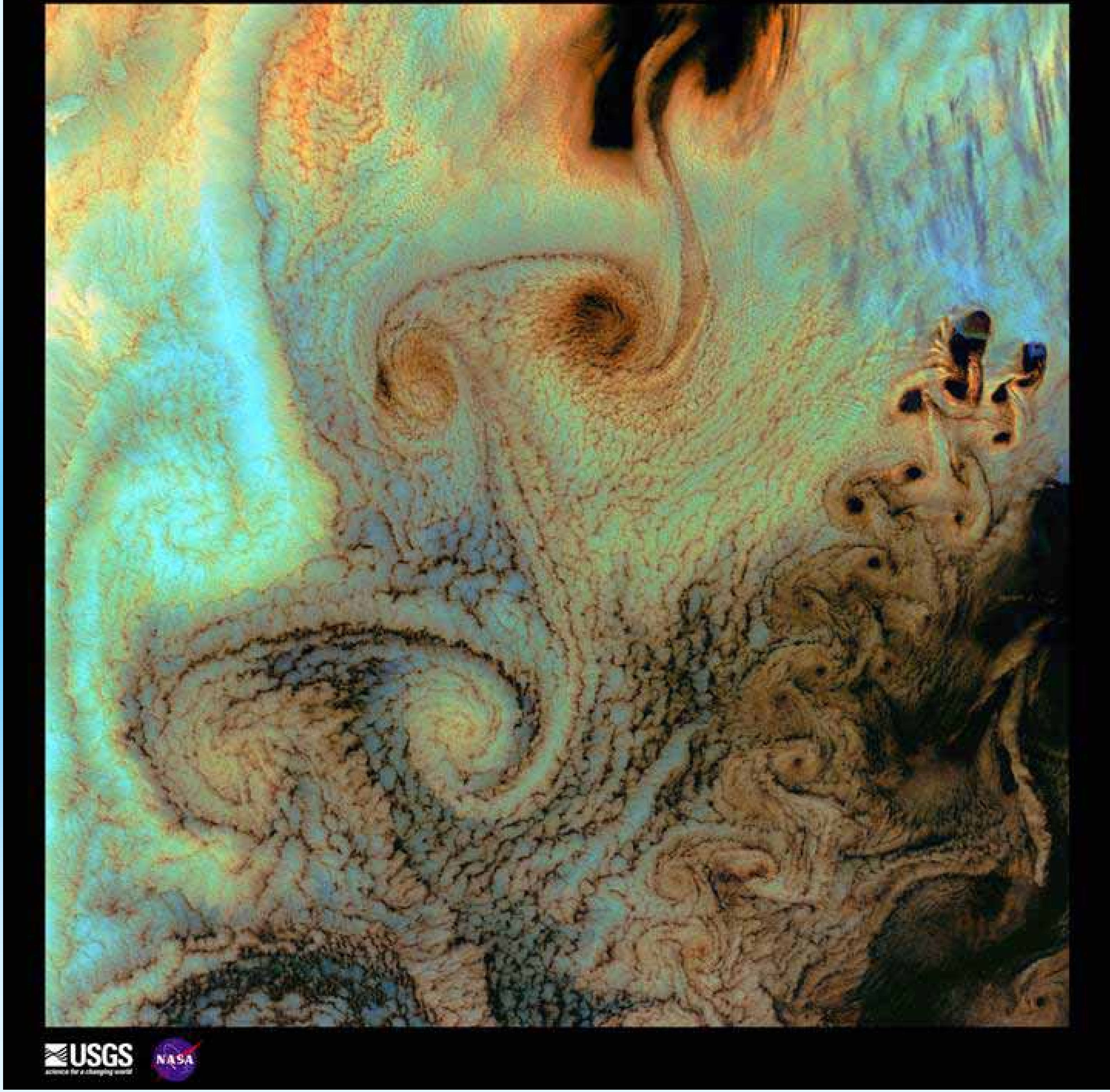

Planetary Rotation:

gives stiffness to the fluid, creates 'tall' flow structures

In our discussion of vortex line tipping and stretching we can now replace vorticity ω by absolute vorticity $\omega + 2\Omega$:

the planetary vorticity *amplifier*

Rotating fluids are filled with 'tall' structures

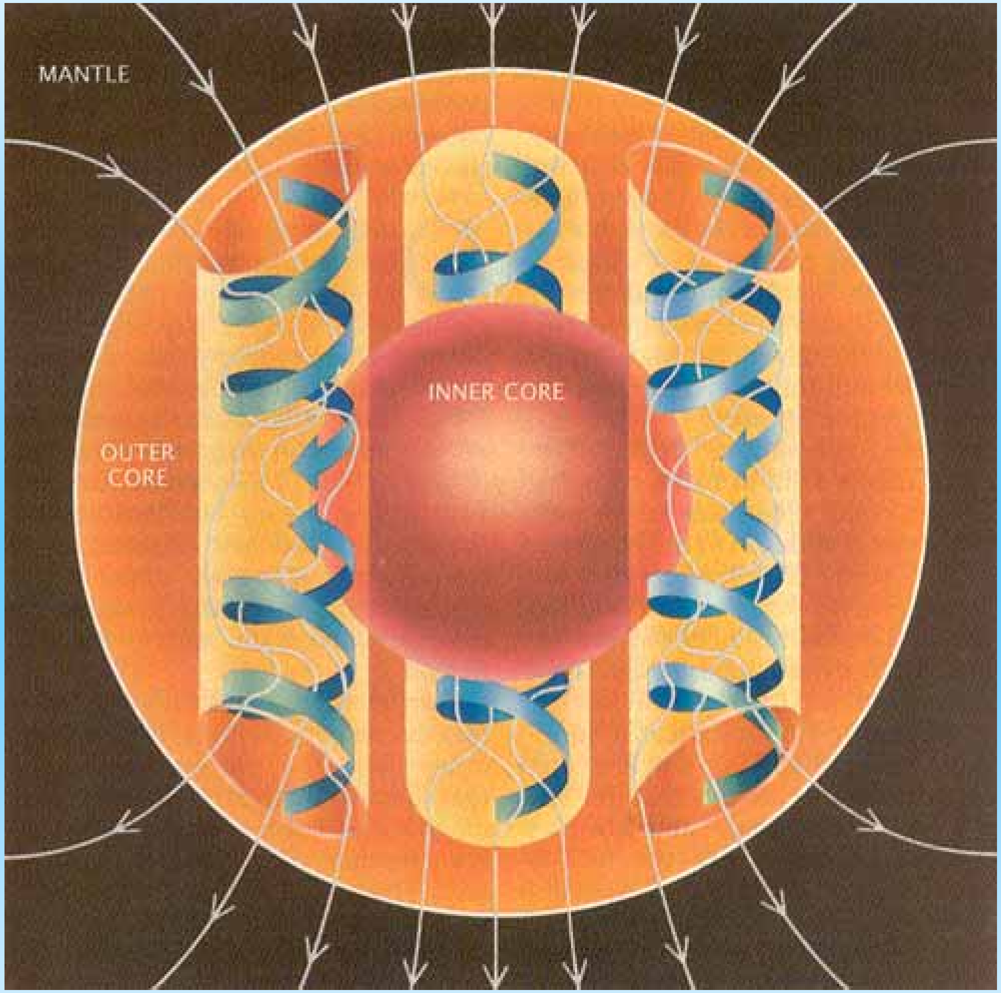

Andy Jackson, WUN 2004

Influence of rotation I:

The Earth’s inner solid core is visible in the magnetic field; note the two maxima of the normal non-dipole field

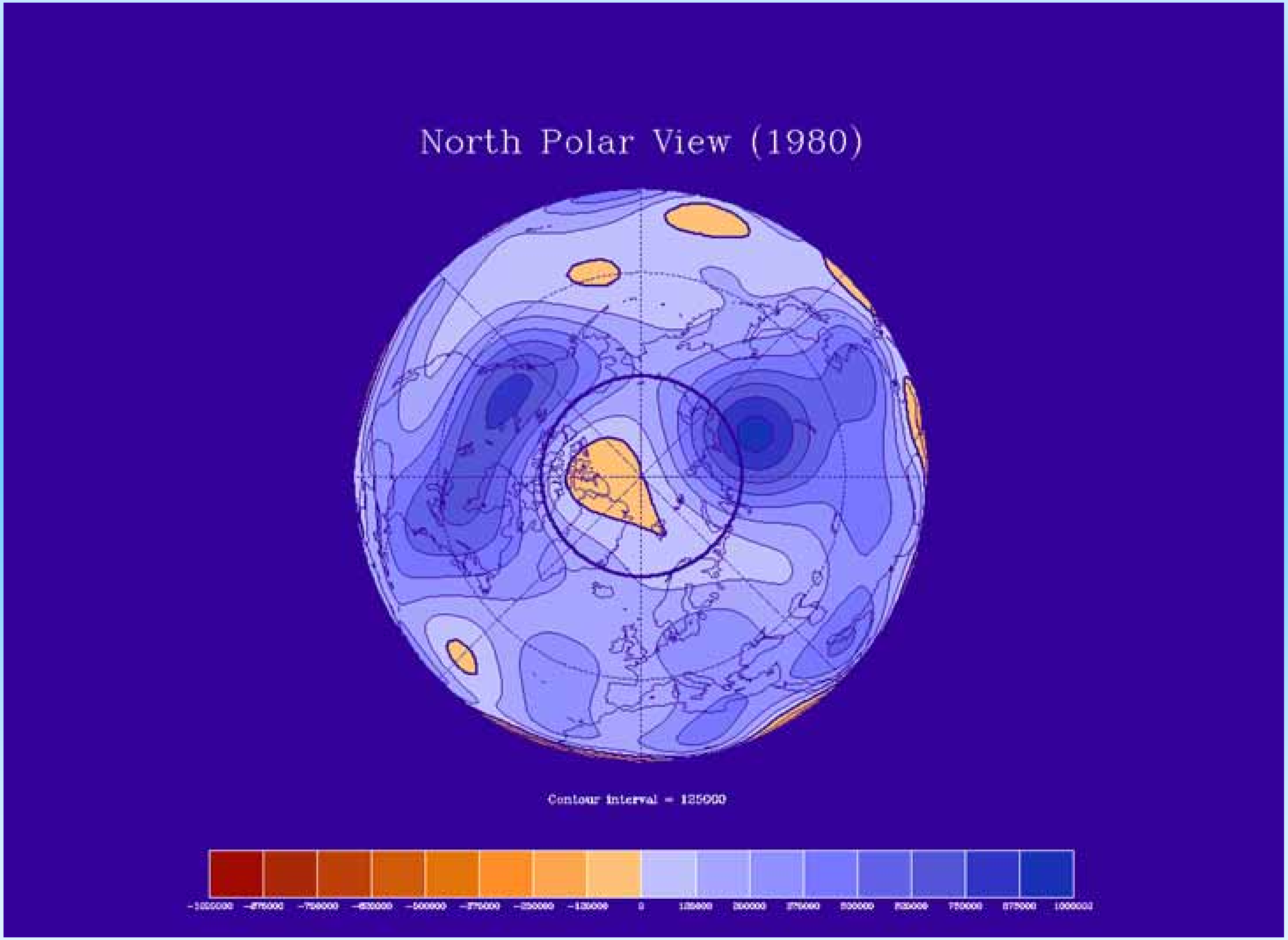

After Gubbins & Bloxham (1985)

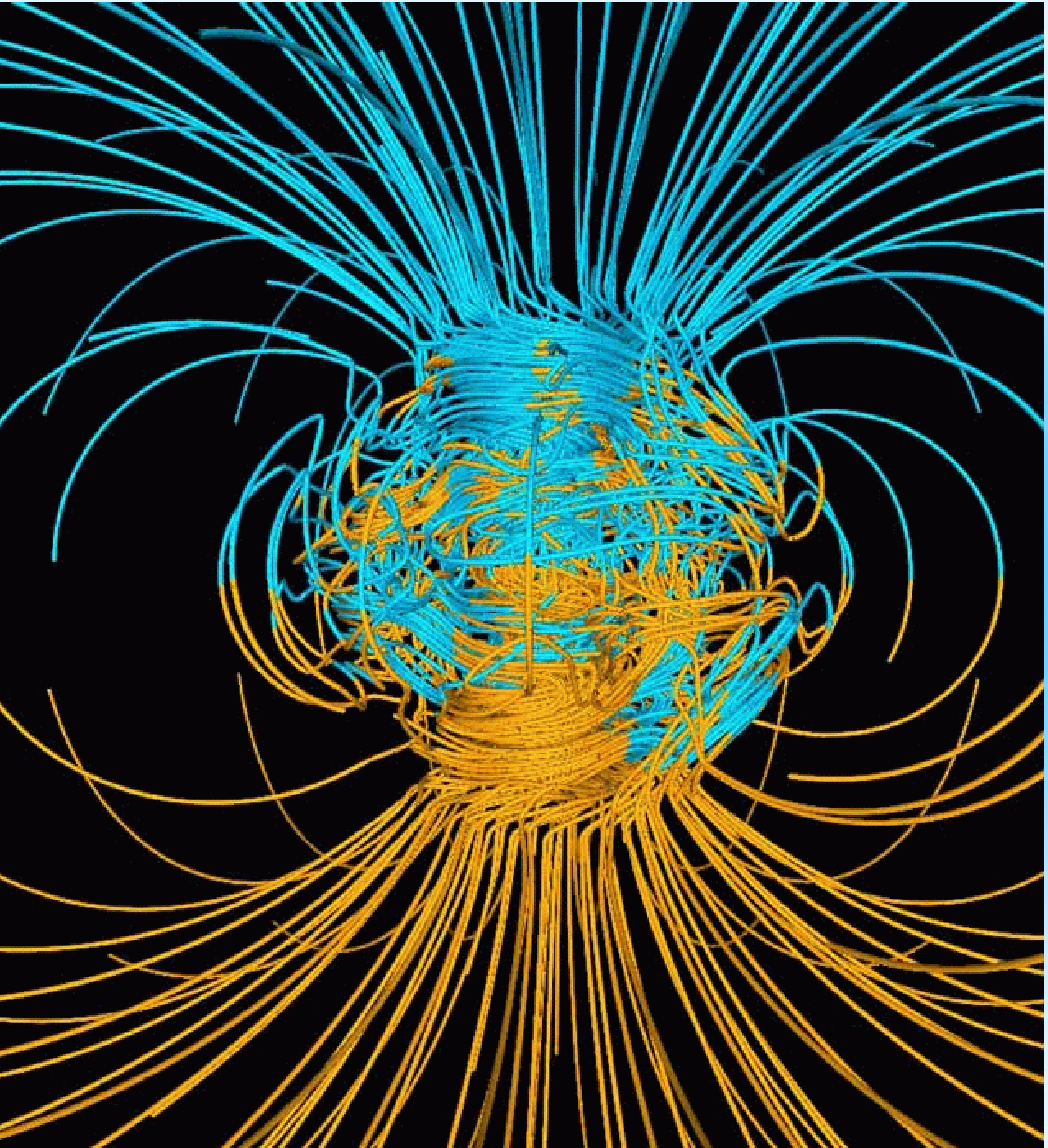

Morphology of magnetic field lines from numerical dynamo simulation (Glatzmaier & Roberts, 1995)

Jets on Jupiter: a good place to think about tall structures vs.thin, gravitationally stable layered Earth atmosphere. Here a deep, non-hydrostatic numerical model allows structures to line up with the rotation axis.

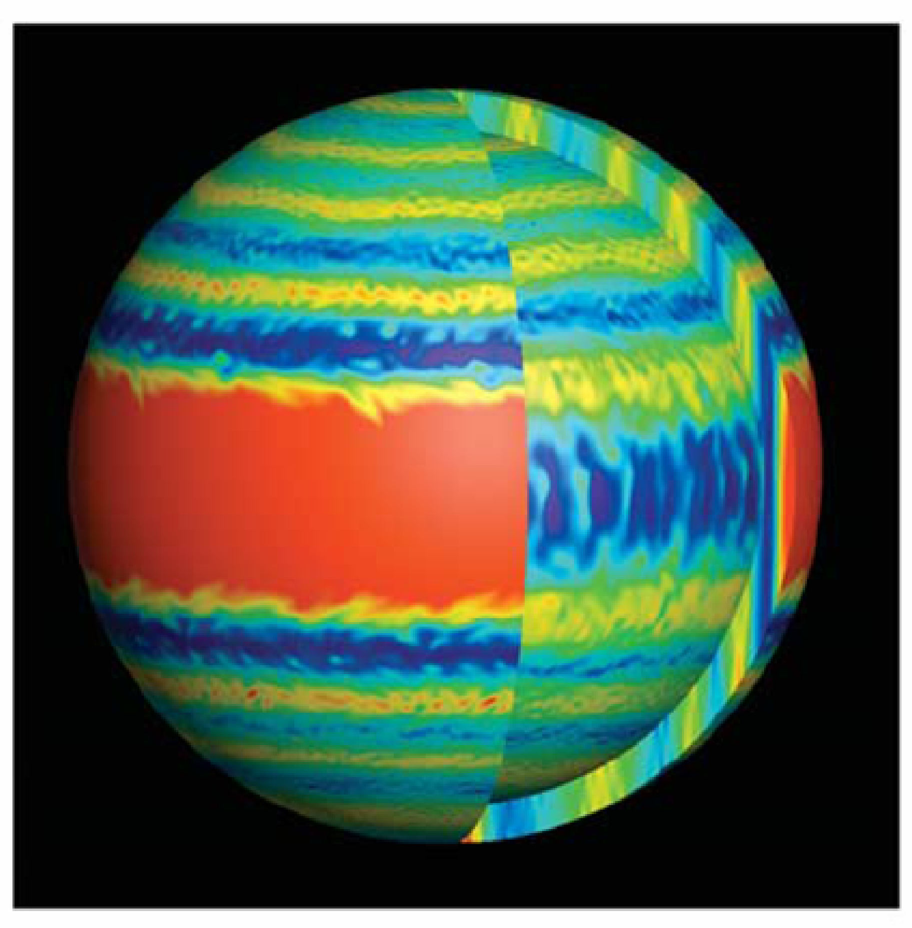

(Heimpel, Aurnou & Wicht, Nature 10 Nov 2005)

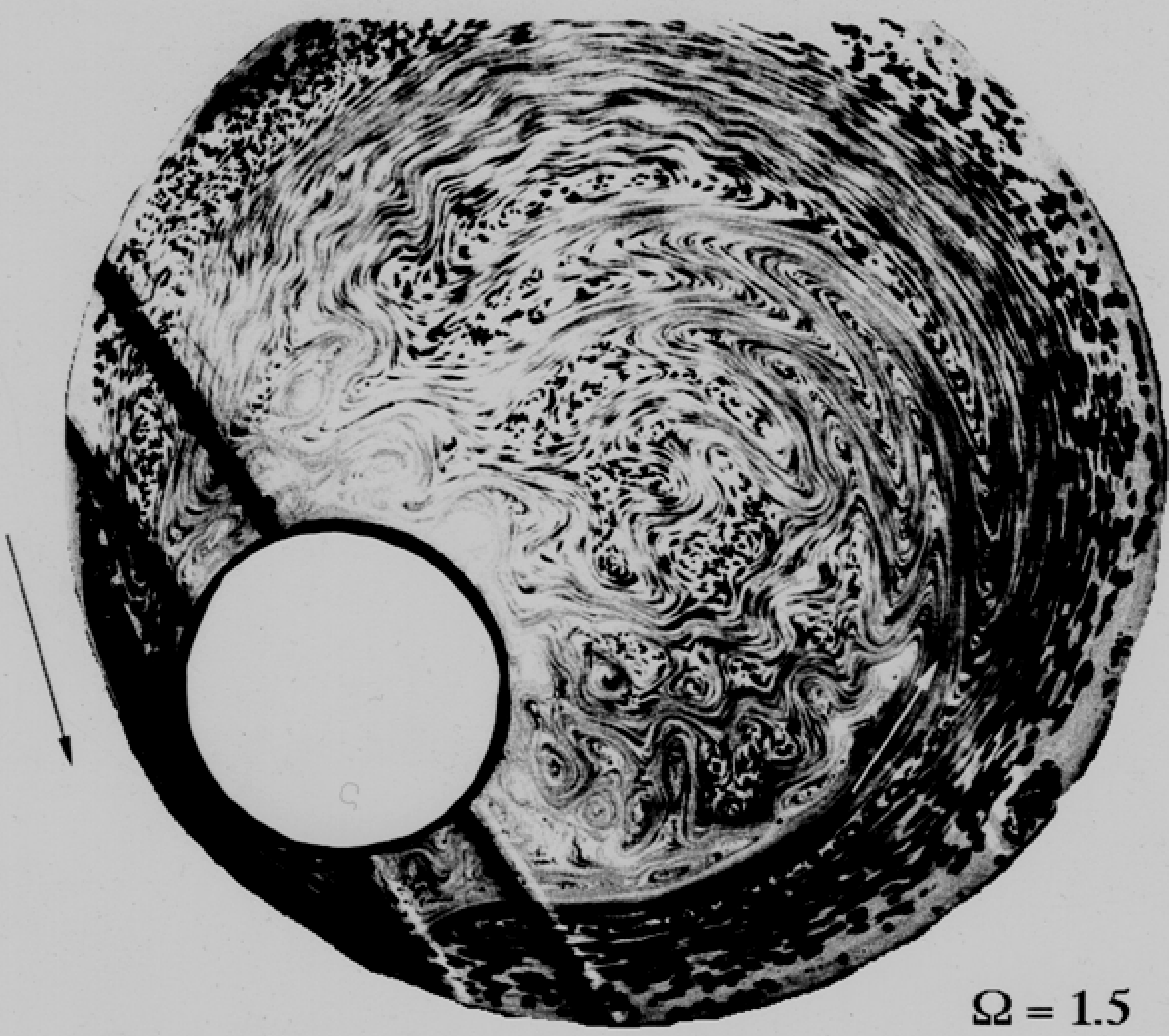

Figure 7b. As in figure 7a, except at double the rotation rate. Now an intricate banded circulation occurs, in which the basic pair of gyres is riddled with jets directed primarily along depth contours, but connecting across them (Boubnov and Rhines, priv. comm.)

planetary rotation can organize the chaotic textures of turbulent flow into coherent structures

GFD lab Univ of Washington

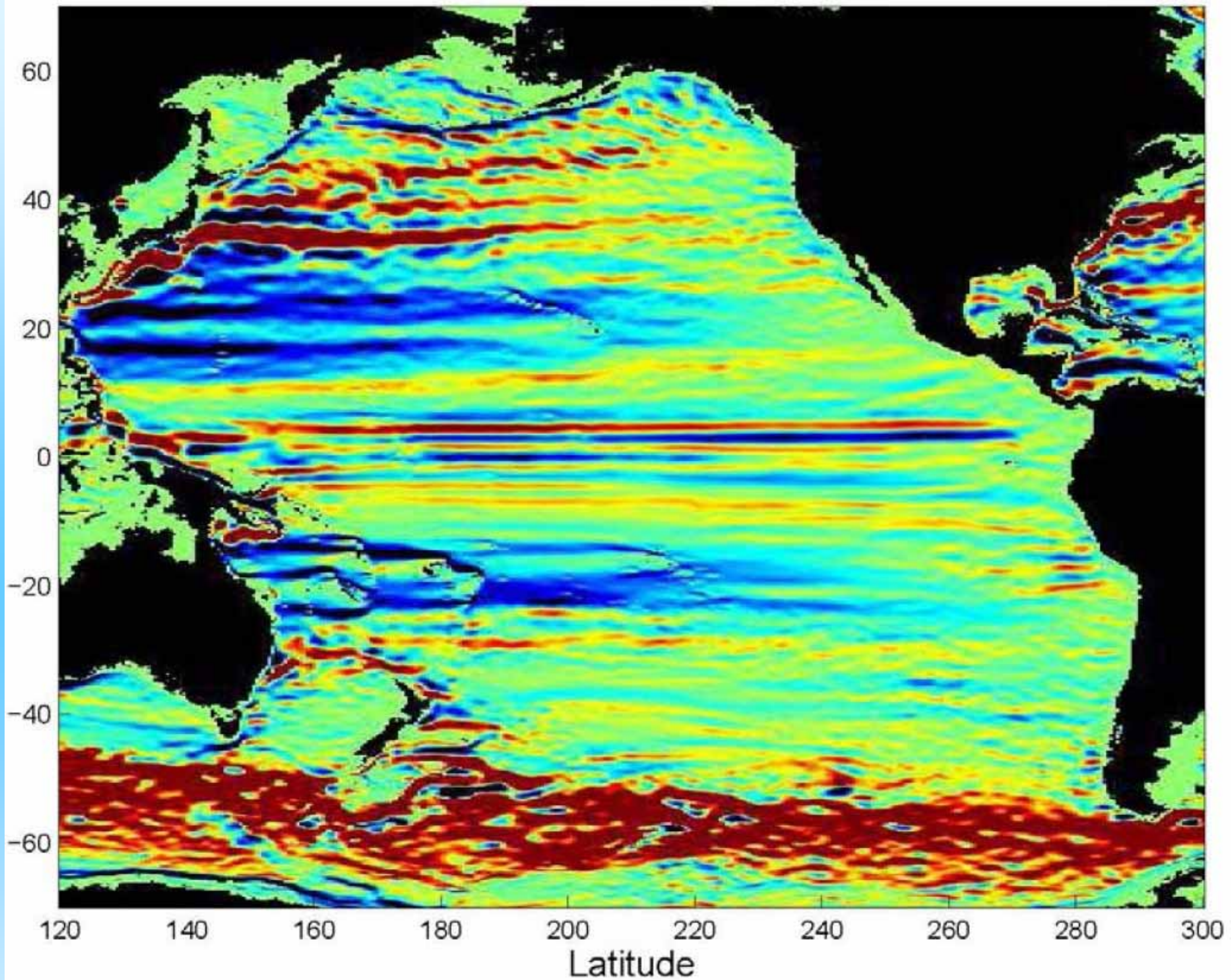

re 1. Zonal component of velocity averaged over 3 years at 400m depth
a high resolution ocean model. Color saturates at +/- 0.06 ms^{-1}.

Maximenko et al 2005

The geopotential: potential function Φ for gravity and centrifugal rotation effects

the geoid Φ: for a symmetric model of Earth's gravity

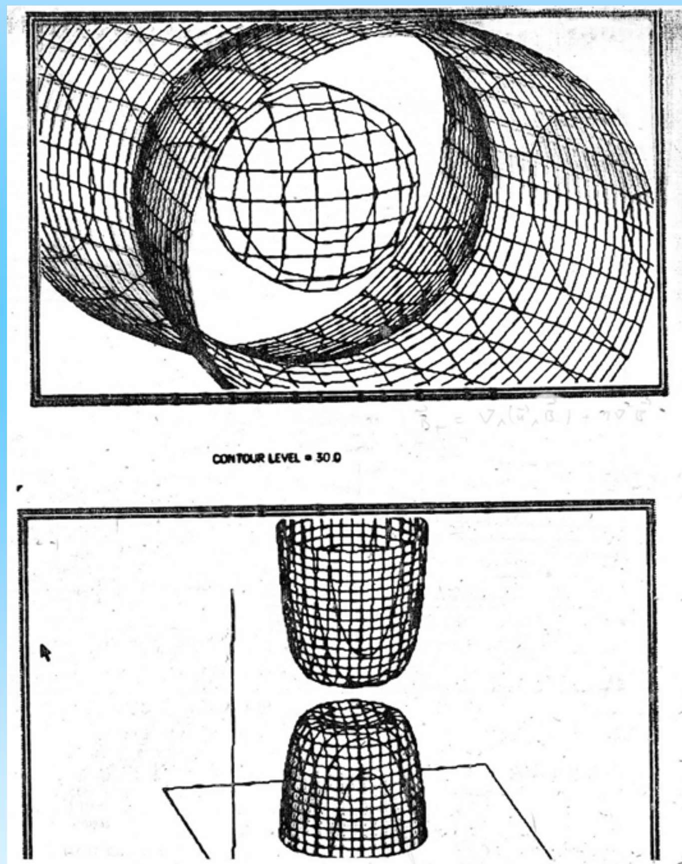

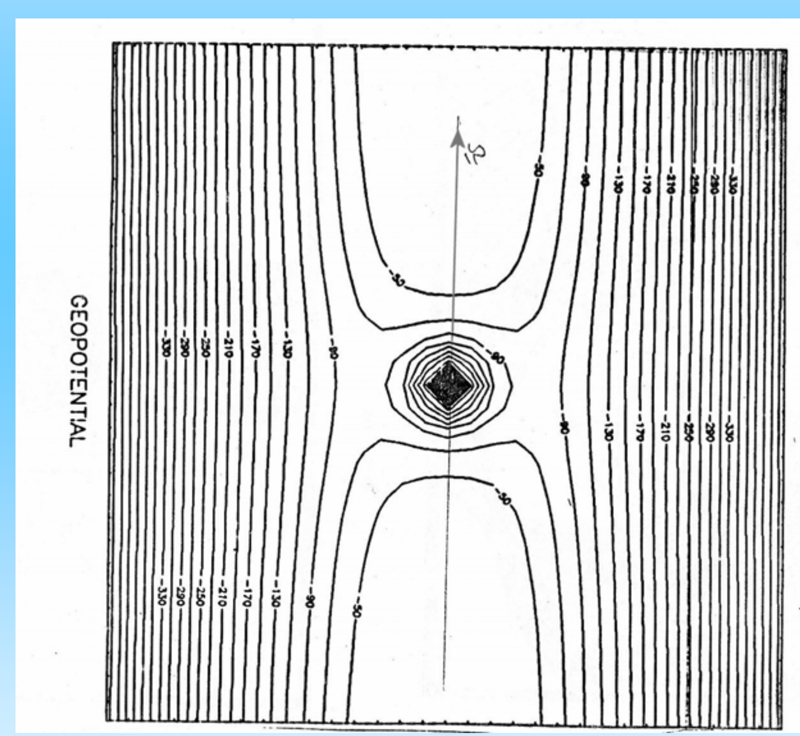

The presence of planetary vorticity amplifies effects of line-stretching:

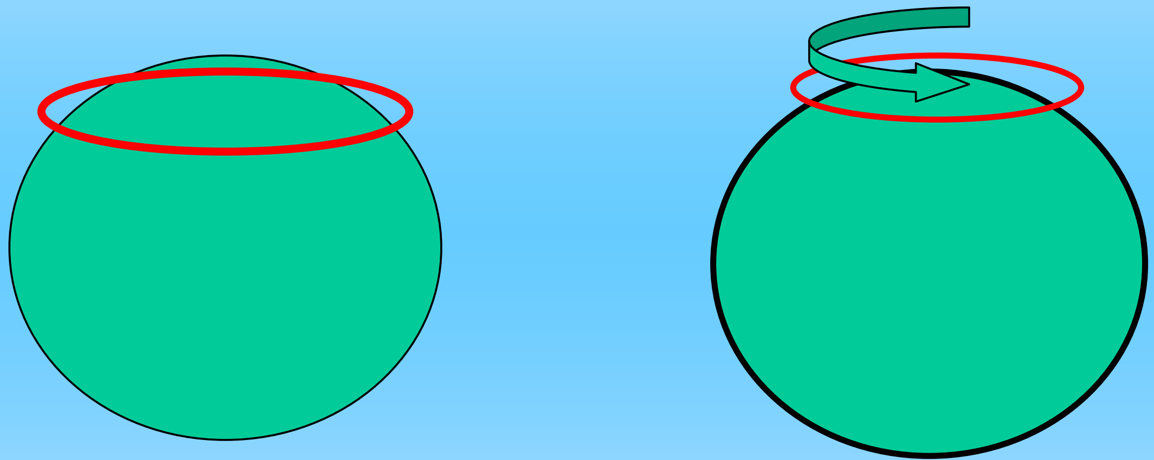

a ring of air moved 1000 km north gains westerly velocity of about 100 m sec^{-1} (for $f=10^{-4} sec^{-1}$) There is not enough energy available to utilize this mode: the Hadley cell is limited in north-south extent.

Forces (eddy momentum flux from PV stirring) and non-symmetric circulation are required to support extensive meridional excursion.

A 2mm glass cylinder is held vertically…at rest in the non-rotating frame…in a rotating fluid…

Its 3D turbulent wake generates cyclonic tall vortices

(Cormac Flynn, GFD Lab, Univ. of Washington also see computer sims of Smith & Waleffe Phys Fl 99 Morize,Moisy & Ribaud, PhysFl 05)

cylinder removed, showing final barotropic cyclones

Turbulent flows exhibit remarkable transformation between non-geostrophic and quasi-geostrophic flow, in both directions. Here, a 3D turbulent cylinder wake converts into a 2D field of cyclonic vortices. This is as if you inserted your finger in the fluid as it rotates rapidly.

the surface of a rotating fluid, slightly moving (Rossby number << 1)

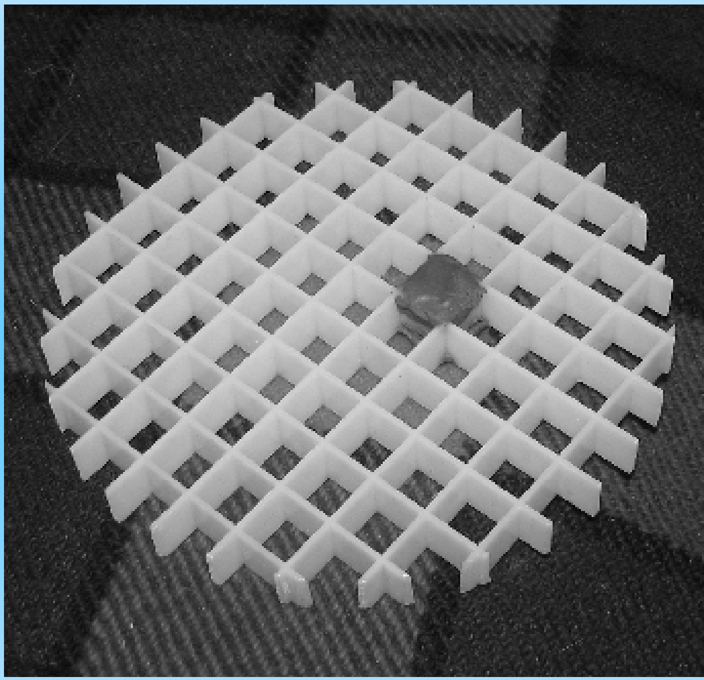

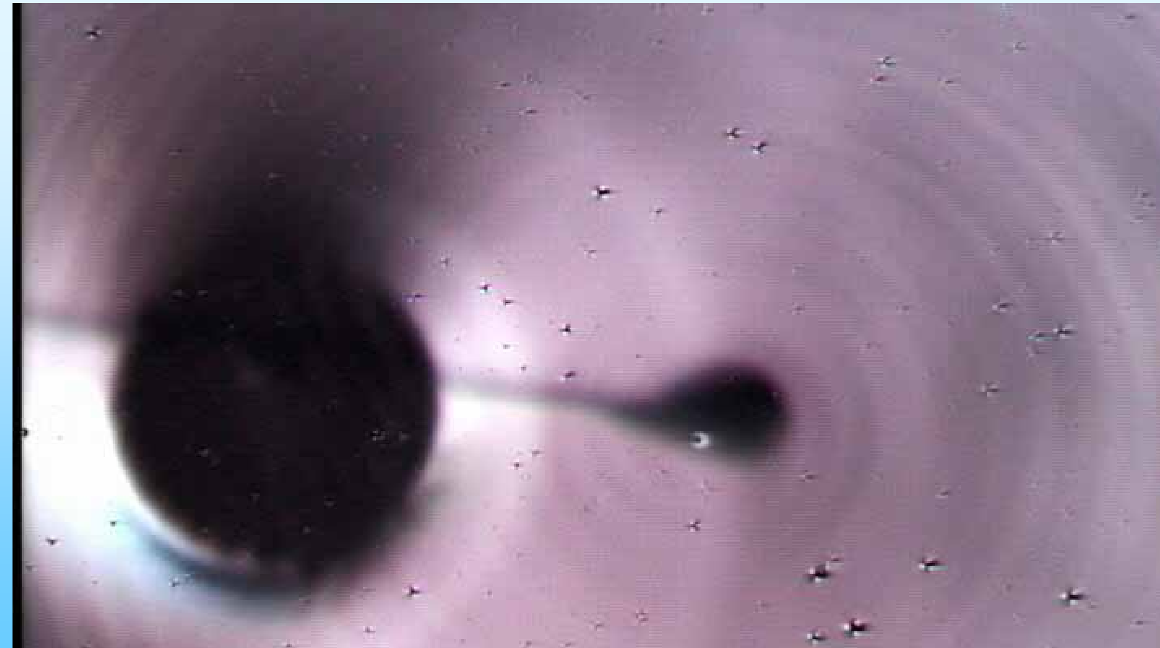

Dynamic height along latitude 60N from surface to stratosphere (1000 HPa to 30 HPa) for days 1-100 in 1996

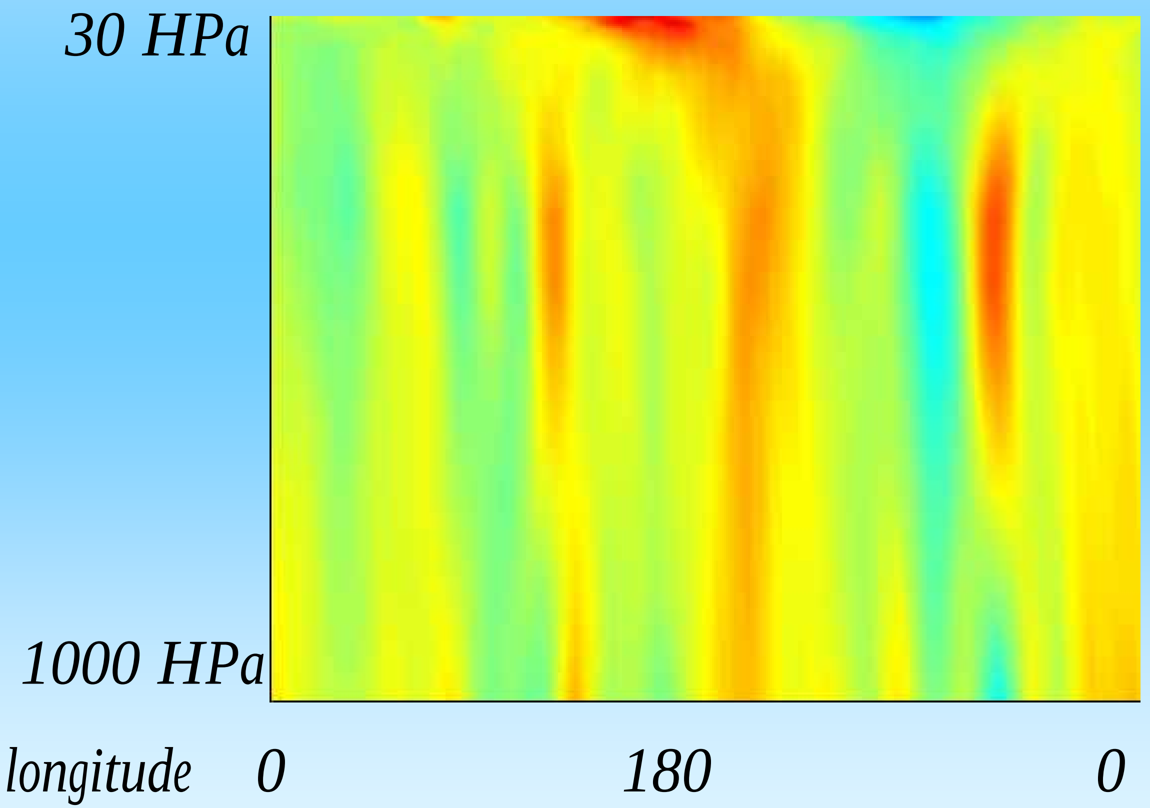

Ocean currents at 50W longitude southeast of the Gulf Stream, over 7 months, showing very similar structure throughout water column: a strong barotropic mode

each line is a horizontal current vector plotted with eastward flow pointing upward

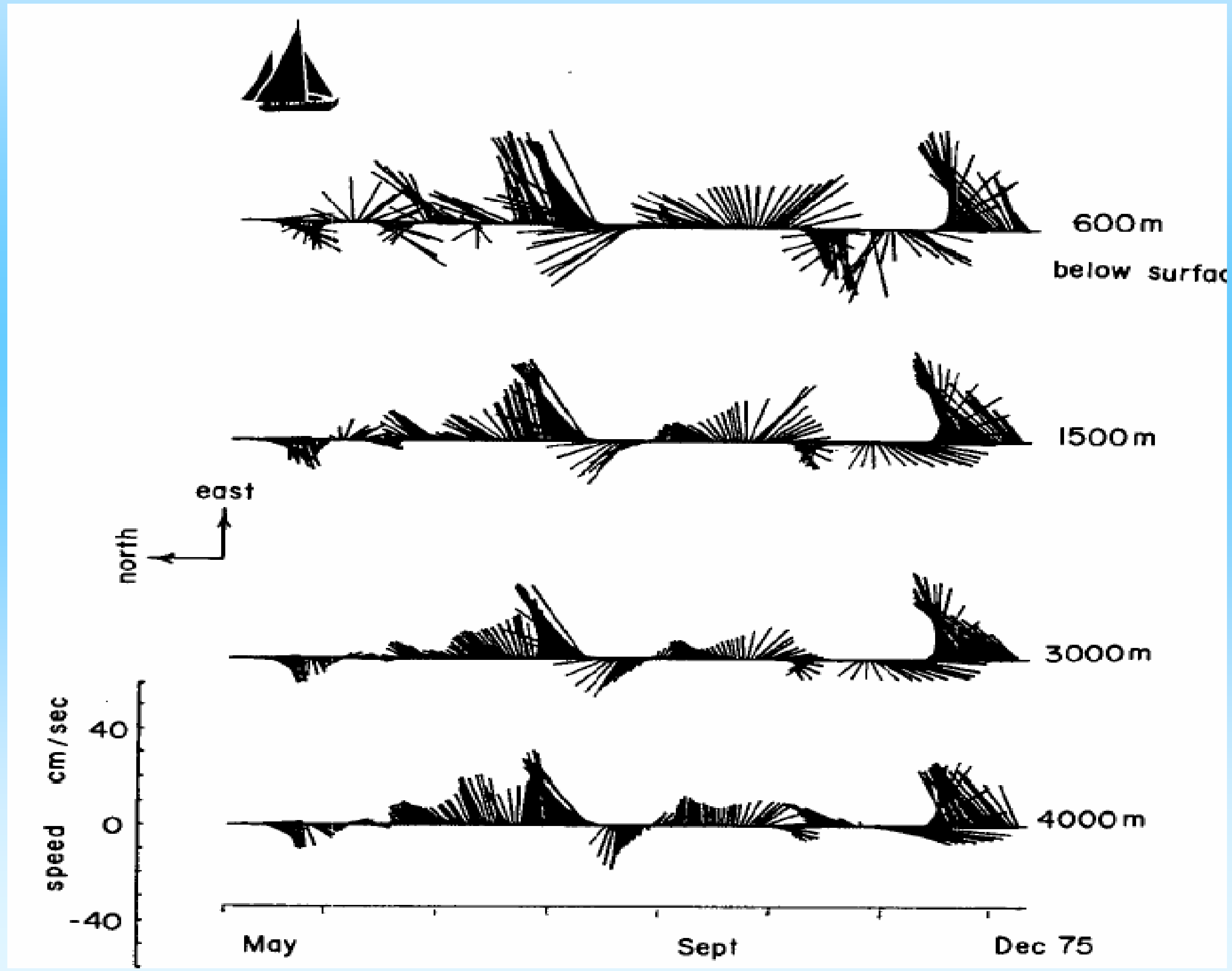

rotational stiffness is related to inertial waves (often wave motions express restoring forces that strongly effect steady circulations too).

inertial oscillations viewed by the movement of the water surface (essentially a pressure field).

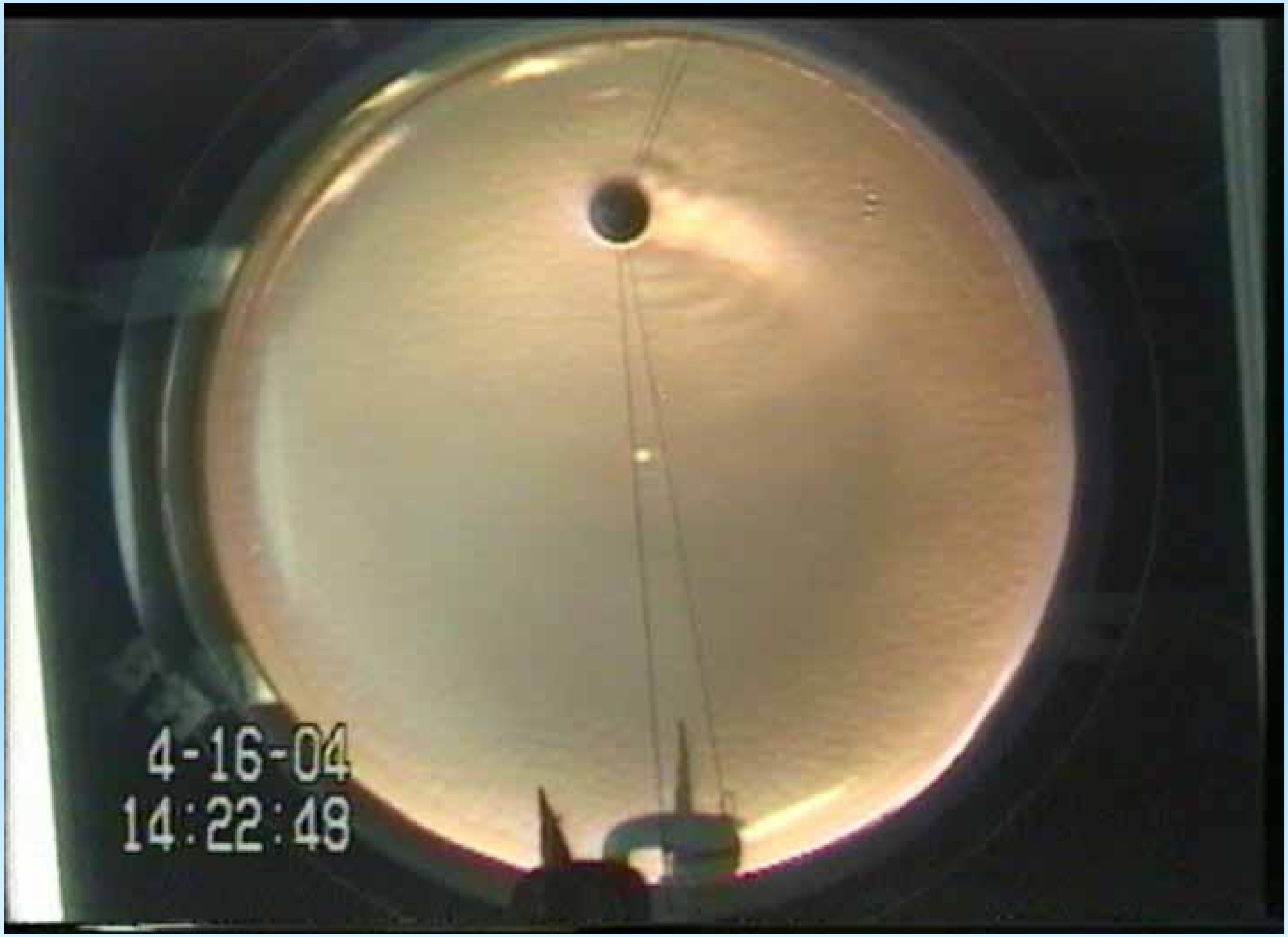

geostrophic balance: the sea surface at the Gulf Stream *Tom Rossby, Oleander project, adcp based*

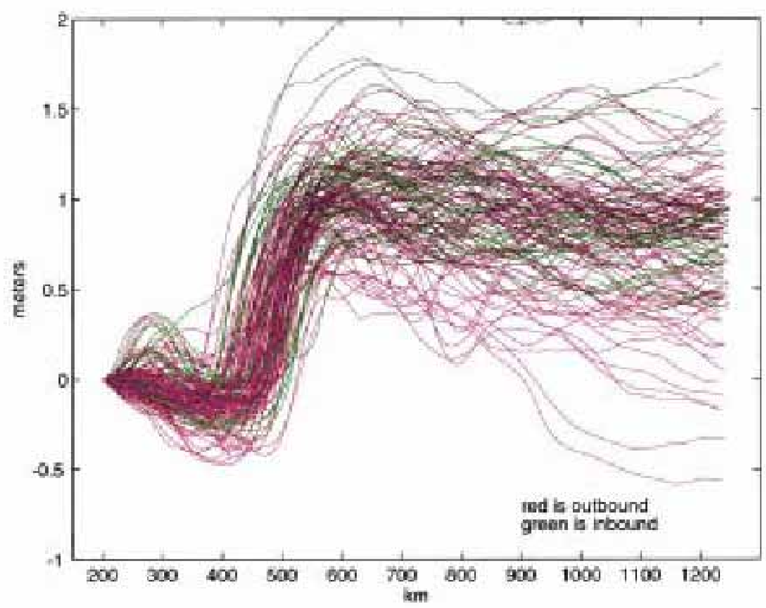

FIG. 7. Geostrophic sea level relative to 39°23′N, 72°29′W, just north of the shelfbreak, estimated from cross-track velocities from south- (red lines) and northbound (green lines) transits. The outliers (two to the south and one to the north) presumably result from a persistent compass errors of O(1°) during those transits. The mean difference and standard deviation across the GS alone equals 1.25 ± 0.21 m ($N = 87$) and 1.27 ± 0.15 m ($N = 39$) for the south- and northbound transits, respectively.

geostrophic balance: the pressure field along north-south lines in the atmosphere; day 1 1996 and day 180 1996

blue: 500 HPa dynamic height

red: sea-level pressure NCEP reanalysis data

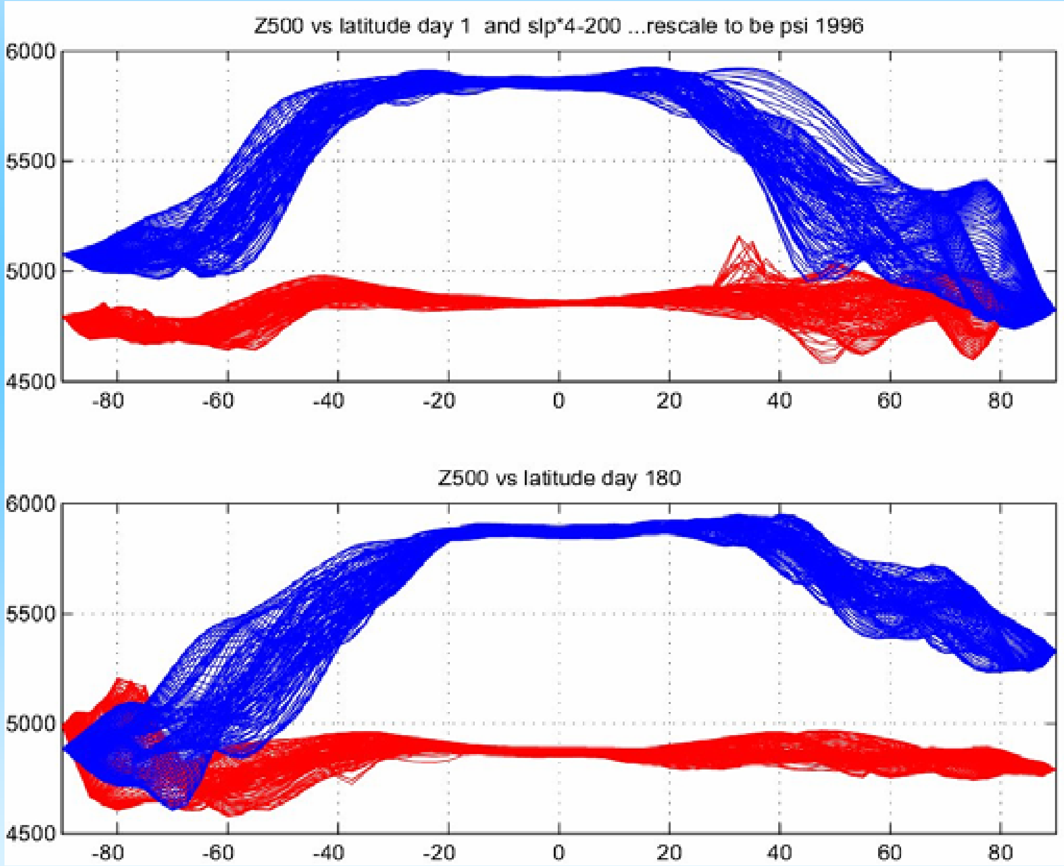

steady, non-dissipative flows have a powerful Bernoulli function conservation principle: both the pressure variation along a streamline and across streamlines is known from the velocity field.

- example: 2-dimensional flow around a circular cylinder. Adding rotation simply adds a pressure field that is a function of ψ. This shows how geostrophic flow has pressure gradient nearly perpendicular to the velocity, yet always with important pressure variations along streamlines

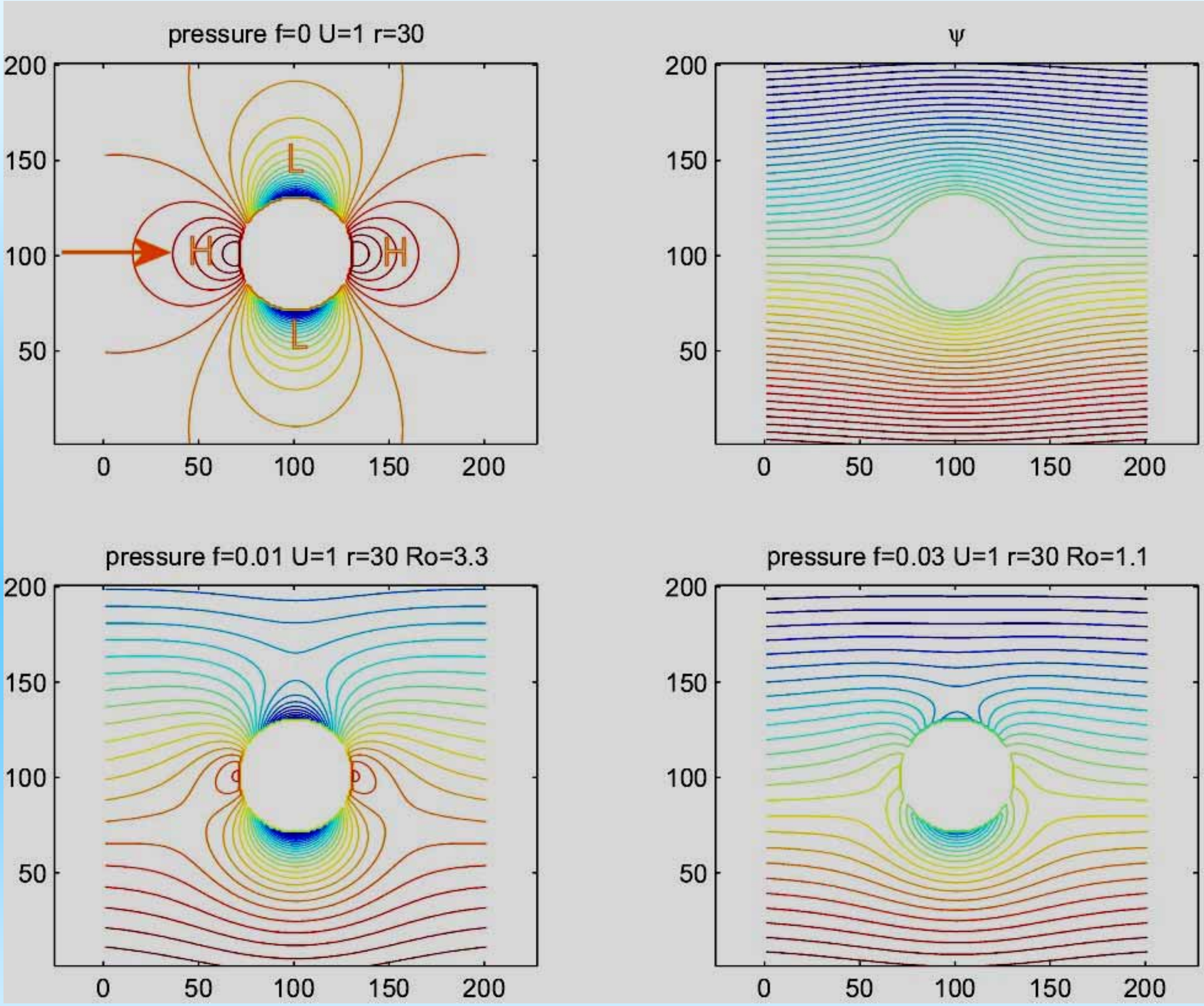

2D flow around a circular cylinder

Fig. The flow field (**ψ**) is at upper right. The pressure field for different values of the Rossby number, Ro = **∞**, 3.3 and 1.1

- The pressure field for flow round a cylinder in a single-layer rotating fluid, at moderate Rossby number is simply the pressure for a non-rotating flow plus a function of ψ

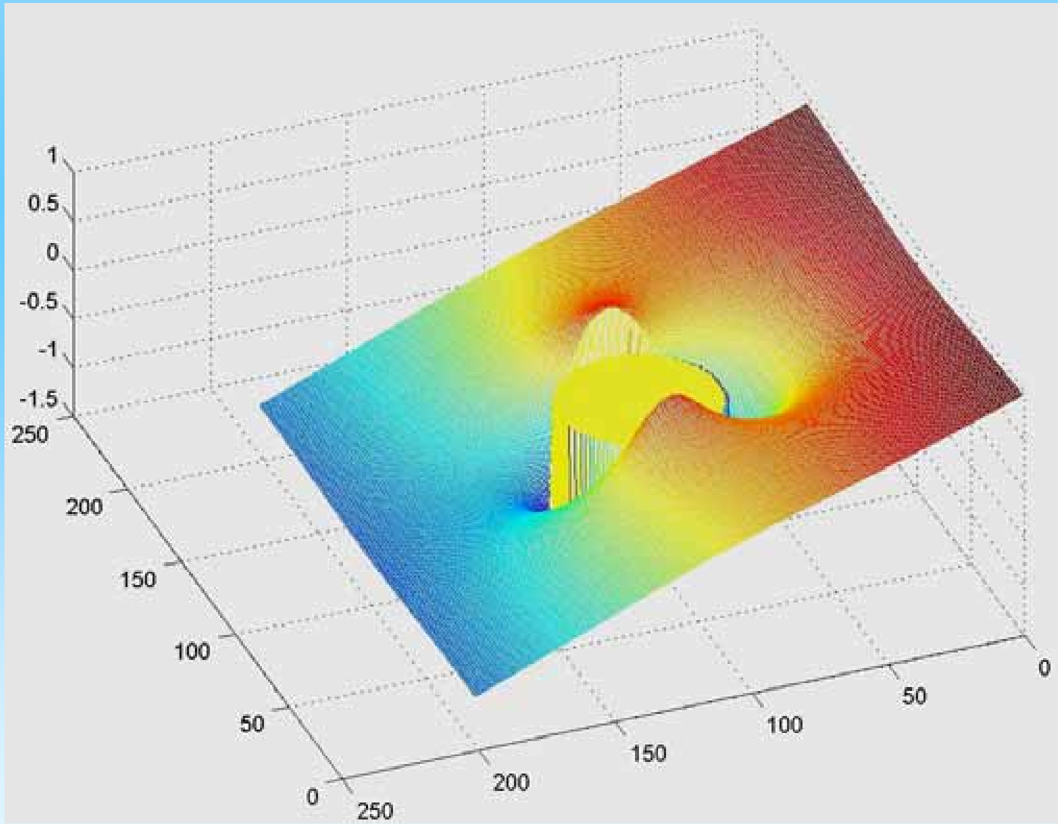

buoyancy: it's tricky

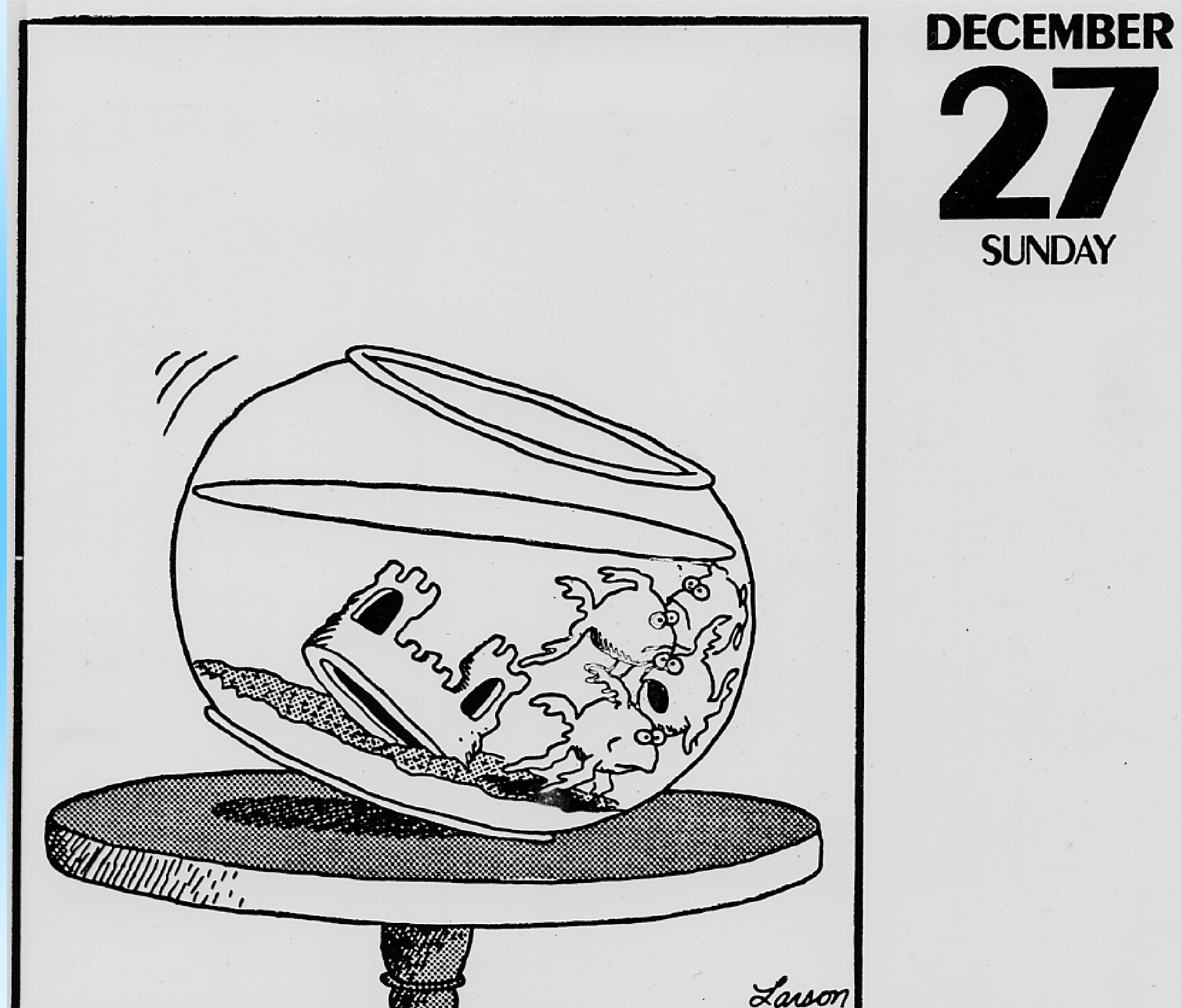

"Trim the bowl, you idiots! Trim the bowl!"

Geostrophic adjustment: initial value problem that ends up as a geostrophic flow

geostrophic adjustment: scenes from the North Pacific subtropical front region: Gregg, Brainerd, Hosegood, Alford

Mixing Versus Mixed Layers

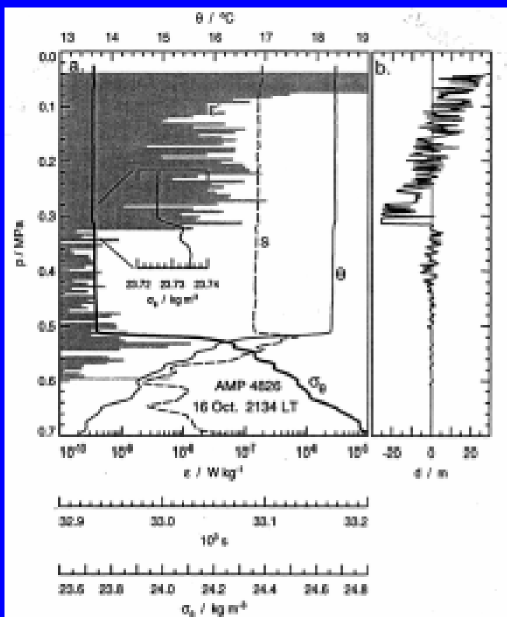

- Mixed Layers: Relatively homogenous relative to deeper water, e.g., $\Delta\sigma_\theta \lesssim 0.1\ \mathrm{kg\,m^{-3}}$
- Mixing Layers: active turbulence generated at the surface, e.g., $\Delta(\log_{10}\epsilon) \leq 2$
- In this example, mixing drops where $\Delta\sigma_\theta \approx 0.001\ \mathrm{kg\,m^{-3}}$
- Mixed layers may not have been mixing for hours to days
- To compare with Ferarri & Rudnick, we considered mixed layers

Brainerd & Gregg (1995)

3

- Because insolation accounted for only ≈ 60% of restratification during a diurnal ML cycle observed with continuous microstructure profiling, Brainerd & Gregg (1993) inferred that observed θS changes resulted from 'slumping'
- Rudnick & Ferrari (1999) and Ferrari & Rudnick (2000) reported that 20 m to 10 km ML T & S gradients have compensating density effects

Rudnick & Ferrari (1999) Wavelet Coefficients

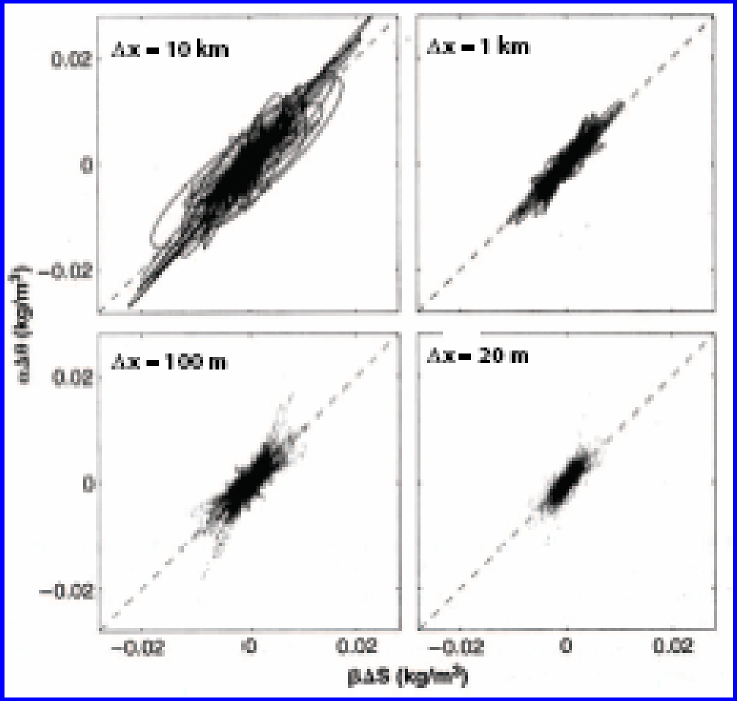

Rudnick & Ferrari (1999)

- Morlet wavelet: $e^{(x^2/2)}e^{2\sqrt{2}\pi j x}$
- Constant-depth run at 50 m
- Max variability 0.02 $\mathrm{kg\,m^{-3}}$
- All are close to $R_\rho = 1$, density compensation

Evolution of Density Surfaces in Float-centered Coordinatess

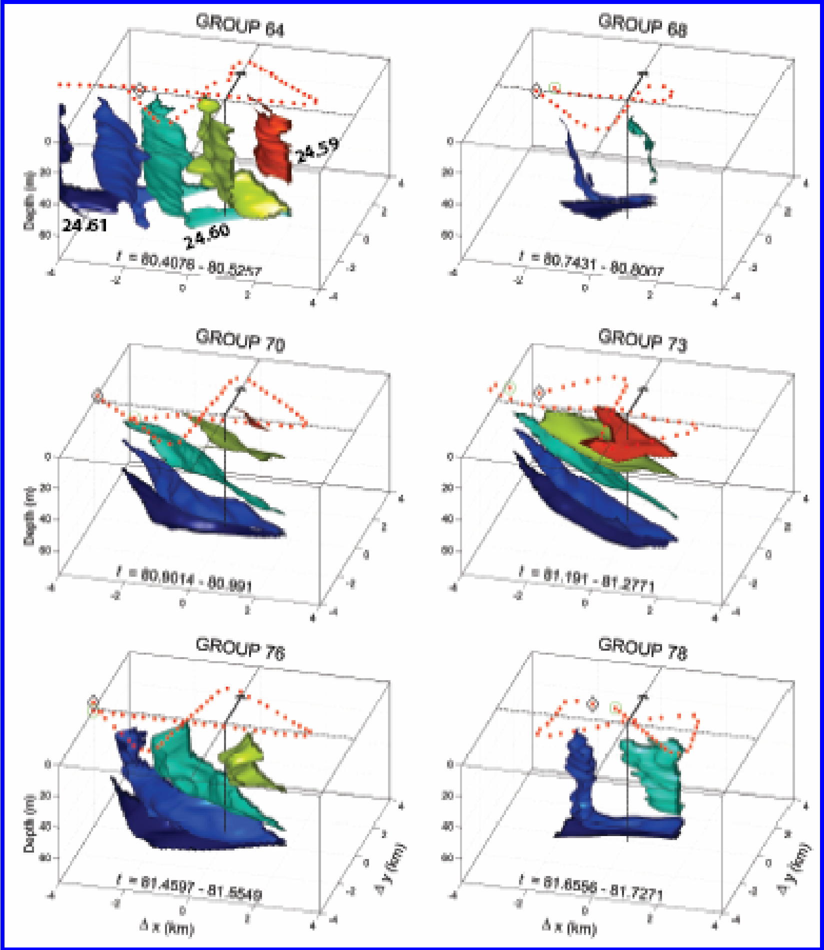

- Group 64: Convecting with vertical isopycnals
- Group 68: Slumping began just before convection ended
- Group 70: Mixed layer restratified 5.2 hours after convection ended
- Group 73: Light water added at surface
- Group 76: 8 hrs of convection homogenized top half of ML
- Group 78: 12 hrs of convection homogenized all of ML

Hosegood, Gregg, Alford (2007)

Mixed Layer Evolution at 28 °N

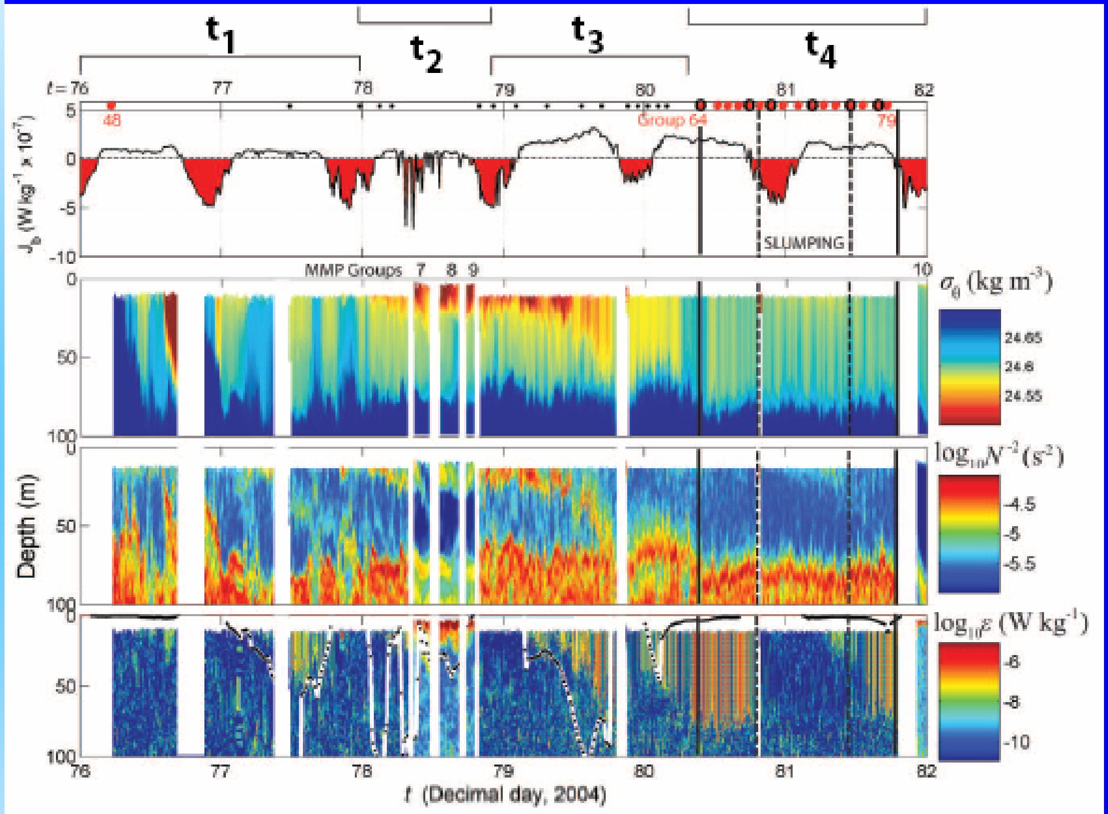

- t1: $h_m = 20 - 80$ m, light winds, weak convection
- t2: Heavy rain capped remnant ML
- t3: Winds & cold air deepened ML to 80 m
- t4: ML 'slumped' without rain or wind

Hosegood, Gregg, Alford (2007)

- ϵ estimated from scales of density overturns
- SWIMS data available below 15 m, missed restratification start during t_4

Comparison with Tandon & Garrett (1994, 1995)

- **Storm-driven homogenization of surface water with a horizontal buoyancy gradient, b_x, leaves a mixed layer with vertical isopycnals**
- **Geostrophic adjustment after the storm generates near-inertial motions that displace the isopycnals about their average position**

$$\zeta = \frac{b_x(z + H/2)}{f^2}(1 - cos\, ft)$$

- **Resulting in an oscillating stratification:** $N^2 = \frac{b_x^2(1 - cos\, ft)}{f^2}$

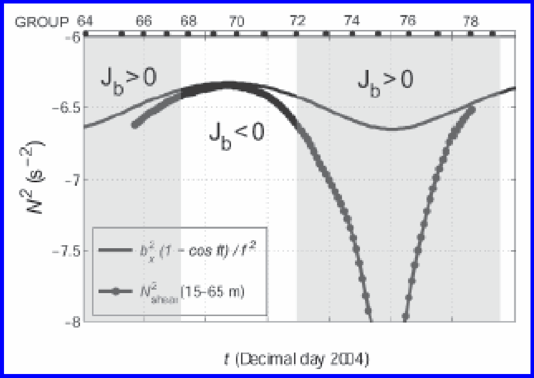

– The model does not consider a diurnal cycle after the storm

Wavelet Coefficients Scaled by Density Contribution of T', S'

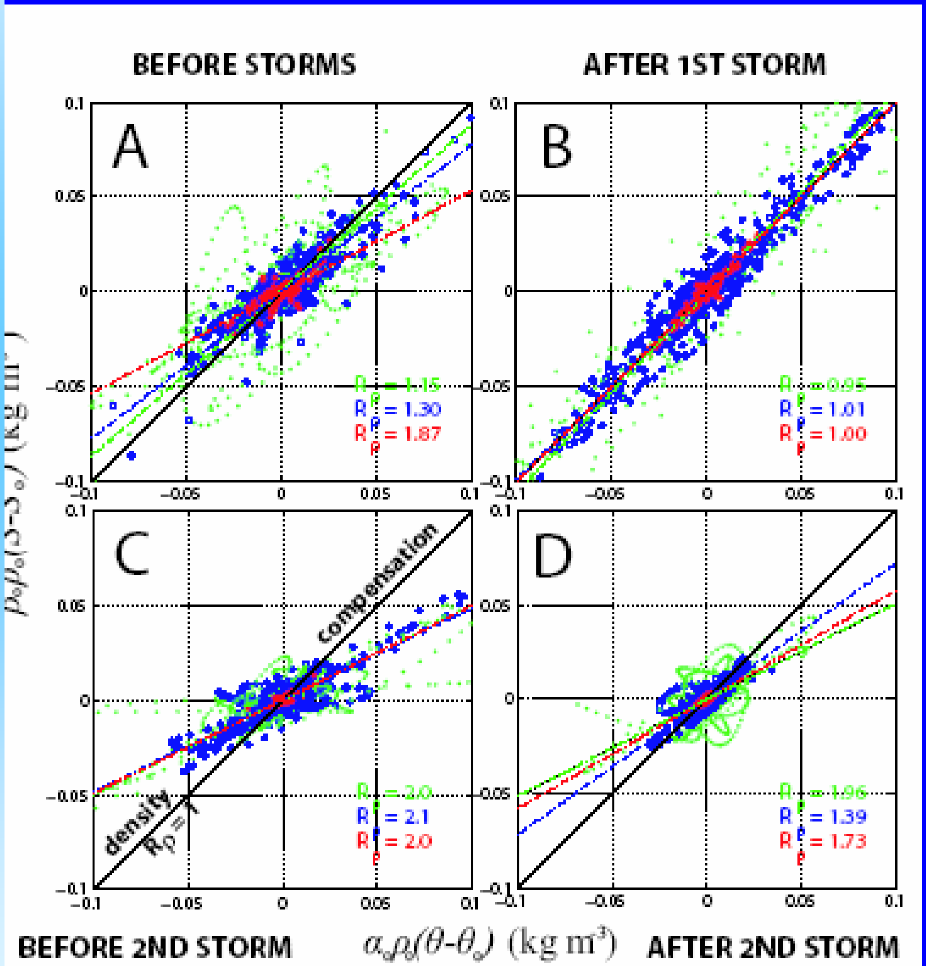

- Morlet wavelet: $e^{(x^2/2)}e^{2\sqrt{2}\pi j x}$
- Data interpolated to 20 m
- Scales are 2 km (red), 5 km (blue) and 10 km (green)
- Dash-dot lines are fits with slopes at lower right
- A & B tend to $R_\rho = 1$, consistent with northern front
- C & D tend to $R_\rho = 2$, T-dominated, consistent with southern front
- D conditions closest to those of Ferrari & Rudnick

Velocity spirals: thermal wind balance

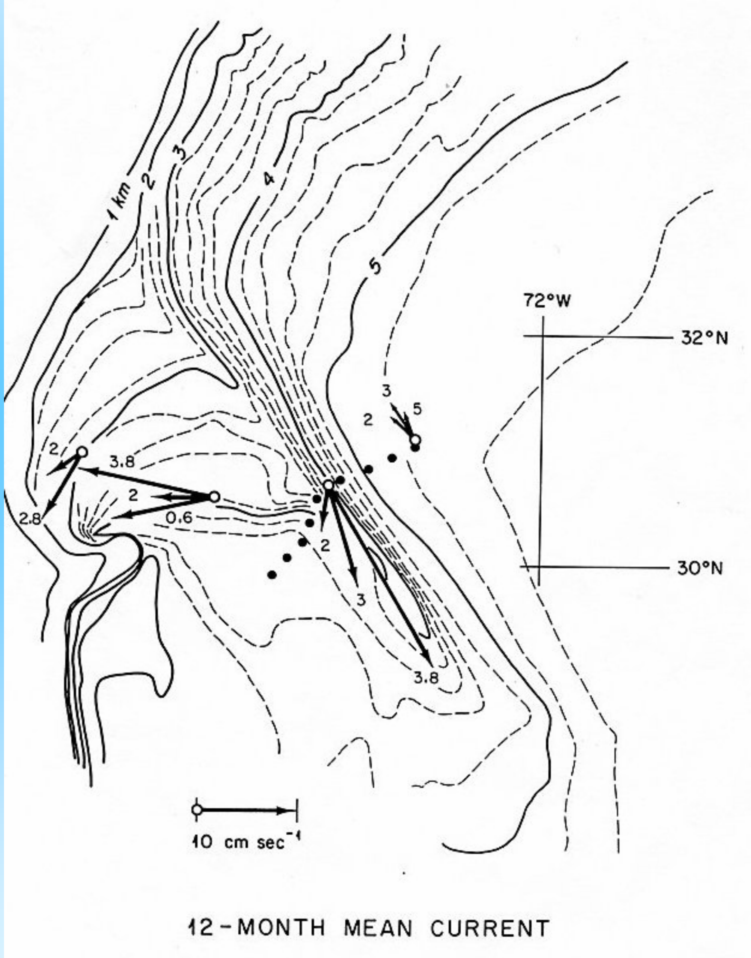

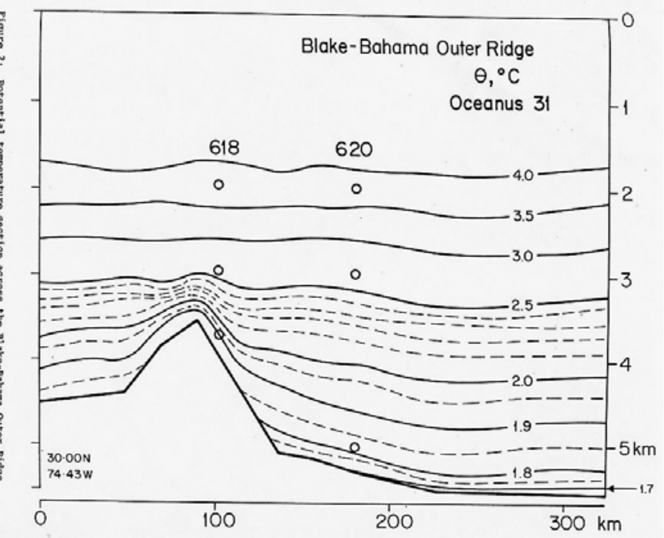

Figure 2: Potential temperature section across the Blake-Bahama Outer Ridge (8 August 1977). The track is indicated on fig. 2. Current-meter locations are shown. The deep boundary current flows southward along the eastern slope of the Ridge, and returns northward on the western slope. The mooring records show, however, that the long-term mean flow is narrower than would be inferred from the region of tilted isotherms (at 620 the 12-month mean is northwestward: fig. 4, and page 14).

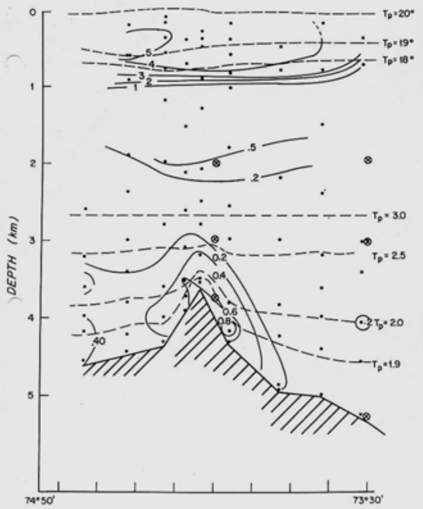

Figure 3: Tritium concentration, showing the high values associated with the deep boundary current. Dashed curves are potential isotherms. The tritium concentration essentially vanishes at 3000 m, and rises once again above the thermocline. A subsurface maximum is seen in the 18° water, associated with recent winter renewal farther north.

one year current records at 2000, 3000, 3800m depth in the deep western boundary current

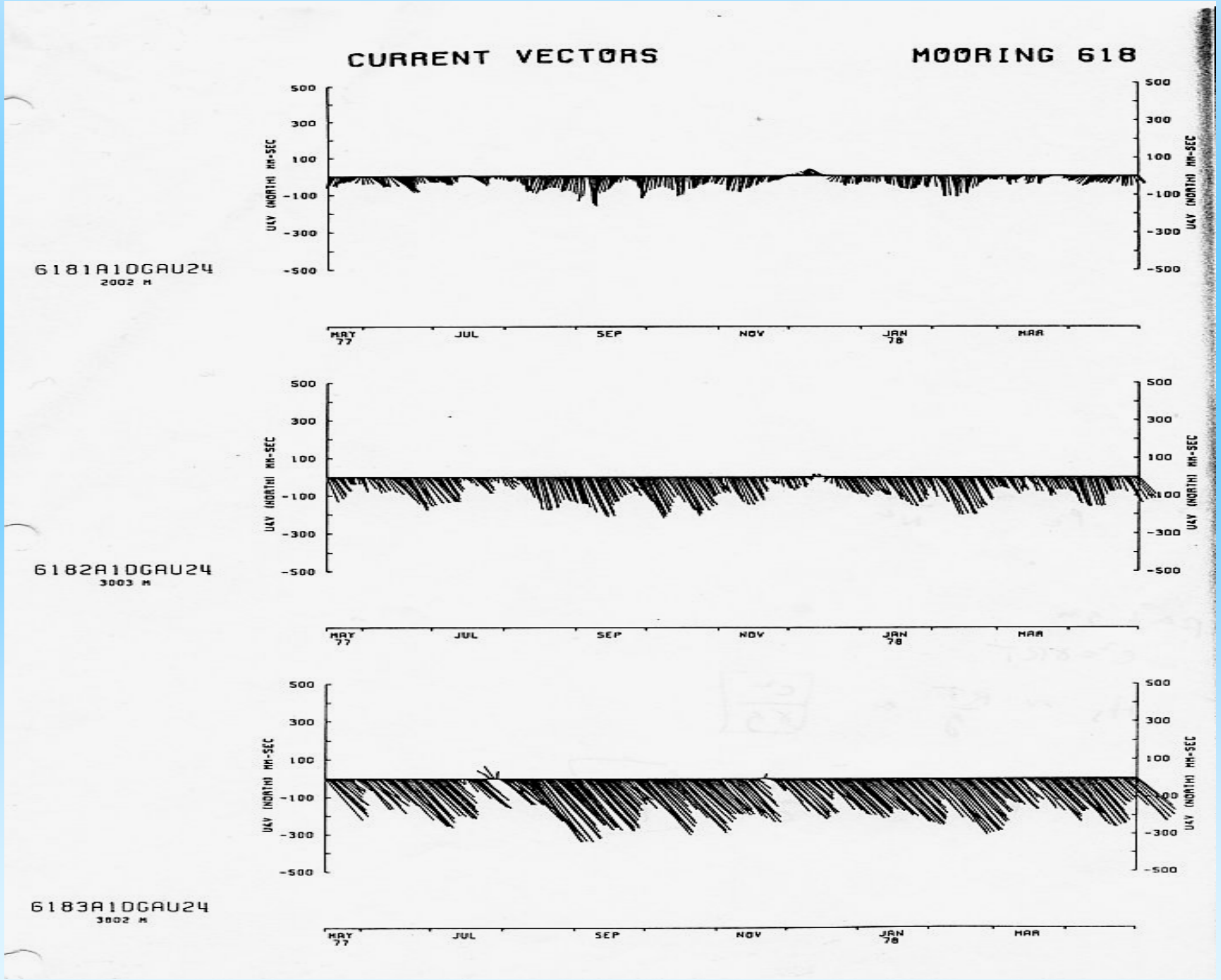

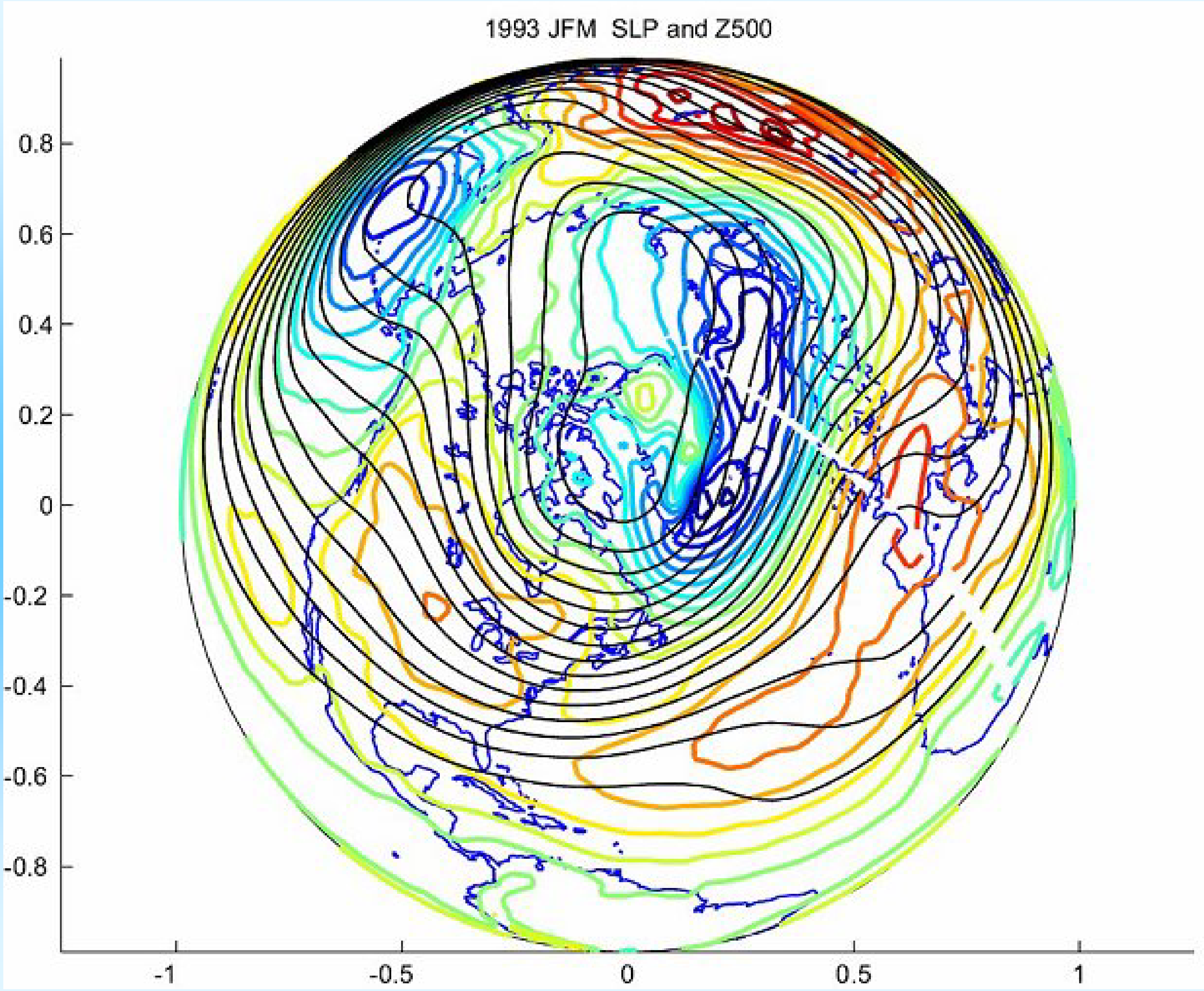
1993 JFM SLP and Z500
0.8
0.6
0.4
0.2
0
-0.2
-0.4
-0.6
-0.8
-1
-0.5
0
0.5
1

Stommel's cooling spiral at OWS Juliette (52.5N, 20W) is a symptom of upward Qnet

Plot of (u,v) velocity components with depth as a parameter from hydrographic data

Stommel, PNAS 1979

Proc. Natl. Acad. Sci. USA 76 (1979) 2519

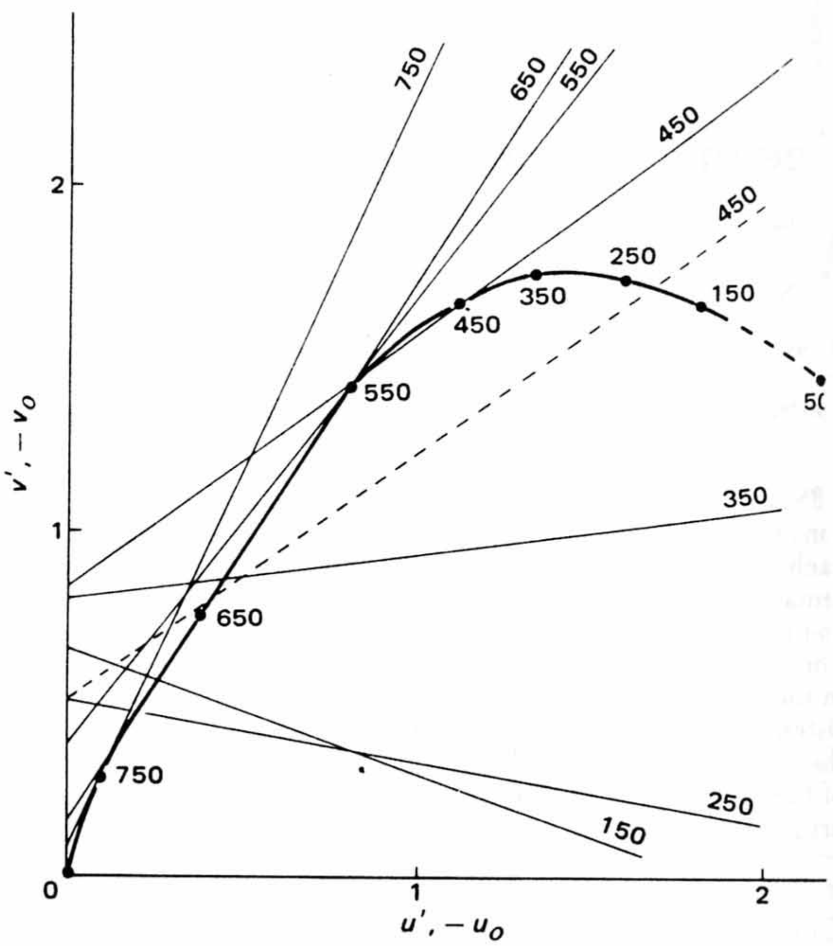

FIG. 1. The curved hodograph, with depths marked in meters, is in geostrophic velocity (u',v'), relative to 850 m, at "Juliette" (52.5° N, 20° W) computed from the horizontal density charts in Dietrich's *Atlas* (1). The lines are the u_o, v_o [3] displayed on the $-u_o, -v_o$ plane. The rather broad common intersection defines that value of $-u_o, -v_o$ which satisfies all the equations best.

rotating and stratified flows..over simple mountains

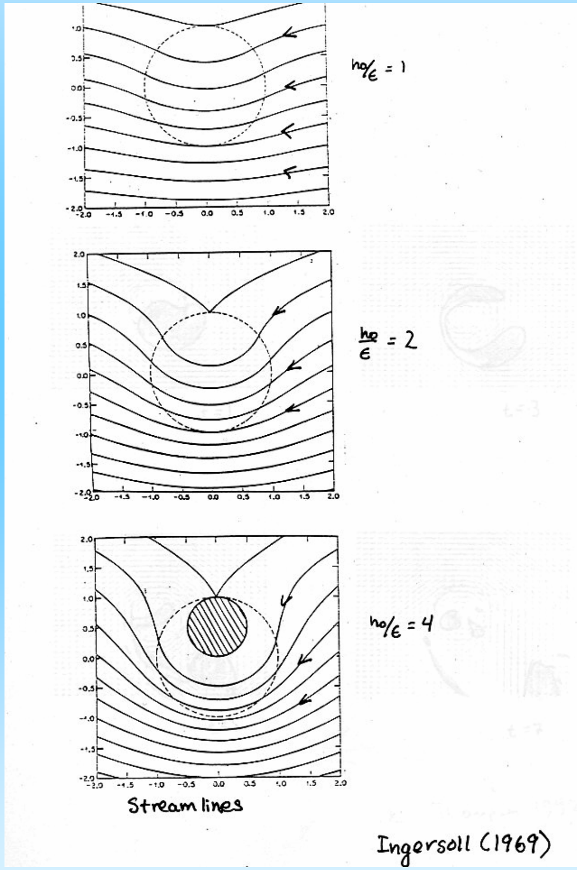

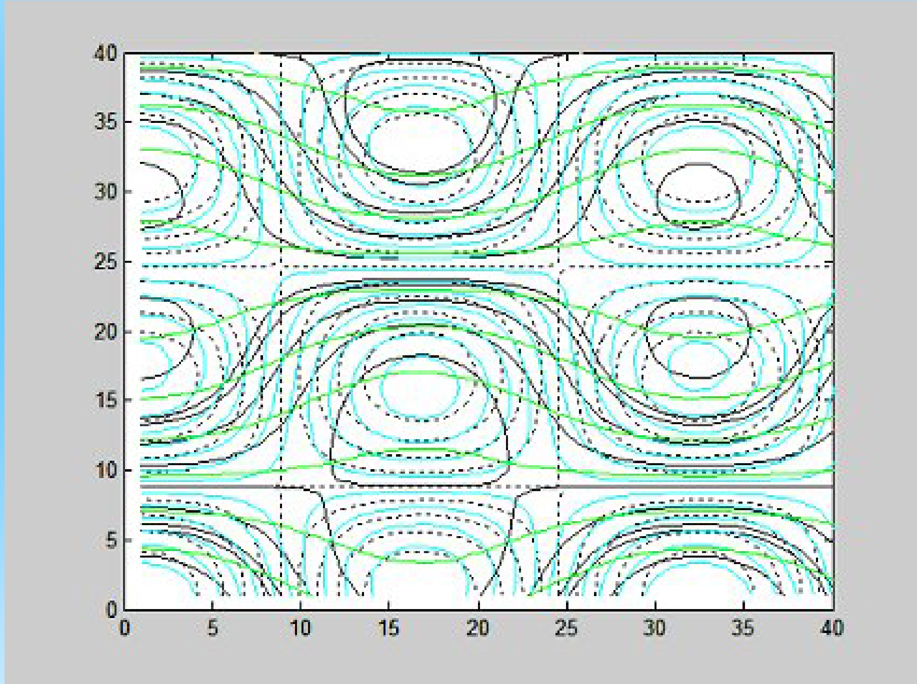

Waves

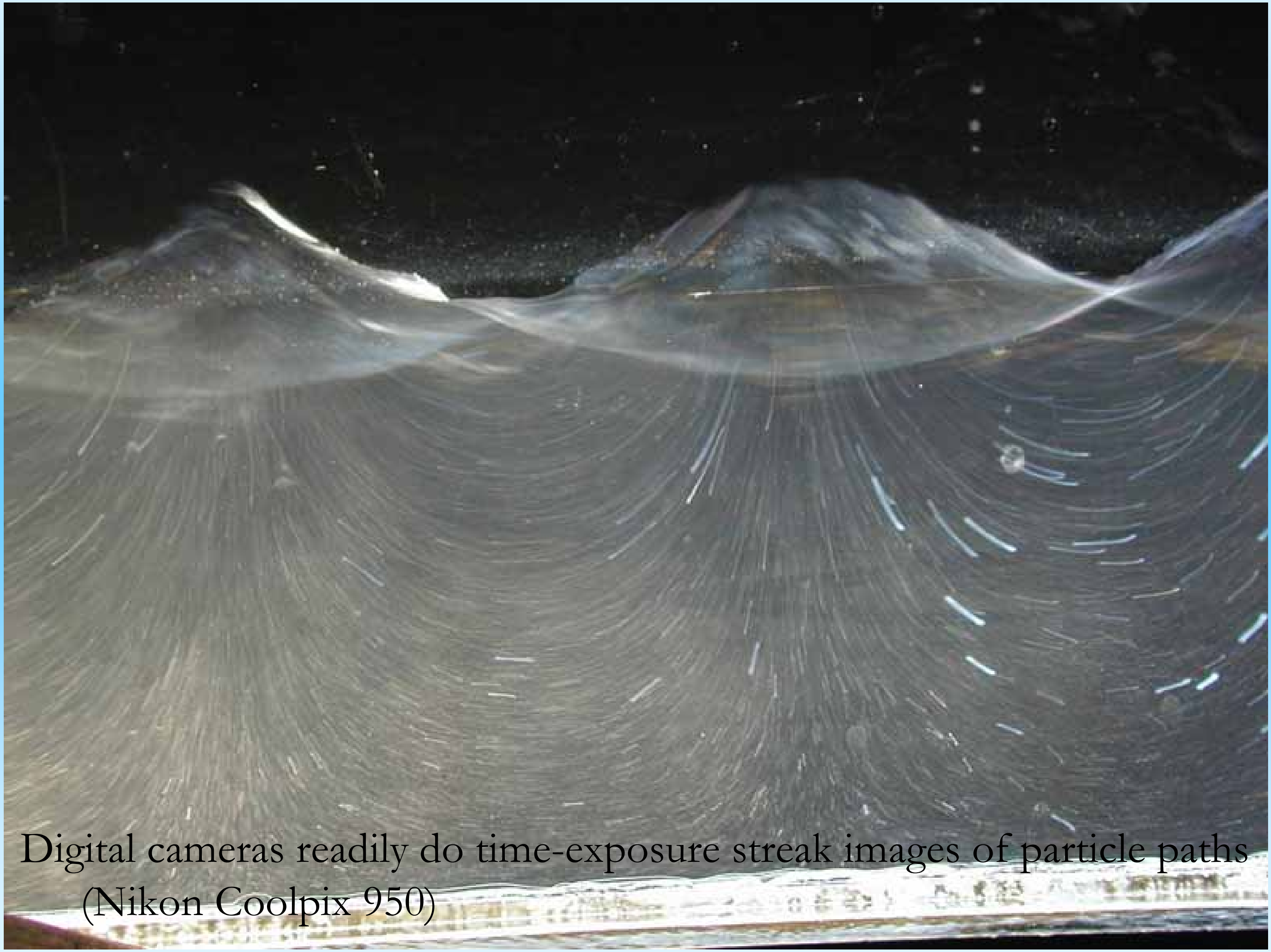

Digital cameras readily do time-exposure streak images of particle paths (Nikon Coolpix 950)

group velocity theory: stationary phase integral

Moiré patterns and group velocity

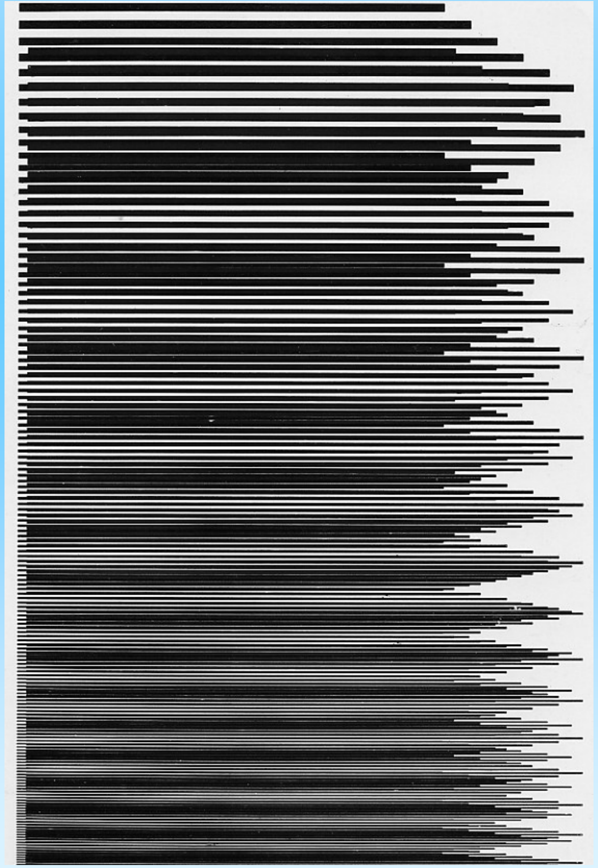

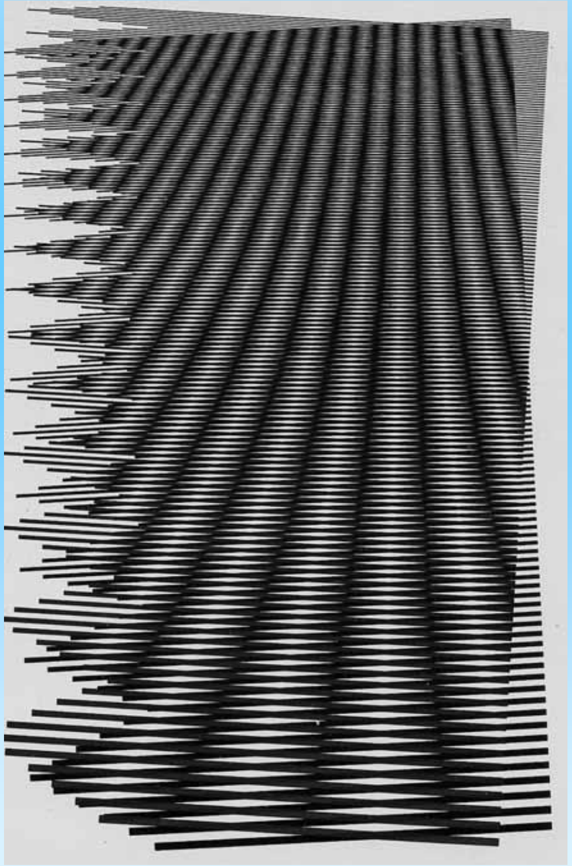

In very shallow water, undular bores occur with both gravity- and capillary nature (backward and forward of the bore front, respectively); here in a 5m channel.

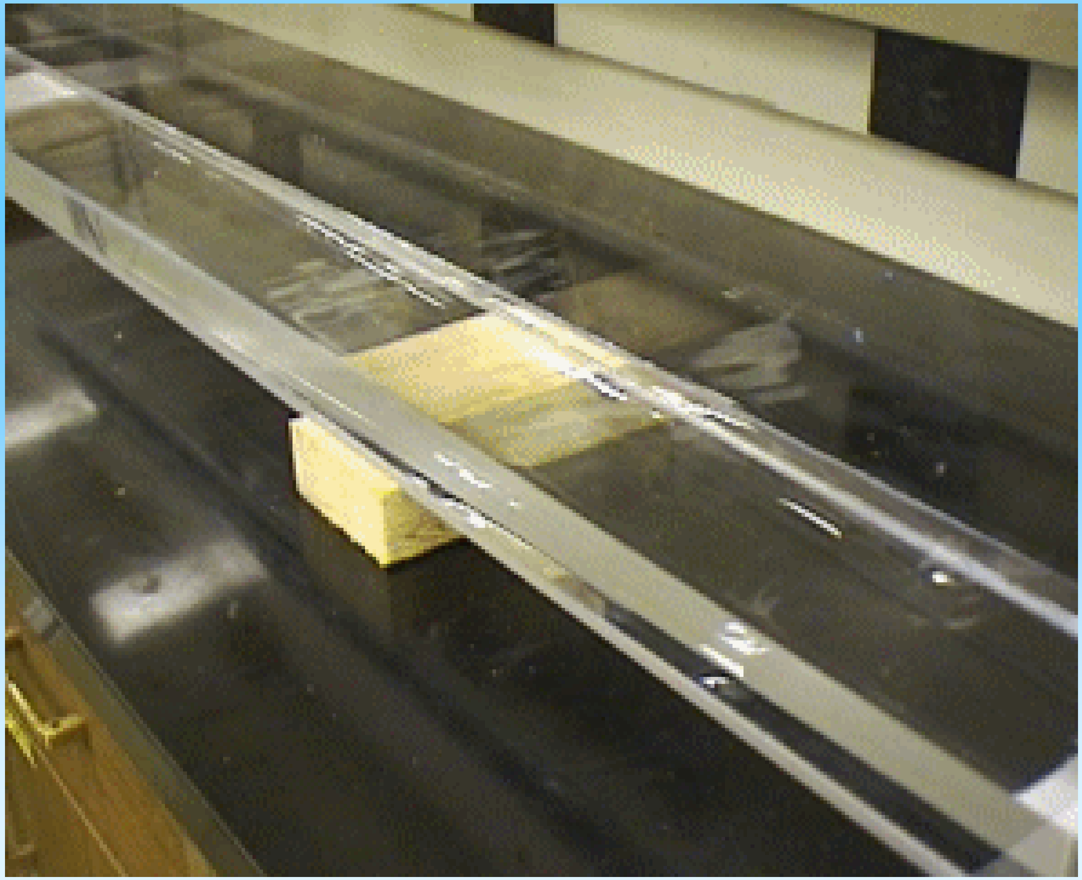

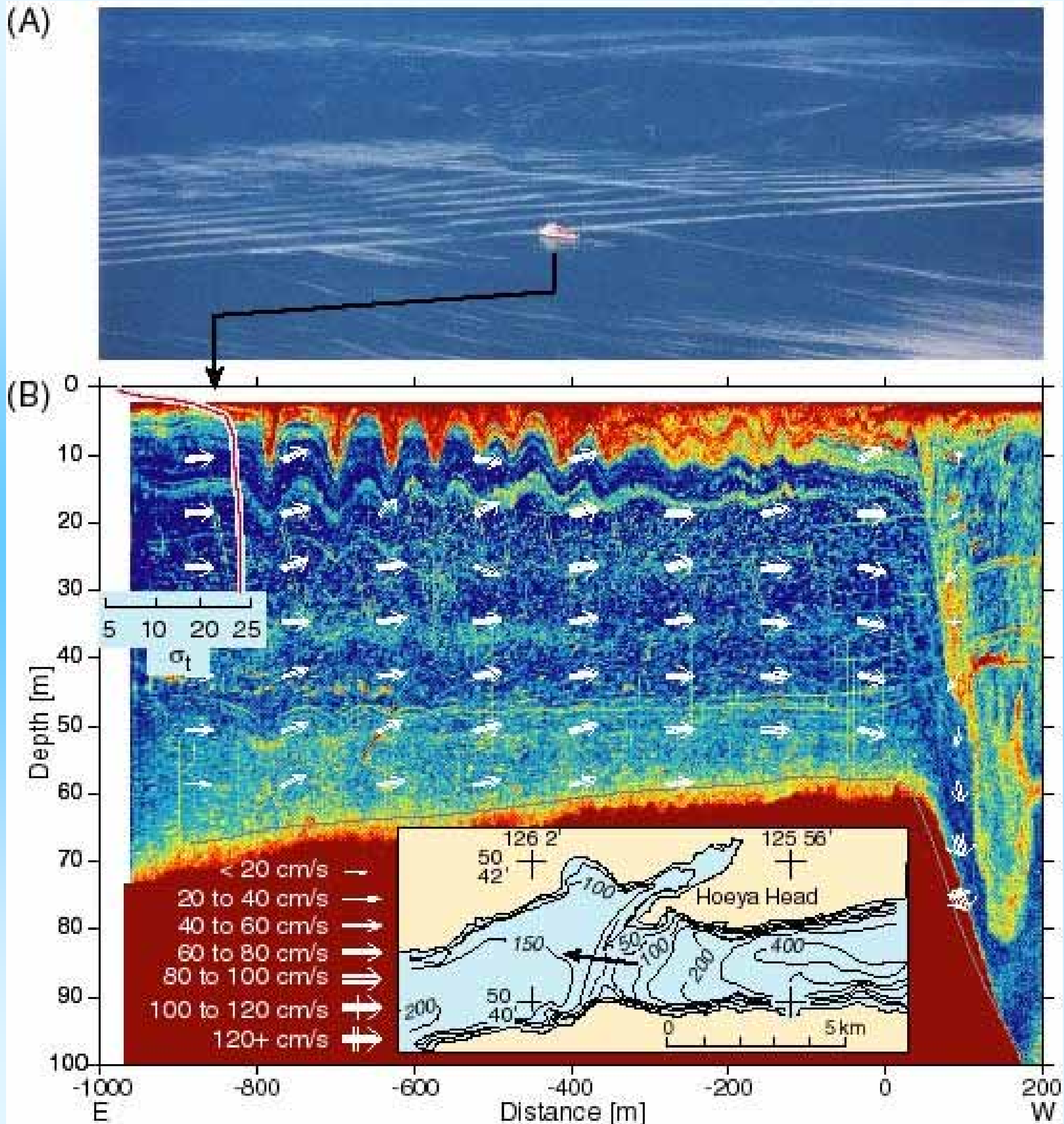
(A)
(B)
Depth [m]
Distance [m]
E
W
-1000
-800
-600
-400
-200
0
200
0
10
20
30
40
50
60
70
80
90
100
5 10 20 25
σ_t
< 20 cm/s
20 to 40 cm/s
40 to 60 cm/s
60 to 80 cm/s
80 to 100 cm/s
100 to 120 cm/s
120+ cm/s
126 2'
125 56'
50 42'
50 40'
Hoeya Head
100
150
50
100
200
400
200
0
5 km

The table rotation rate is oscillated about its mean value to excite waves, with a small mountain. Fast, long hydrostatic Kelvin waves ans short non-hydrostatic inertial waves. 1 m diameter cylinder, *GFD Lab Univ of Washington*

Kelvin waves, inertial waves in shallow rotating fluid

internal gravity waves: rays and modes

Jim Renwick, GFD lab Univ of Washington

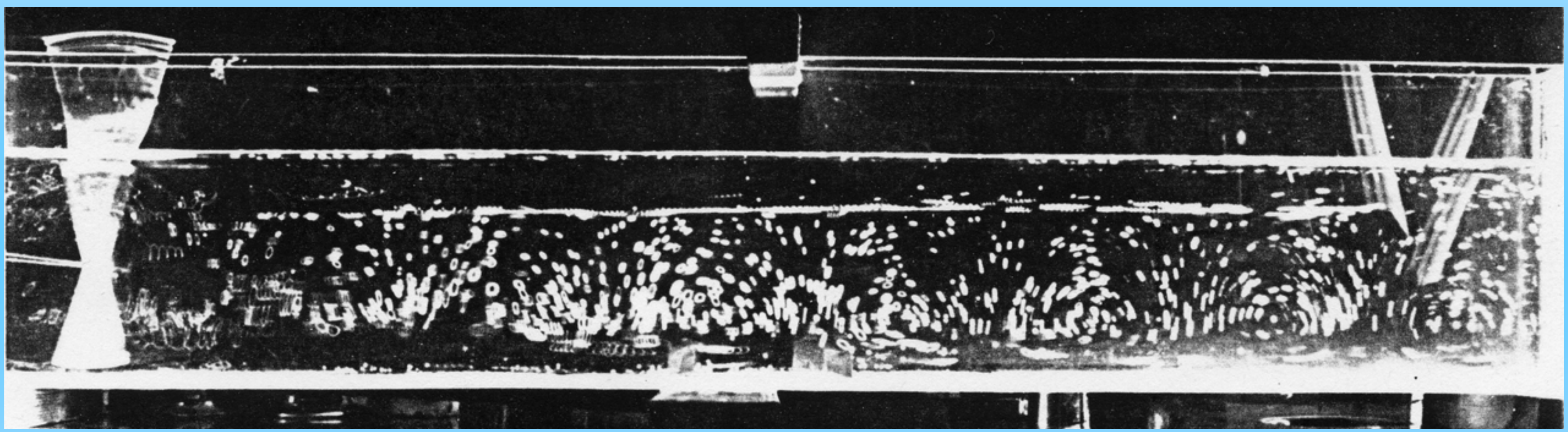

Waves: modes and rays and wave/mean-flow interaction at the base of the mixed layer

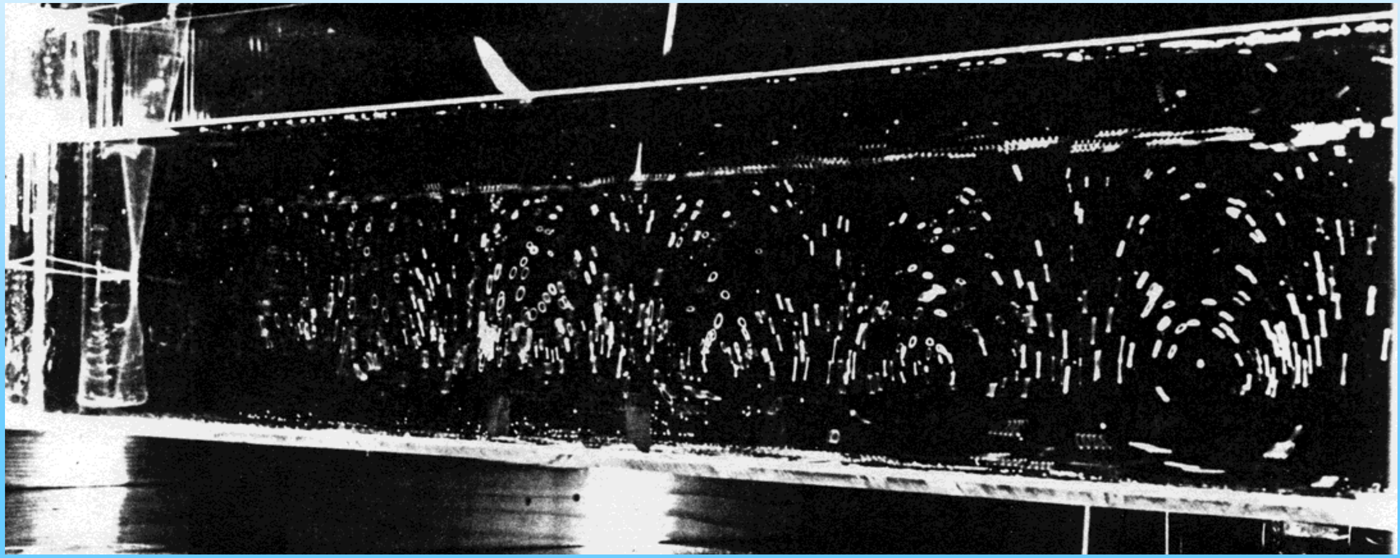

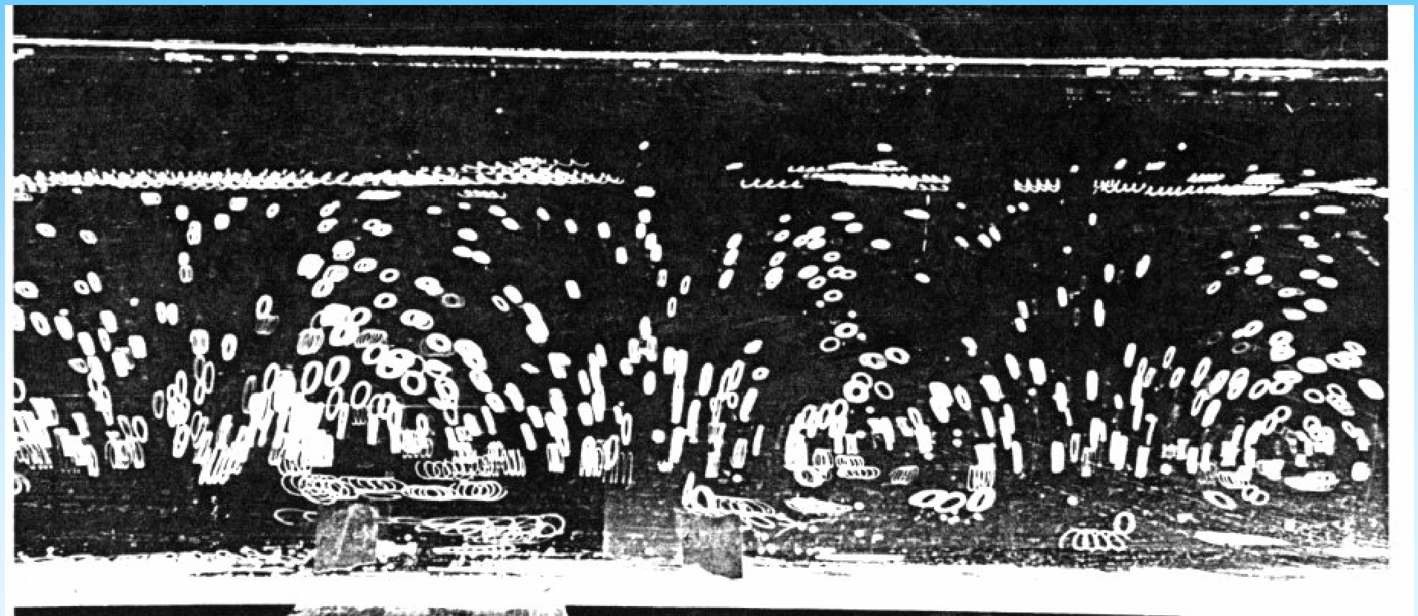

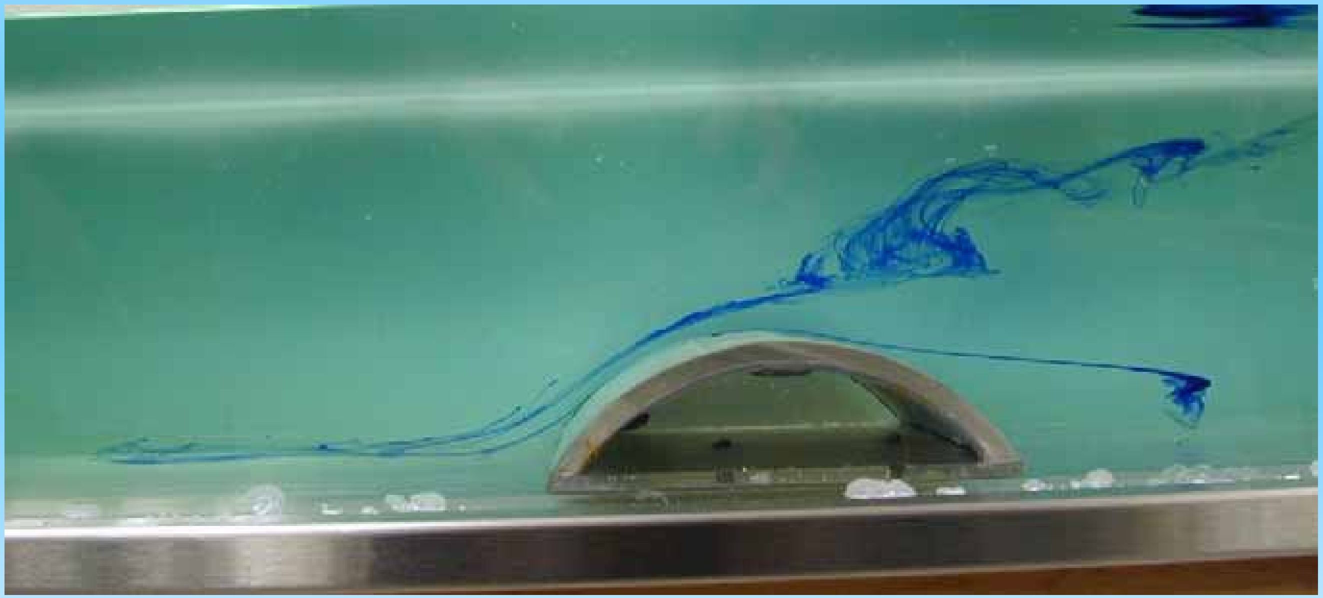

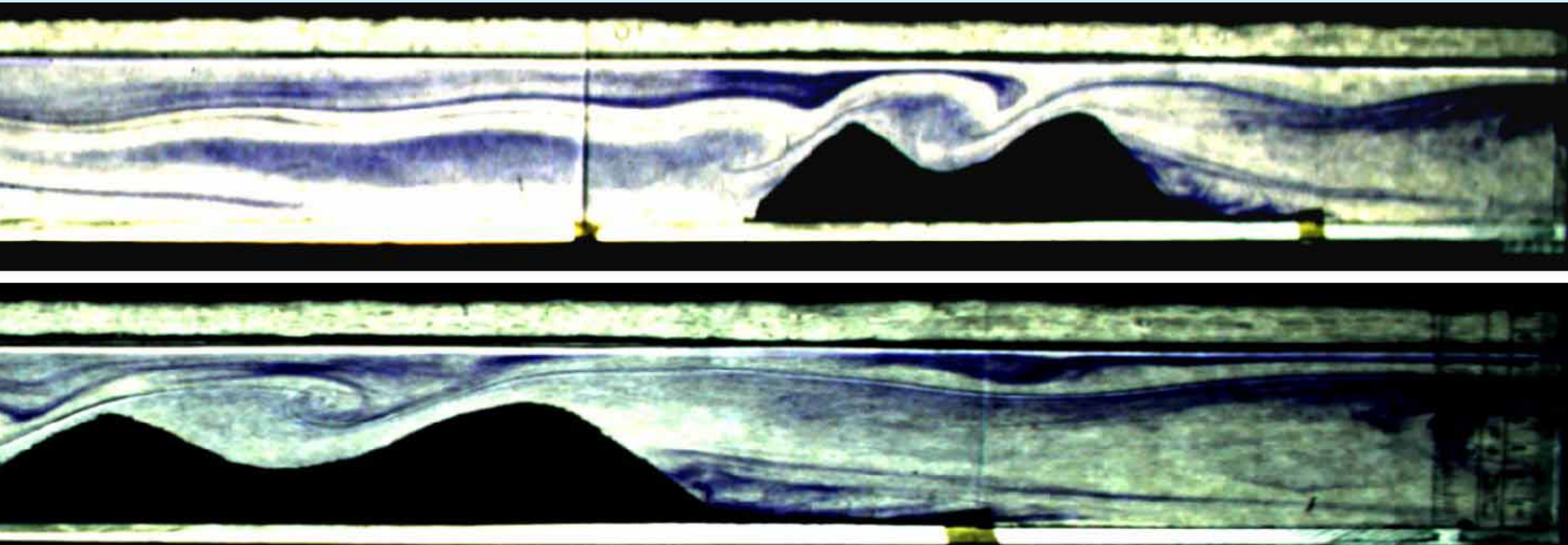

convection in a stratified fluid sends out gravity waves

internal gravity waves driven by oscillating 2 dimensional cylinder. Viewed with shadowgraph
Notice reflection at base of mixed layer

GFD Lab, Univ of Washington

oscillating cylinder

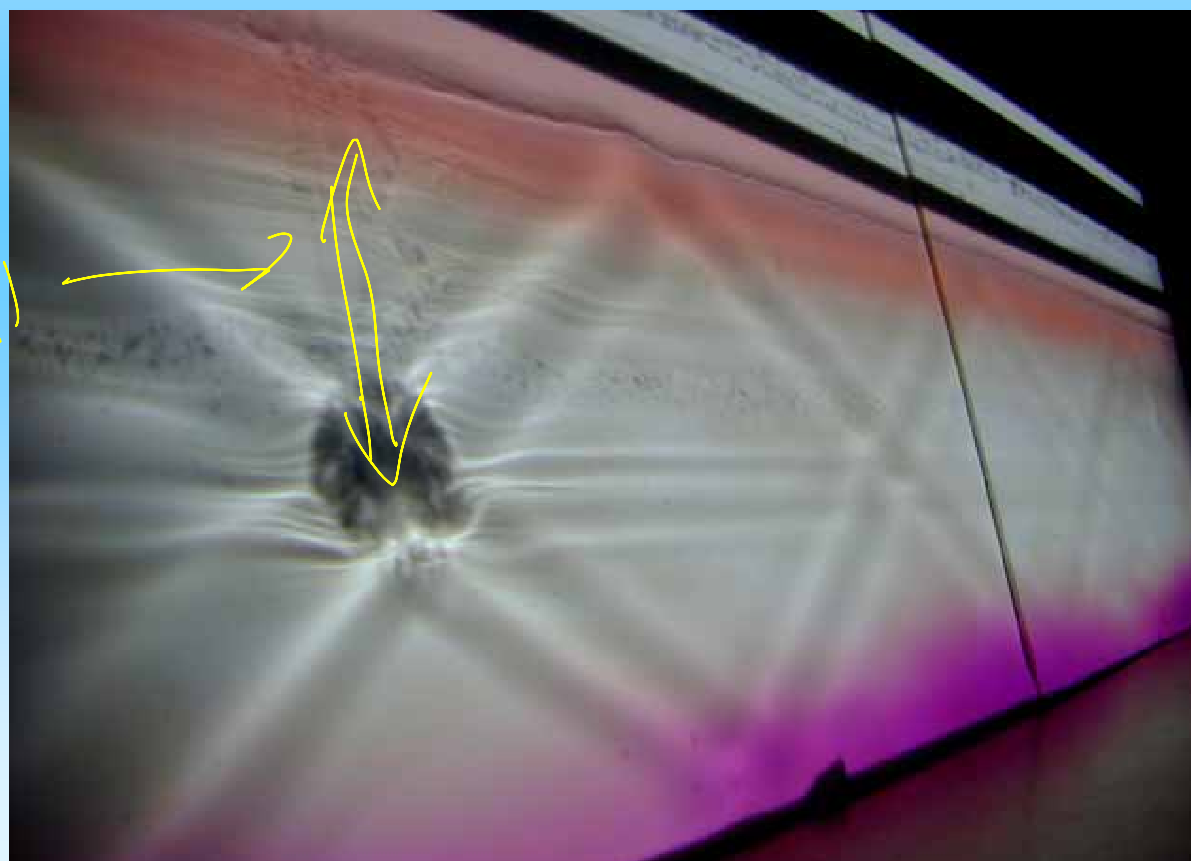

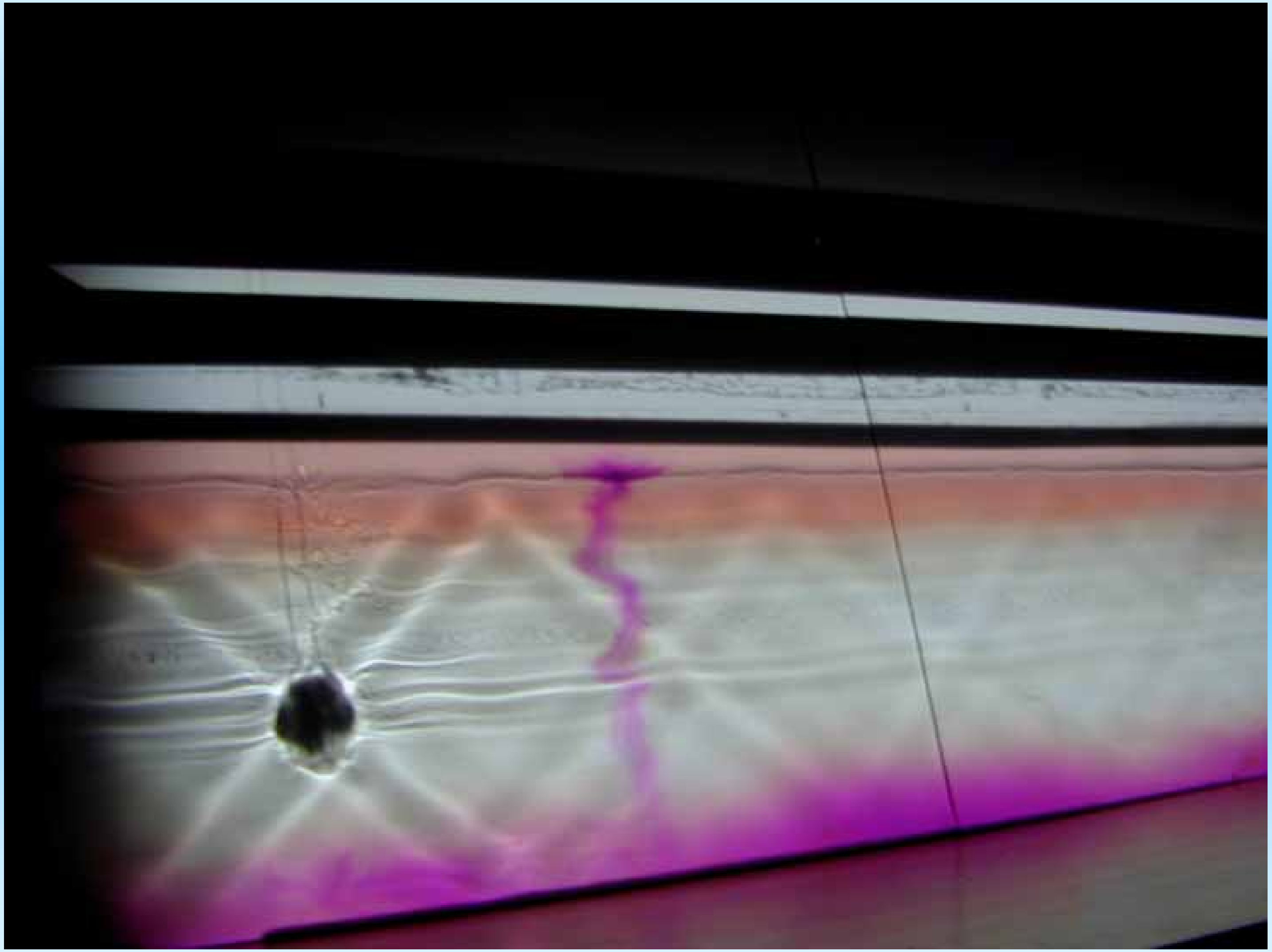

frequency close to N..some generation of harmonics and some turbulent mixing

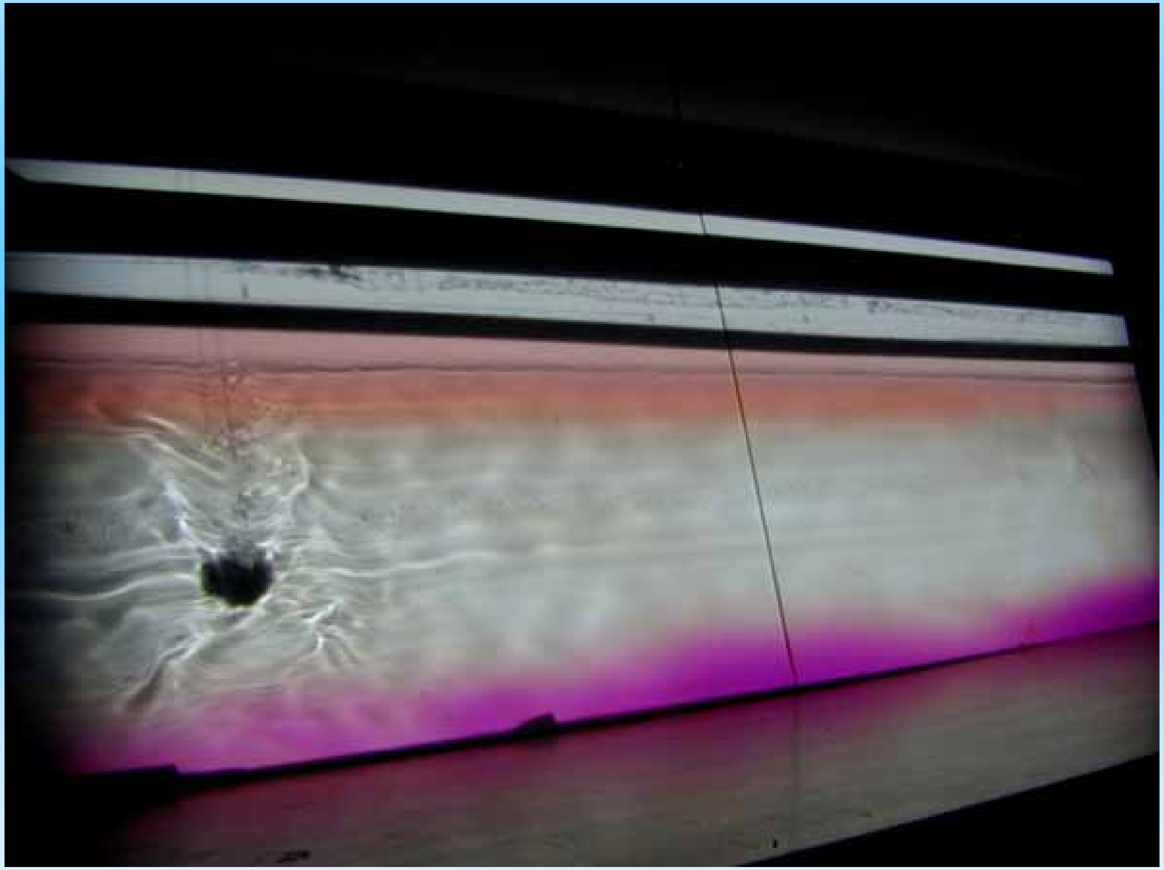

internal gravity waves: a circular cylinder moves to the right steadily, horizontally

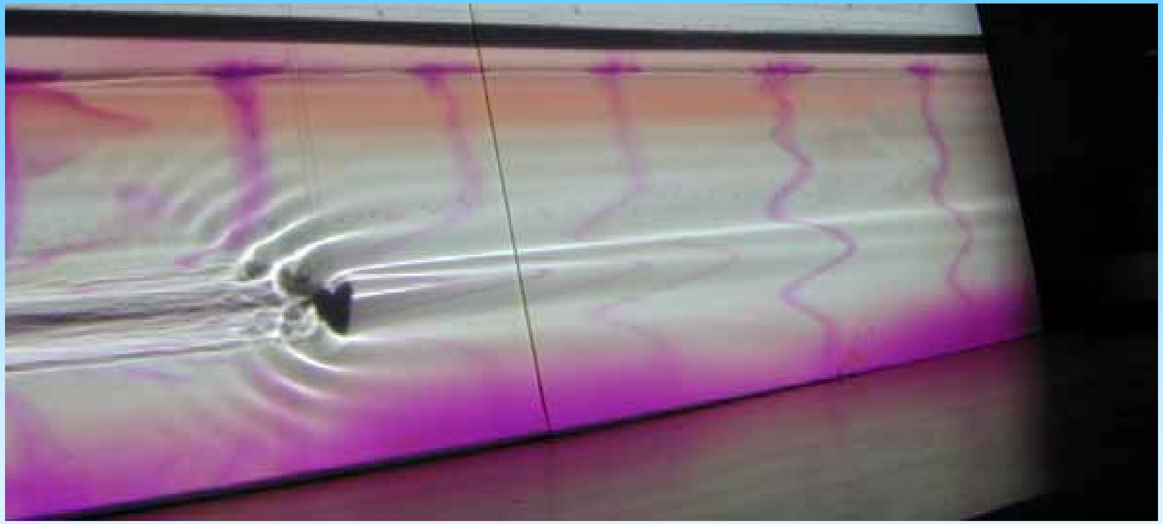

notice the fluid which is pushed ahead of the cylinder, with too little kinetic energy to rise against the stratification. In a reference frame moving with the 'mountain' this would be blocked fluid upstream of the mountain. It is transmitted by long, low frequency gravity waves, visible in previous slide

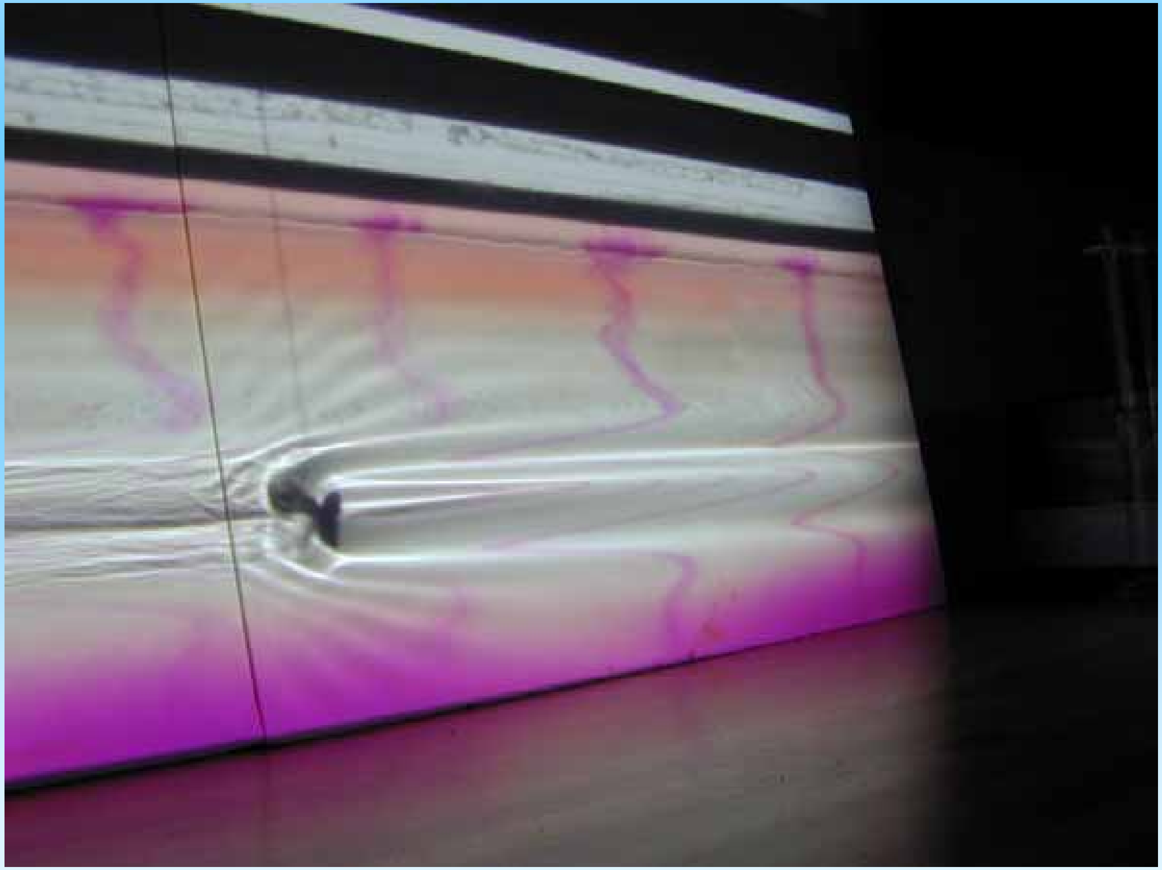

geostrophic adjustment in a cylinder with 2 –layer stratification. A ball of fluid is injected at the interface and allowed to 'slump' and spin. Shall we try this during the lecture?

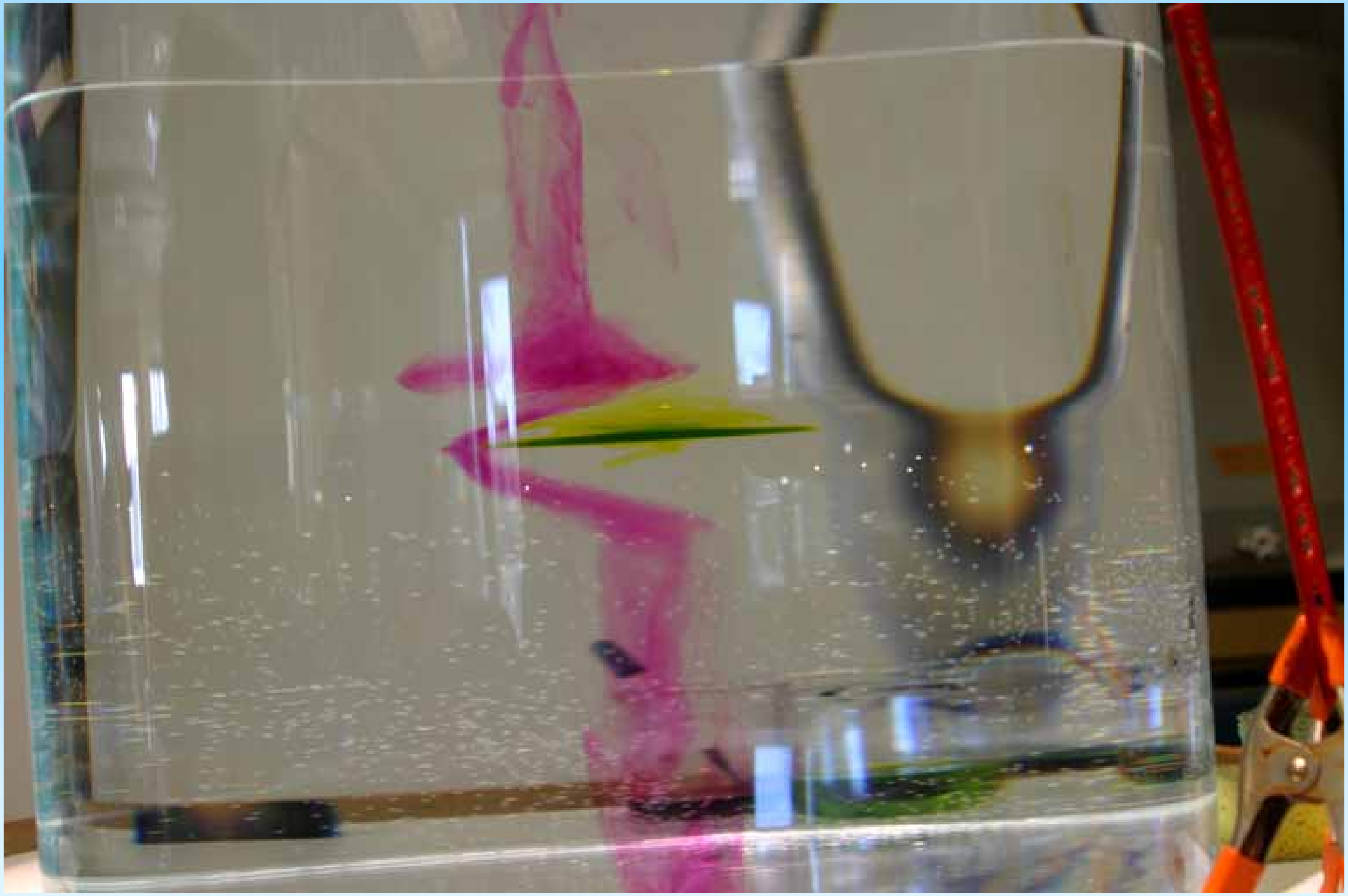

Rossby waves (barotropic mode) evolving in x and time (left); dispersion relation (right)

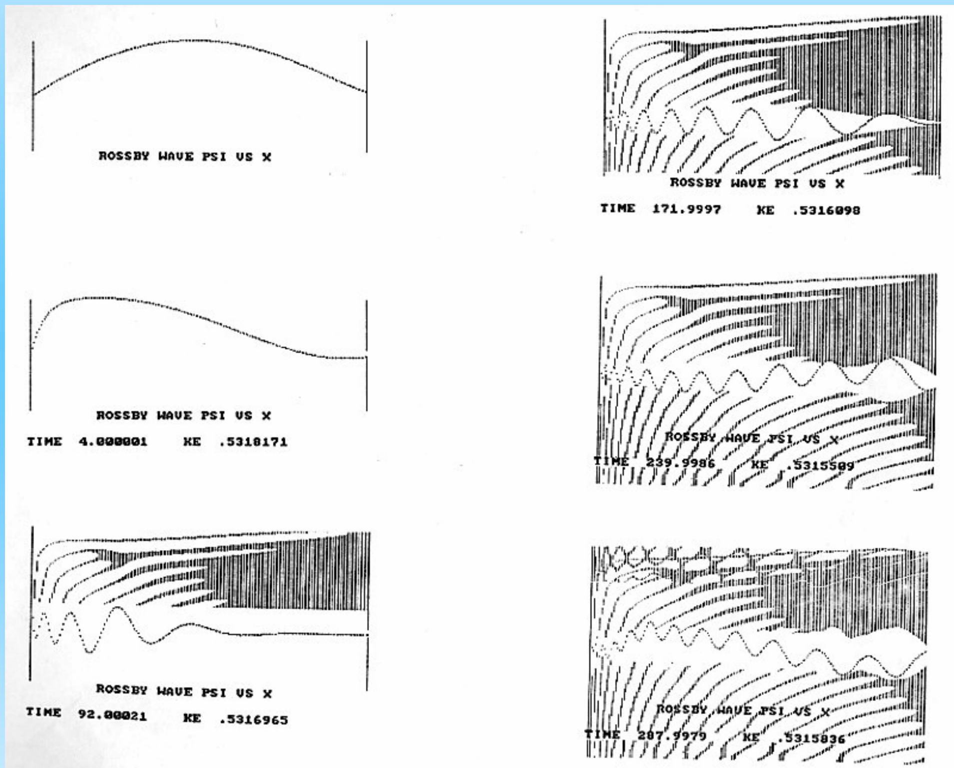

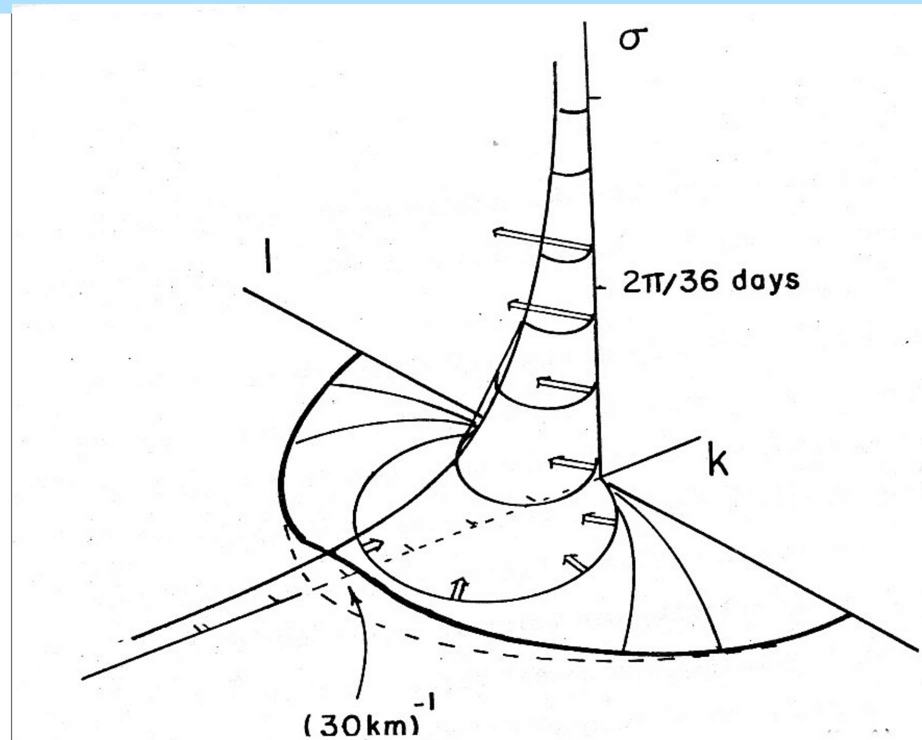

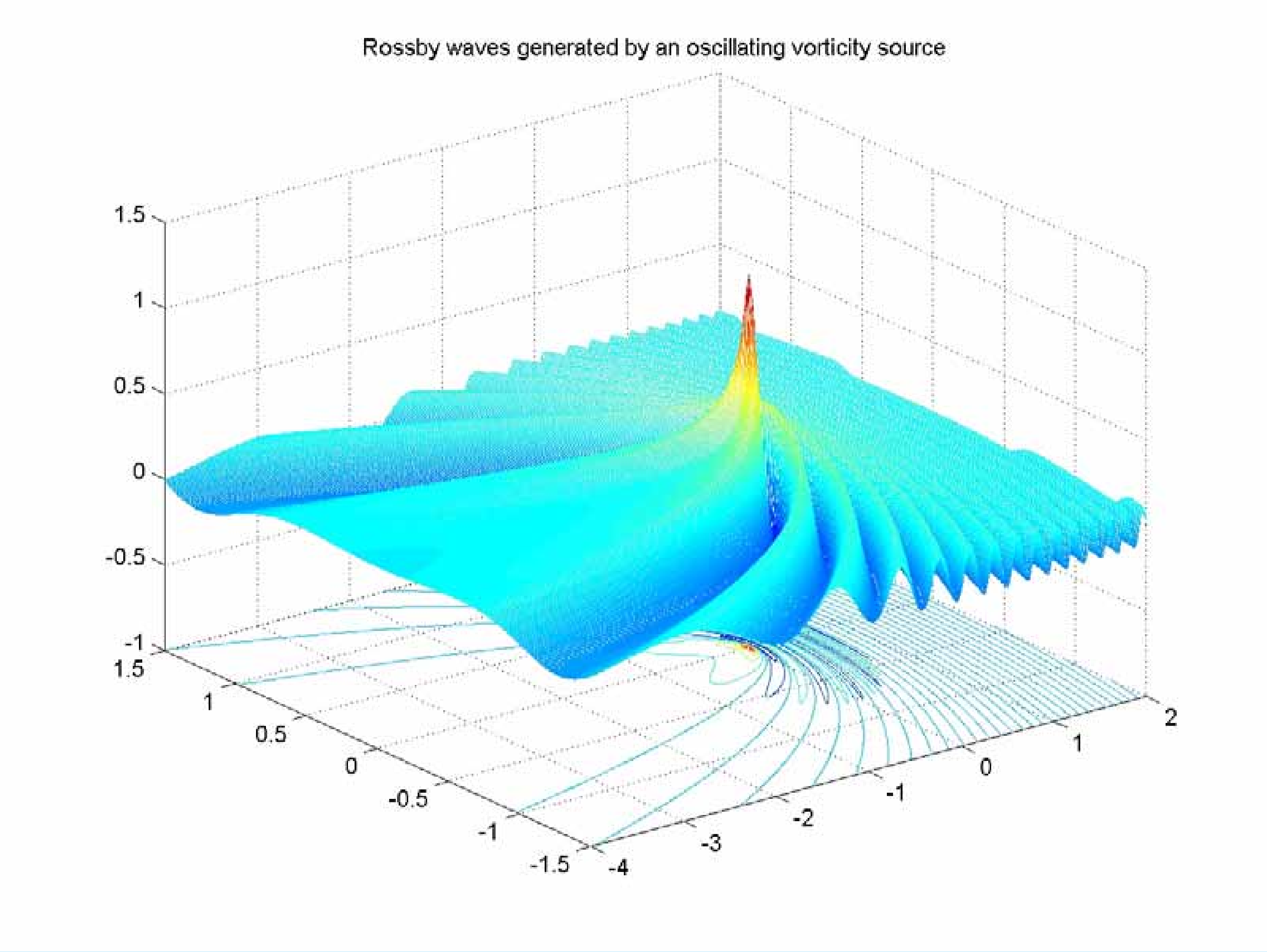
Rossby waves generated by an oscillating vorticity source
1.5
1
0.5
0
-0.5
-1
1.5
1
0.5
0
-0.5
-1
-1.5
-4
-3
-2
-1
0
1
2

Rossby wave Green function for an oscillating vorticity source at the origin: with free-surface divergence

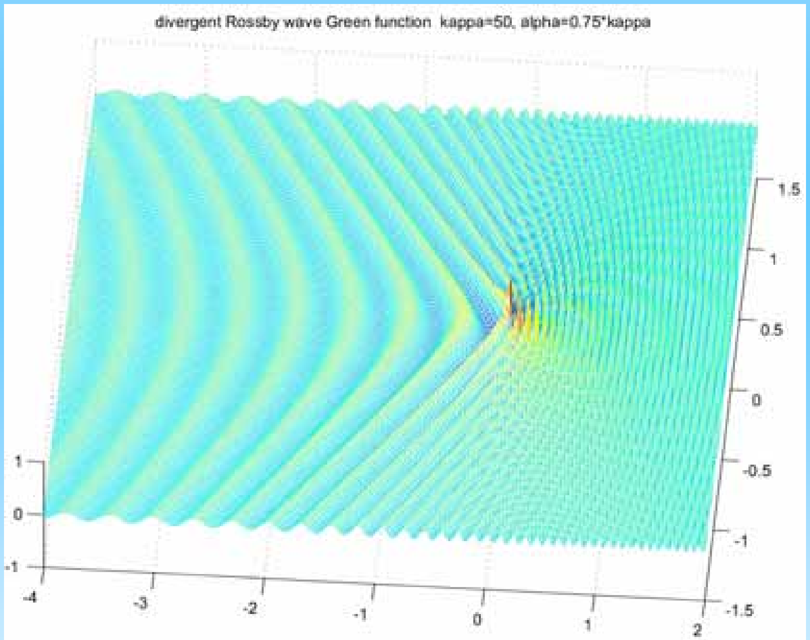

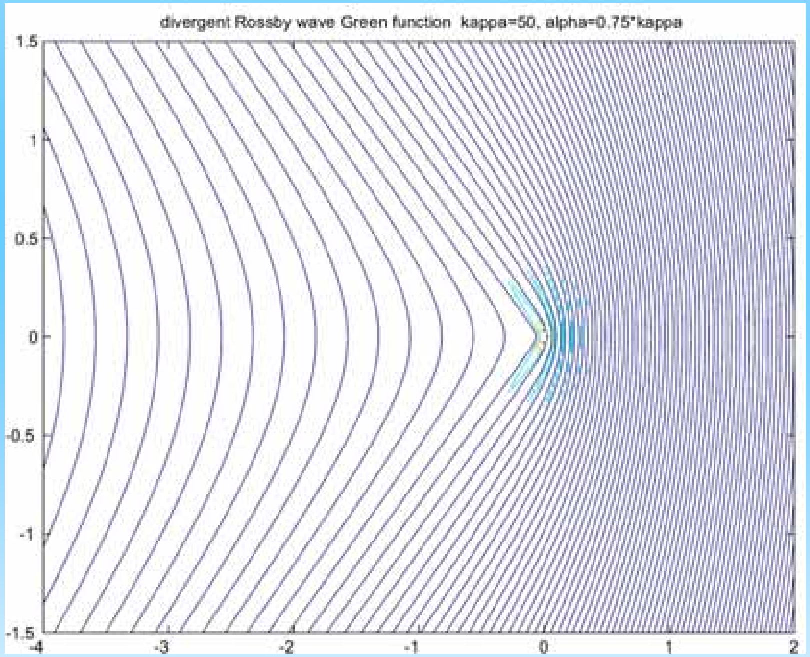

barotropic Rossby waves excited by uniform westerly (eastward) zonal flow past a cylindrical mountain (*McCartney JFM 1975)*

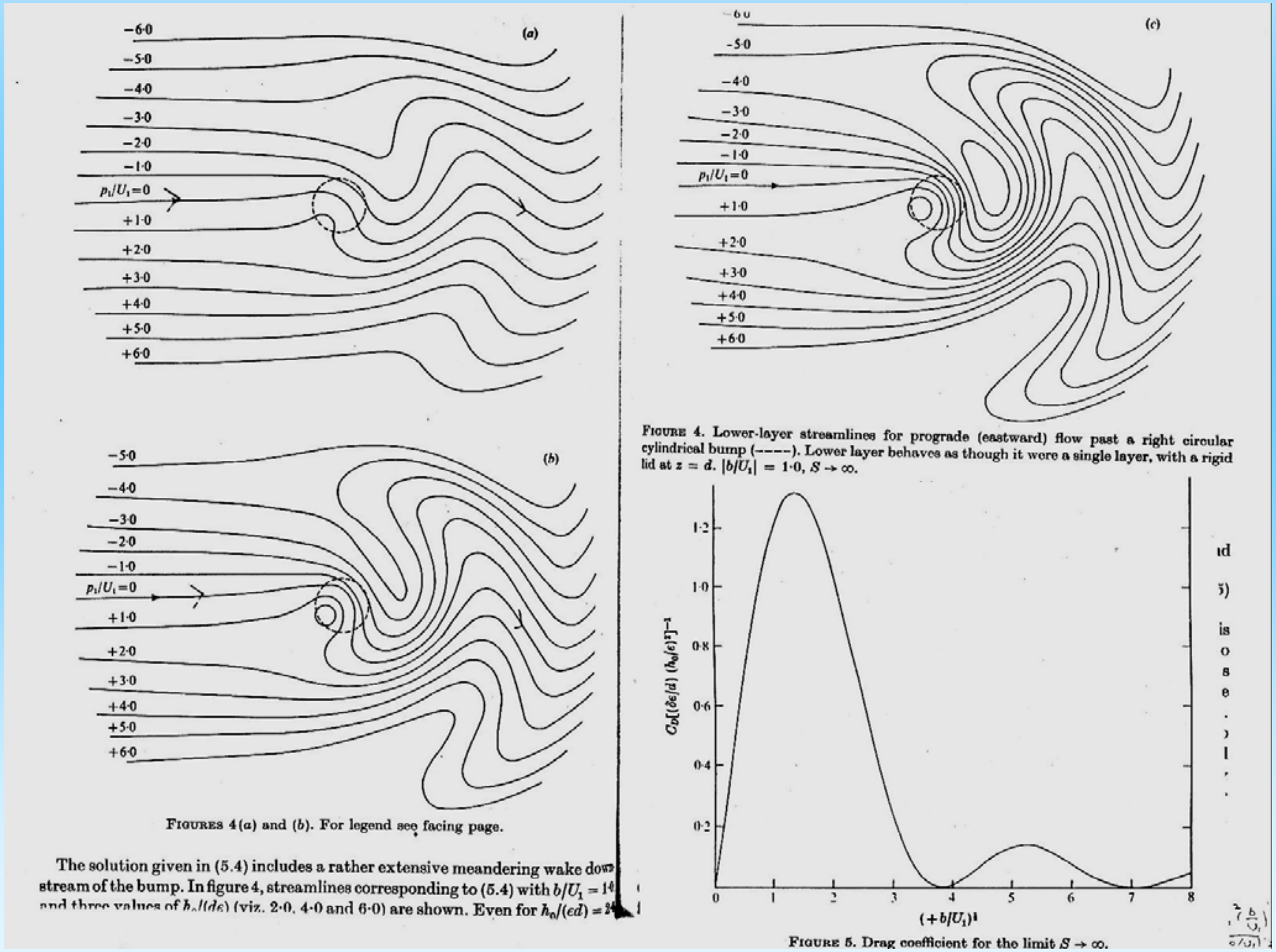

Subtropical gyre dynamics, thermo-dyanamics and biology

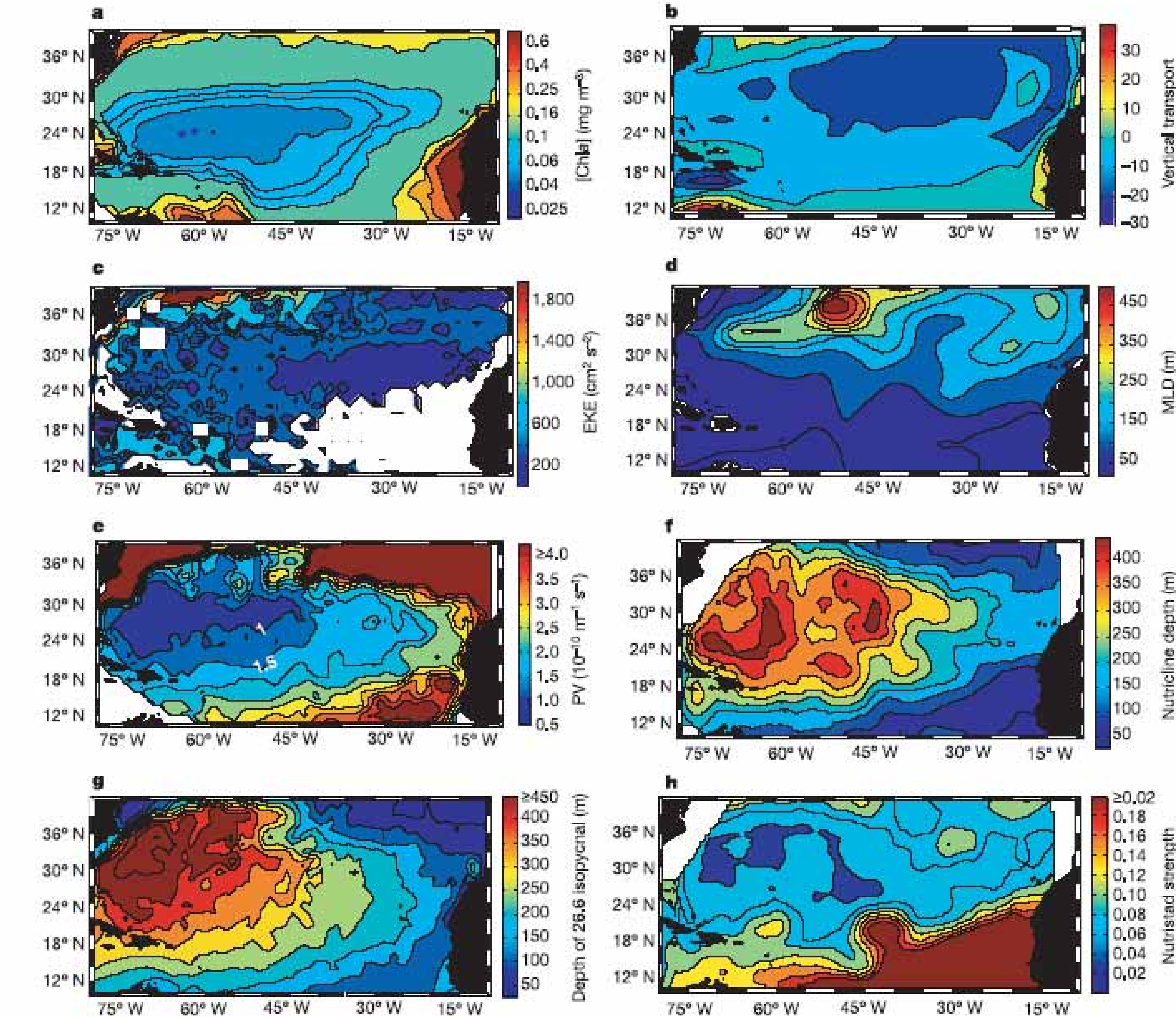

Figure 5 | Properties of the North Atlantic subtropical gyre. **a**, Annual mean SeaWiFS] chlorophyll *a* concentration, [Chl*a*], with a log scale for the colour axis; **b**, vertical transport calculated from the annual mean wind stress curl[25]; **c**, climatological mean eddy kinetic energy[20], EKE; **d**, climatological March mixed layer depth[26], MLD; **e**, potential vorticity on the 26.5 isopycnal, PV; **f**, nutricline depth, as defined by the depth maximum vertical nitrate gradient; **g**, depth of the 26.6 isopycnal, approximation for the base of the STMW; and **h**, the strength of the gradient at the nutricline, showing the wedge of STMW as a deplet nutristad.

Palter, Lozier & Barber Nature 2005

Williams, Follows, Migillicuddy Nature 1998

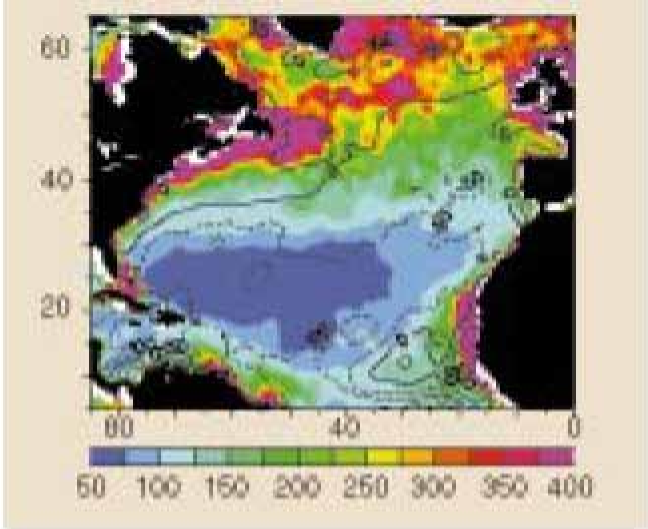

Figure 1 Annual primary productivity (coloured values in g C m^{-2} yr^{-1}), and upwards vertical velocity of water (contoured in m yr^{-1}) in the North Atlantic. Productivity reaches maximum values of 400 g C m^{-2} yr^{-1} where there are high levels of nutrient input from upwelling; and it has minimum values of 50 g C m^{-2} yr^{-1} within the subtropical gyre where there is downwelling (negative contours) and comparative nutrient depletion. Previous estimates of nutrient supply seem inadequate to account for even these low values, hence the proposal[1-3] that eddy circulation may be responsible for supplying them. (Figure derived from satellite estimates of surface chlorophyll from ref. 4, and calculations of vertical velocity at the base of the surface wind-forced boundary (Ekman) layer[6].)

Oschlies, Garcon Nature 1998

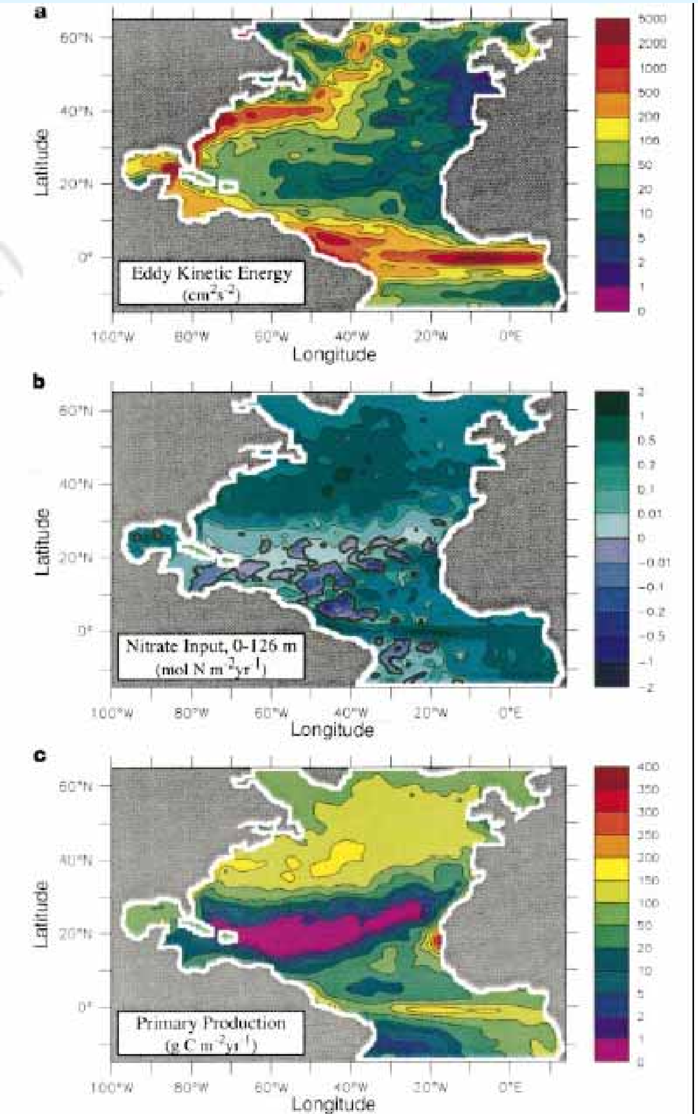

Figure 1 Results from the assimilation experiment A. **a**, Surface eddy kinetic energy (EKE), which contains all deviations from the annual mean, computed for a depth of 60 m to avoid contamination by shallow Ekman currents (in $cm^2 s^{-2}$). **b**, Annual mean nitrate flux into the upper 126 m, which is taken as proxy for the euphotic zone (in mol N m^{-2} yr^{-1}). **c**, Annual mean primary production (in g C m^{-2} yr^{-1}). A constant ratio of C:N=6.6 was assumed to give carbon fluxes from the model. This is a rather conservative assumption[27] and will give minimal estimates of carbon fluxes.

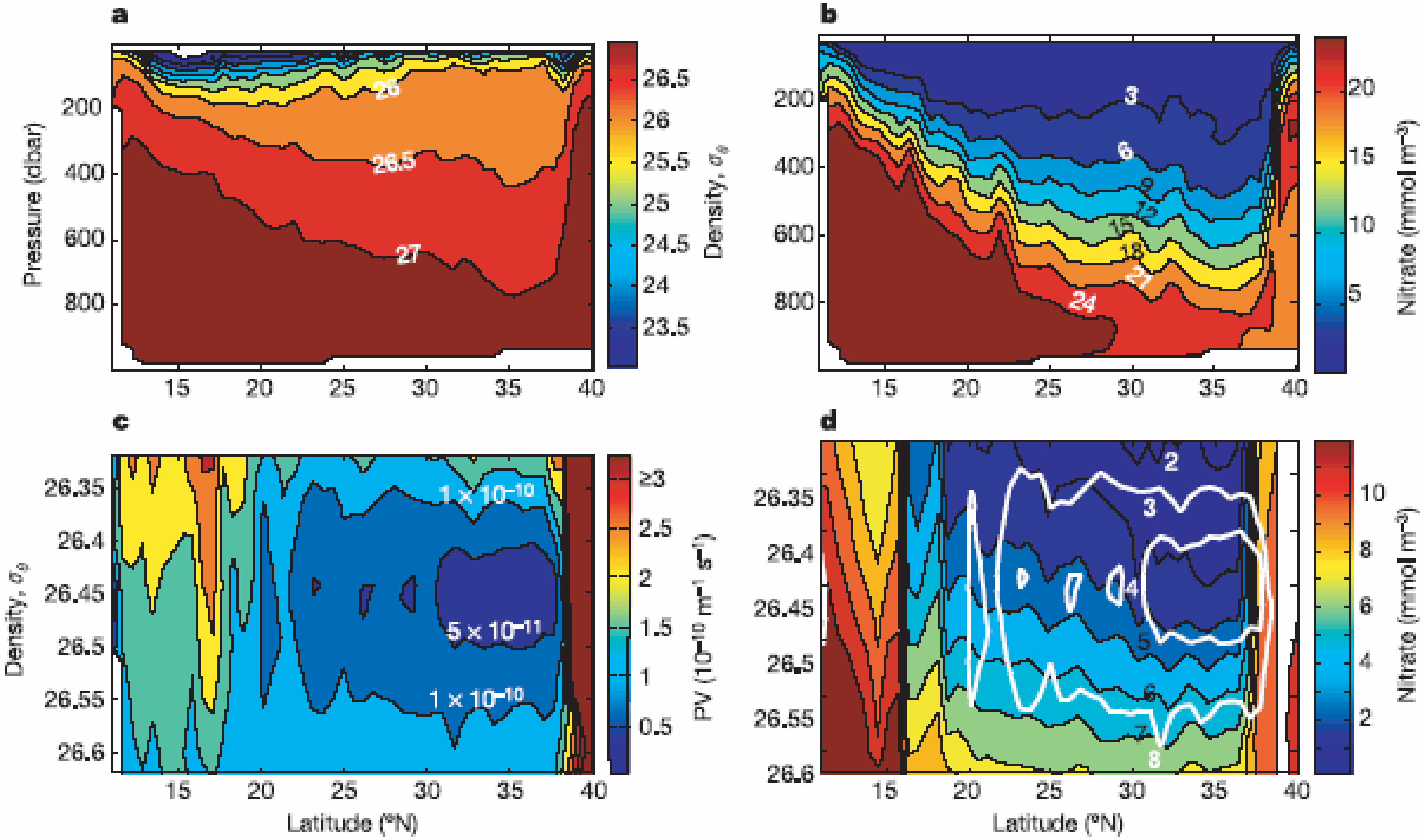

gure 3 | Properties of WOCE section A22 in August 1997. **a**, Potential nsity as a function of pressure. **b**, Nitrate as a function of pressure. Potential vorticity (PV) as a function of potential density; the low-PV aters ($\leq 1 \times 10^{-10}\ \mathrm{m^{-1}\ s^{-1}}$, shaded blue) are considered the core of the STMW. **d**, Nitrate as a function of potential density. The white contour lines in **d** represent PV $= -0.5 \times 10^{-10}$ and $-1 \times 10^{-10}\ \mathrm{m^{-1}\ s^{-1}}$. PV was calculated using $f/\sigma_o\ (\partial\sigma_\theta/\partial z)$, where f is the Coriolis parameter, σ_o the reference density, and $\partial\sigma_\theta/\partial z$ the vertical density gradient.

TABLE OF CONTENTS

- Polar amplification of the two 20^{th} C warming events
- Storms and weather….ocean to stratosphere: continuity of the Atlantic storm track/Icelandic Low from subtropics to high Arctic
- Atmospheric and oceanic transports, strongly coupled, supply continental and polar warmth, fresh water
- The oceanic heat source: northward heat transport essential to wintertime driving of scales of atmospheric circulation,
- Transports by ocean circulation: connecting the Arctic and Atlantic
  – Erika Dan, 60^0N winter in the N Atlantic: deep, shallow and shelf water masses
  – Atlantic – Arctic exchange: Θ-S-transport (~heat, fresh-water transport) diagrams
  – Rapid and slow modes of response of Atlantic overturning: Labrador Sea vs. Nordic Sea overflows
  – What matters to the global overturning circulation:
    - The freshwater cap and its movement: liquid and solid
    - Layering of deep-ocean water masses, and its representation in models
    - Shallow continental shelves and communication with the deep ocean
- Arrays and instruments: establishing the baseline and sustaining it in time

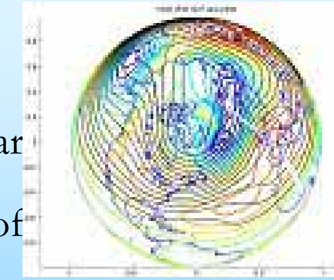

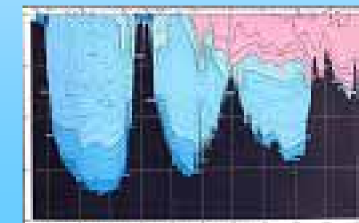

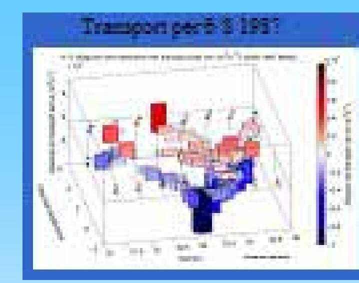

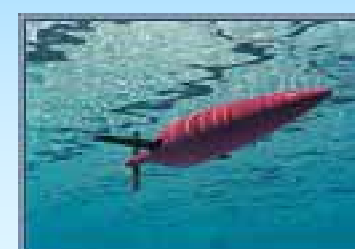

Global surface temperature has seen two major warmings in the 20th Century: in the 1920s-30s, when it was very concentrated around Greenland, and since the 1980s, when it is much more global, yet still concentrated in high northern latitudes.

Cod and herring fisheries responded to the much warmer ocean temperatures, which lasted for more than 25 years.

Ironically we anticipate the ocean circulation slowing during the current warming, whereas it is possible that an accelerated oceanic meridional overturning circulation was a factor in driving the 1920s warming.

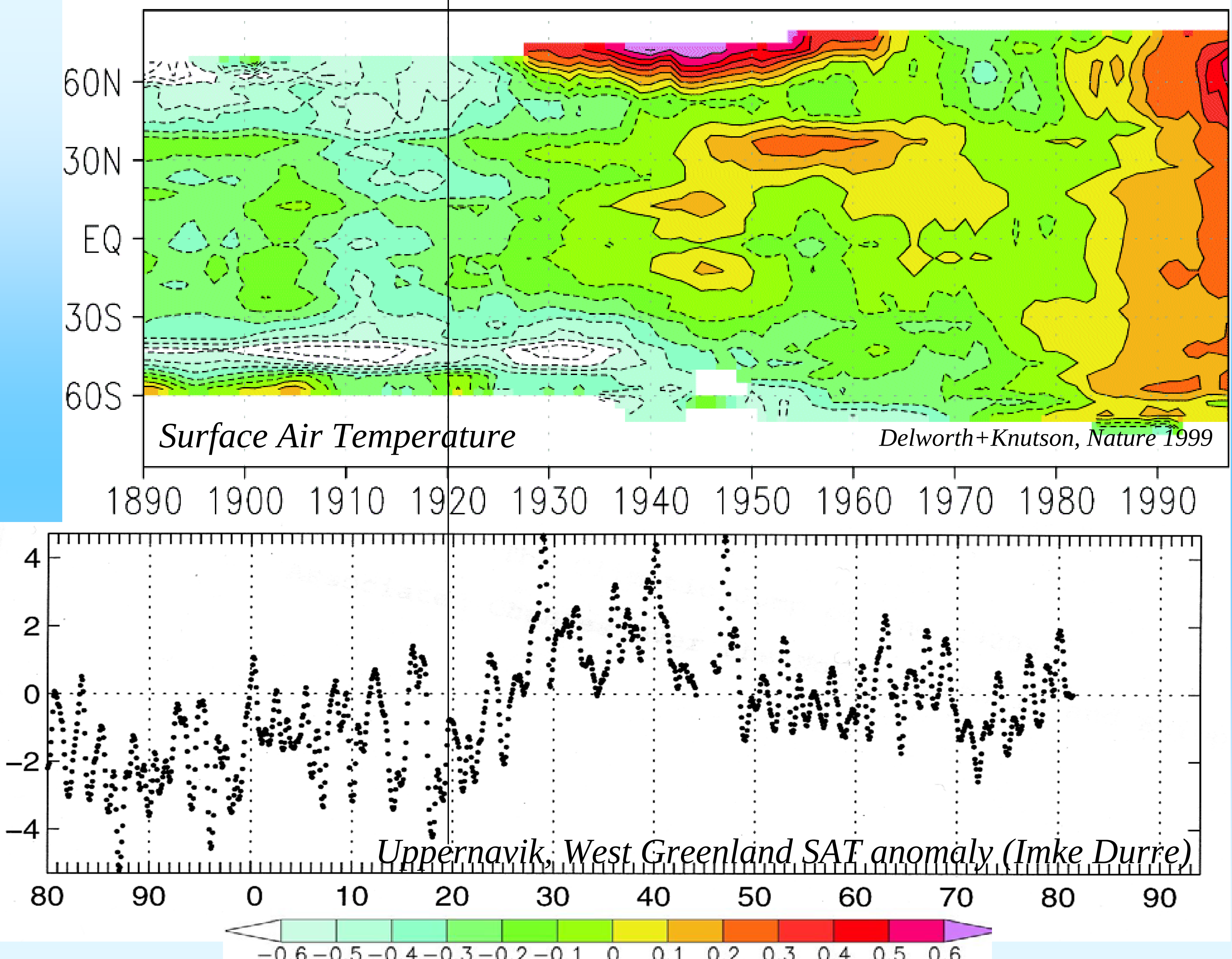
Surface Air Temperature
Delworth+Knutson, Nature 1999
60N
30N
EQ
30S
60S
1890 1900 1910 1920 1930 1940 1950 1960 1970 1980 1990
Uppernavik, West Greenland SAT anomaly (Imke Durre)
4
2
0
−2
−4
80 90 0 10 20 30 40 50 60 70 80 90
−0.6 −0.5 −0.4 −0.3 −0.2 −0.1 0 0.1 0.2 0.3 0.4 0.5 0.6

The standing-wave structure with wintertime Icelandic and Aleutian Lows gives the atmosphere some of the east-west structure and gyre circulation familiar to the ocean. The rapid radiative cooling in fall sets up a cold dome which slumps under gravity, tending to create a surface polar vortex which is anticyclonic, the convergence overhead strengthening the polar cylonic vortex…yet mountains and vertical momentum transport can intervene, opposing the surface high.

In particular, the Atlantic storm-track forms a continuous connection between subtropics and the high Arctic.

Lau's JAS 1979 winter diabatic heating of the 700mb-1000mb lower atmosphere. Peak values are 100-150 watts/m^2 in the subtropical storm track regions

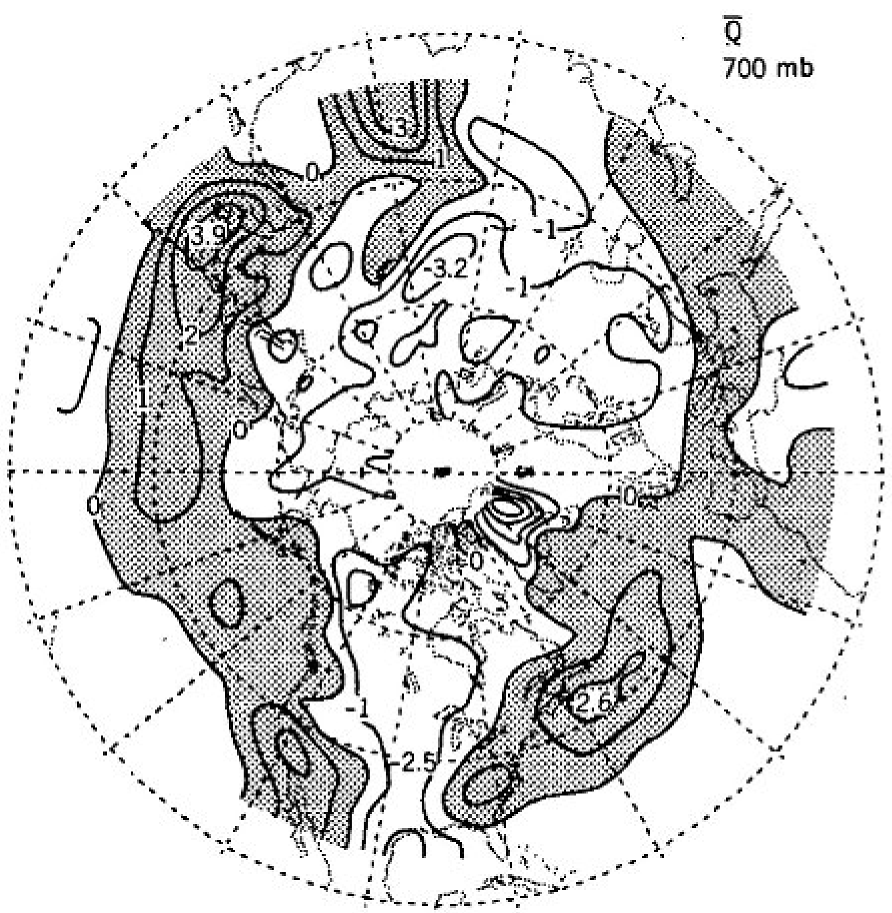

FIG. 21. Distribution of diabatic heating rate $\bar{Q}$ at 700 mb. Contour interval 1°C day^{-1}.

Held et al. (J.Clim.02) 100mb-1000mb diabatic heating for January

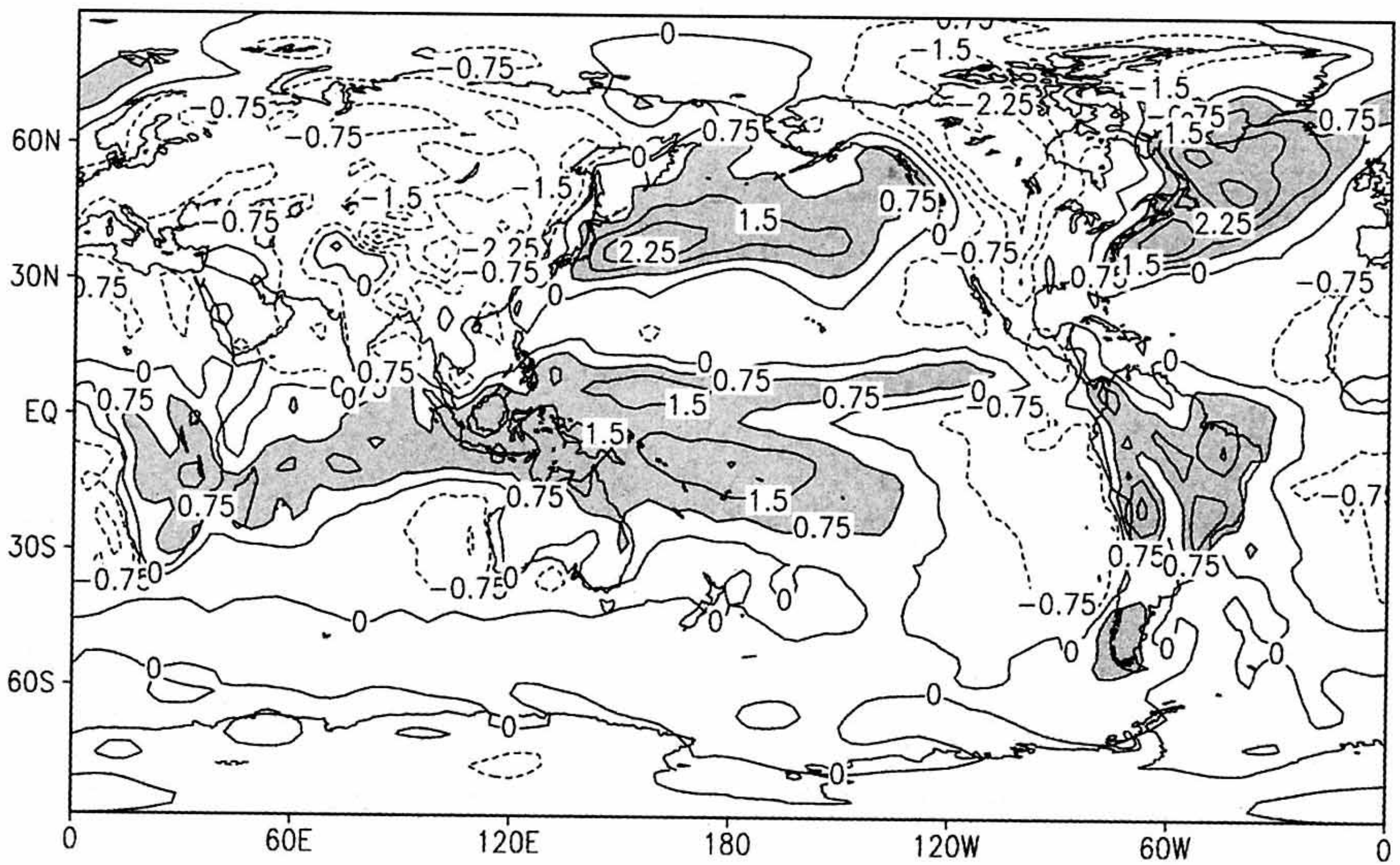

FIG. 8. The column-averaged diabatic heating field in Jan obtained from the NCEP–NCAR reanalysis as described in the appendix. The contour interval is 0.5 K day^{-1}.

Qnet, net atmosphere-ocean heat flux, watts/m^2 (Keith Tellus 95)
(annual average)

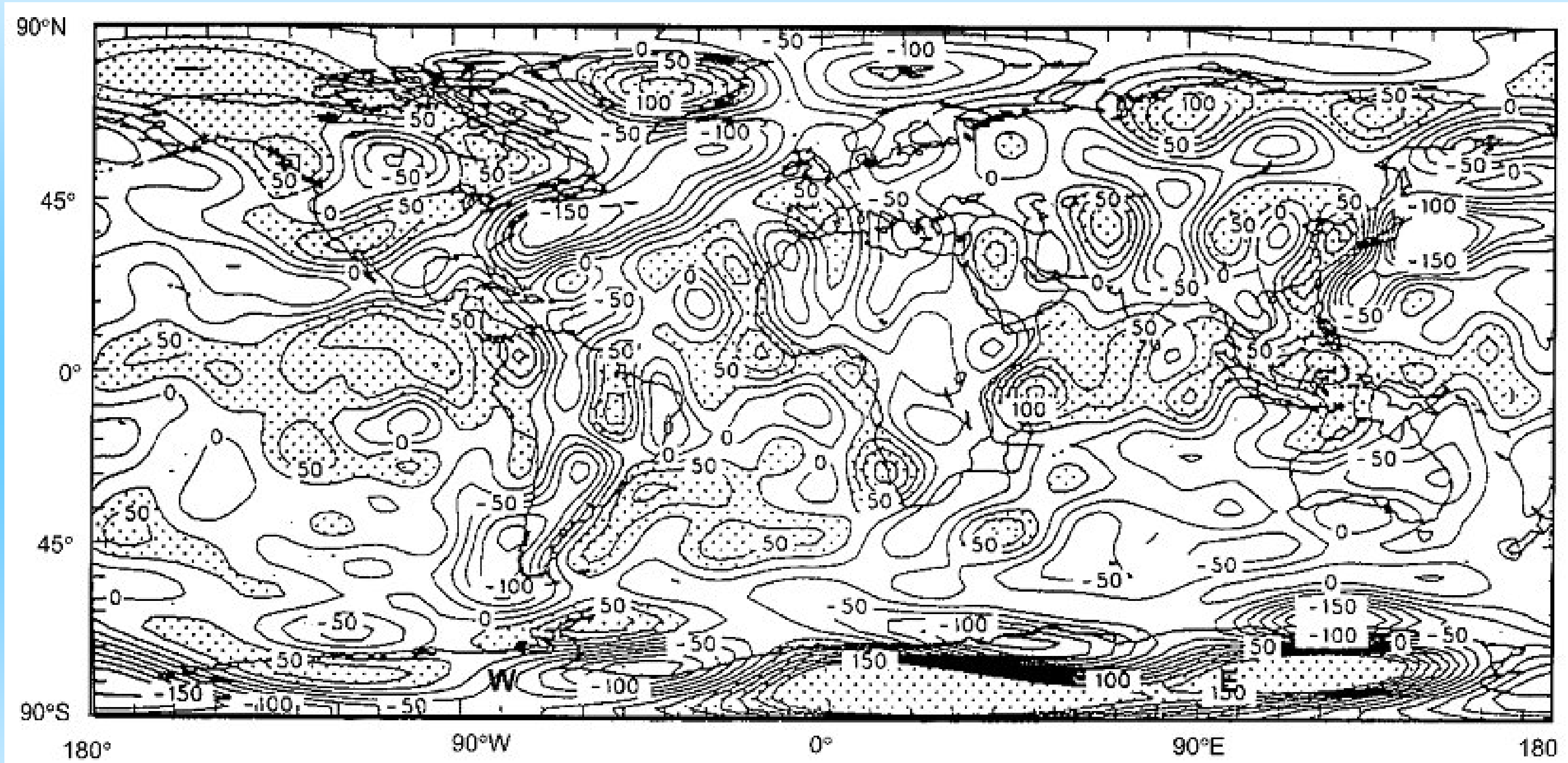

It should be noted that because the sun heats the ocean, O, but does not cool the atmosphere, A, the most useful maps of Qnet for A will differ those for O by the short-wave insolation.

(from *Thompson+Wallace J Clim 2000*)

30 year trend in advection of time-averaged
winter temperature (925-500 Hpa av.)
..anomalous velocity and advection, cooling the ocean while warming the land in both Atlantic and Pacific sectors. Could these oceanic advective heat sources be the root cause of this contribution to global warming over Eurasia?

$$U\partial T / \partial x$$

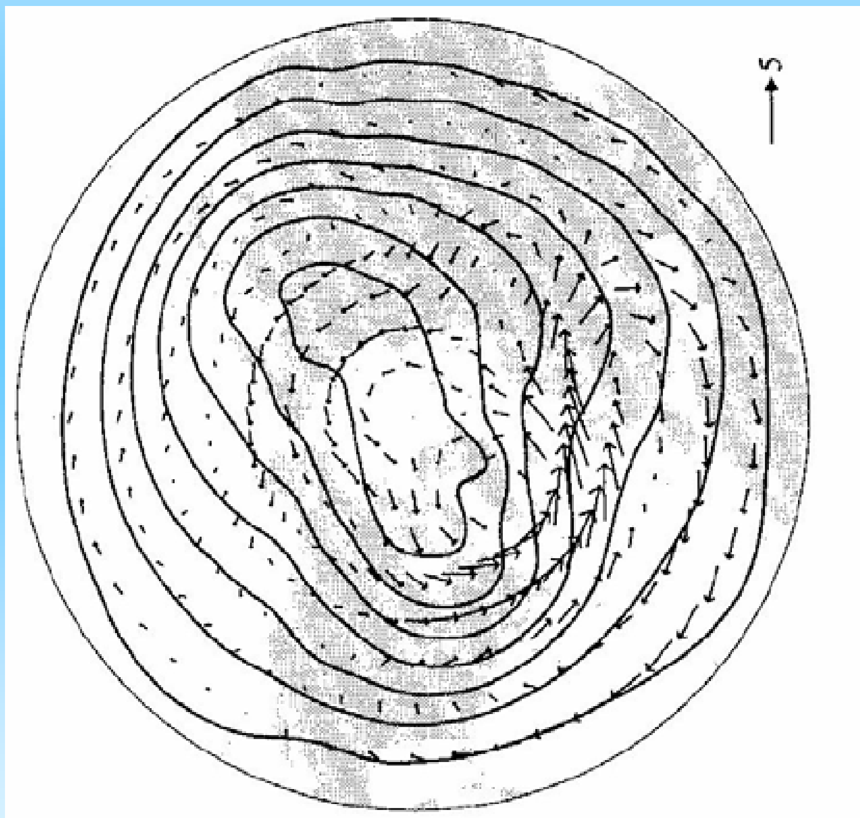

Hudson Strait salinity at 50m August 1965 (*J.Lazier)*
This is part of the only 3-dimensional hydrographic survey ever made of the Labrador/Irminger seas.

Cuny et al. 2003

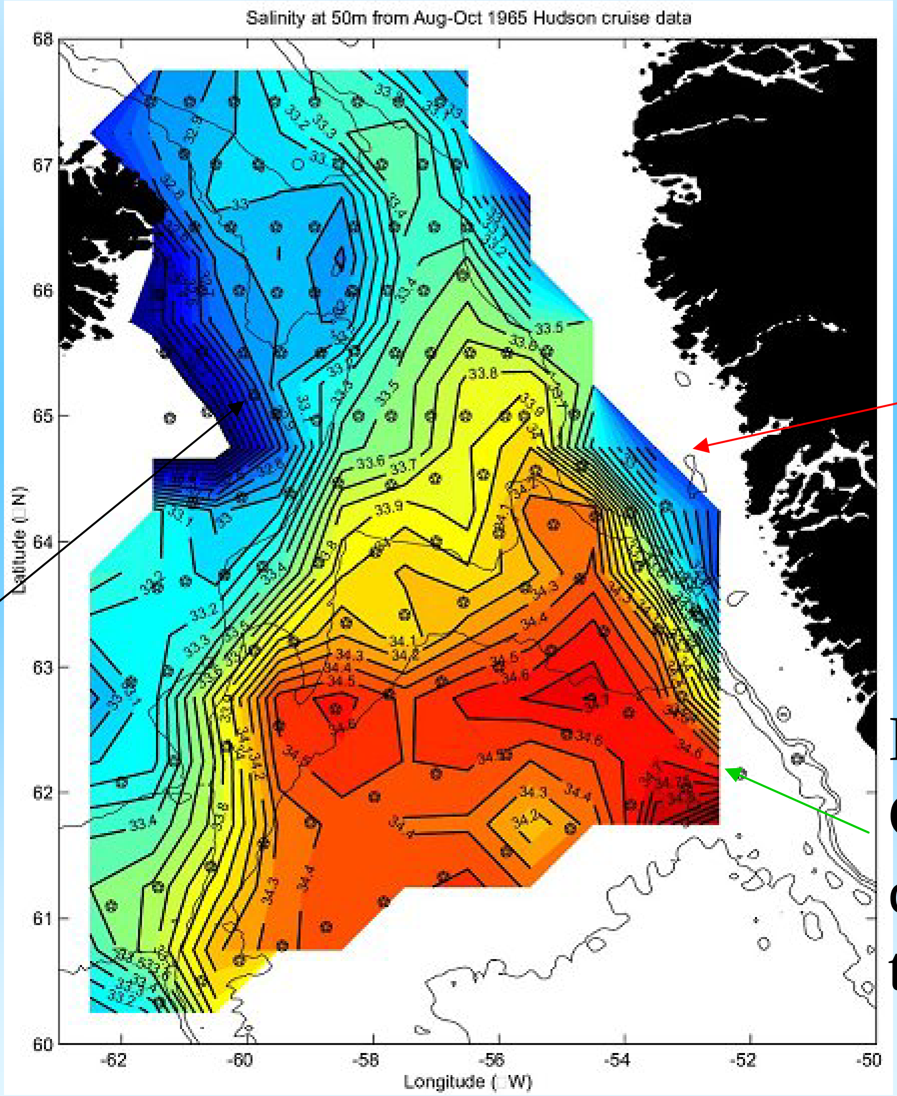

Southward moving low-salinity water from Baffin Bay

Northward moving Greenland shelf water

Irminger Current water circumnavigating the Labrador Sea

The solution? Instrument the Arctic Rim. Do ASOF.
Deploy the Eriksen Seaglider:

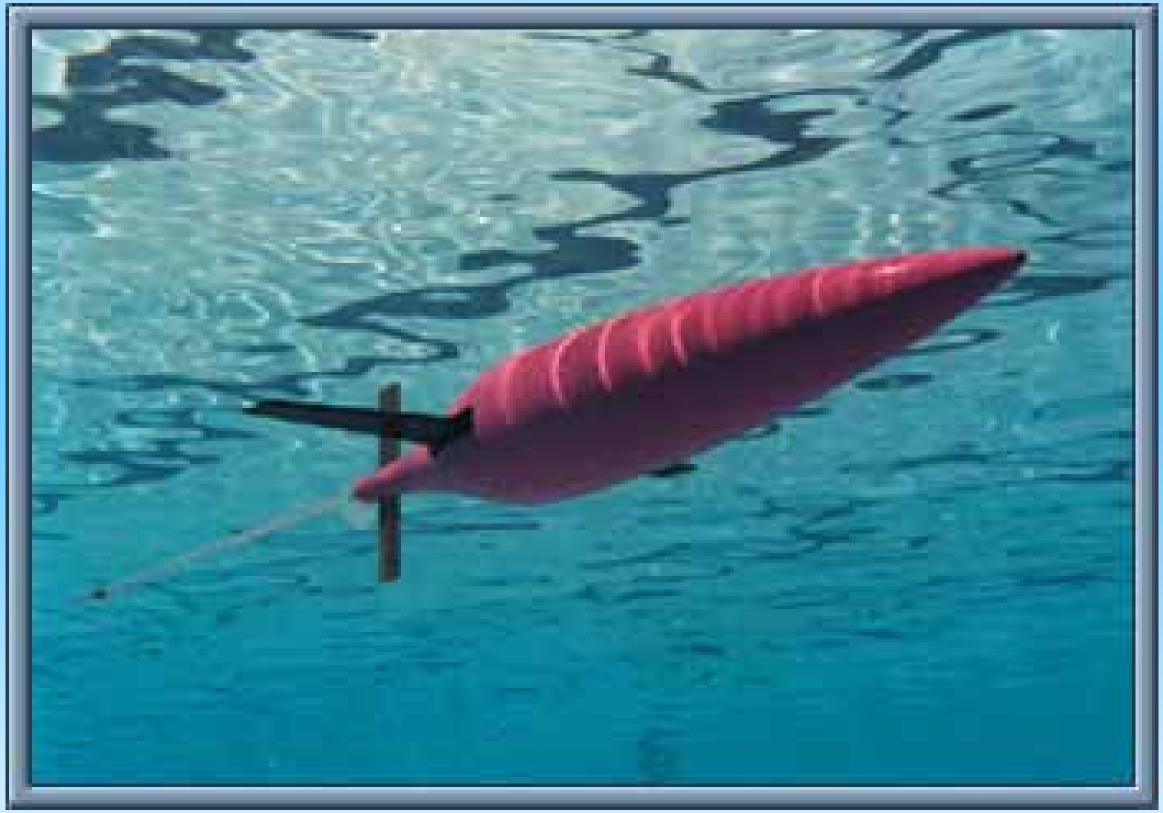

THE END

An evacuated glass vessel with water in it illustrates the Clausius-Clapyron relation between vapor pressure of water and temperature. The water is pushed from the vessel in my hand to the ‘cold ball’, and the vapor pressure difference between the two ends is close to the hydrostatic pressure measured by the column’s vertical displacement. One can fill out the curve and see the greater sensitivity (to temperature) of water vapor production at high, ‘tropical’ temperature. This all works because we shake the vessel so that a thin film of water lies under my warm hand. It illustrates a key variable in the climate system.

When shaken this water ‘clinks’ like metal,vapor cavities opening up and slamming shut.

Ocean advection, Arctic-Atlantic Connections, Climate

P.B.Rhines, University of Washington
Sirpa Hakkinen, NASA Goddard SPC
with David Bailey, Wei Cheng, Jerome Cuny, Trisha Sawatzky

WUN Climate teleseminar, 26iii2003

North Atlantic Oceanic Heat Advection is Important to the Wintertime Storm Track, Eurasian climate and weather and Global Climate

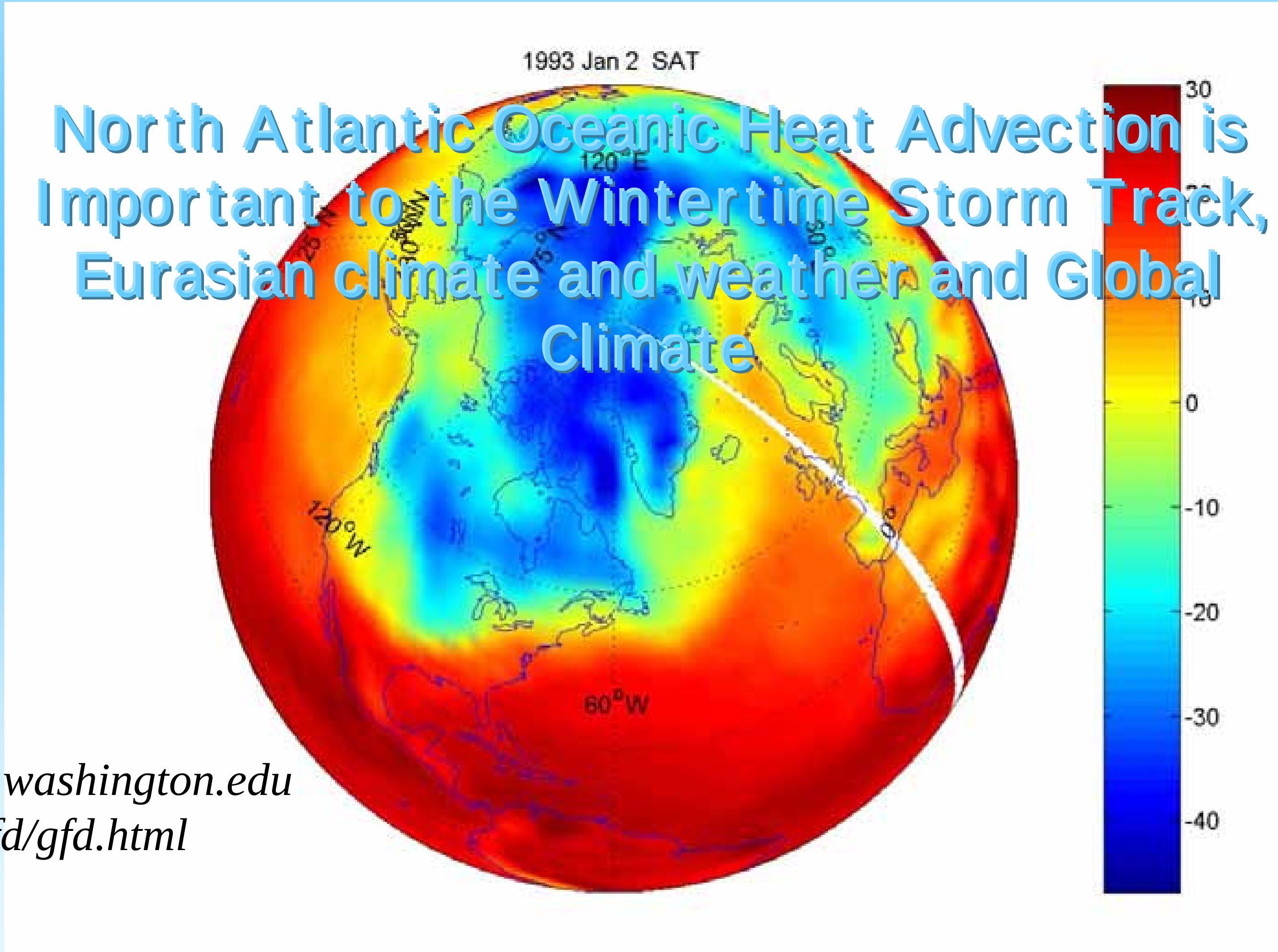

www.ocean.washington.edu/research/gfd/gfd.html

- **FDEPS Lectures, November 2007**
- P.B. Rhines, Oceanography and Atmospheric Sciences, University of Washington
- Rhines@ocean.washington.edu
- www.ocean.washington.edu/research/gfd
-
- These lectures will address the dynamics of oceans and atmospheres, as seen through theory, laboratory simulation and field observation. We will look particularly at high latitudes and climate dynamics of the ocean circulation coupled to the atmospheric storm tracks. We will emphasize the dynamics that is difficult to represent in numerical circulation models. We will discuss properties of oceans and atmospheres that are both fundamental, unsolved questions of physics, and are also important, unsolved problems of global environmental change.
- **Lecture 1**:
- Is the ocean circulation important to global climate ? Does dense water drive the global conveyor circulation? Fundamental questions about oceans and atmospheres that are currently under debate.
-
- The field theory for buoyancy and potential vorticity.
- Basic propagators: Rossby waves and geostrophic adjustment.
- Potential vorticity: inversion and flux.
- **Lecture 2**:
- How do waves and eddies shape the general circulation, gyres and jet streams?
- Almost invisible overturning circulations.
- Lessons from Jupiter and Saturn.
- The peculiar role of mountains, seamounts and continental-slope topography.
- **Lecture 3**:
- Dynamics of ocean gyres and their relation with the global conveyor circulation.
- Water-mass transport, transformation and air-sea exchange of heat and fresh water.
- Ocean overflows and their mixing.
- Decadal trends in the global ocean circulation.
- **Lecture 4**:
- Heat, fresh-water, ice: convection in oceans and atmospheres and the texture of geophysical fluids.
- **Lecture 5**:
- Teaching young students about the global environment using the GFD laboratory: science meets energy and environment in the lives of Arctic natives
- **Seminar**:
- *Exploring high-latitude ocean climate with Seagliders and satellites*

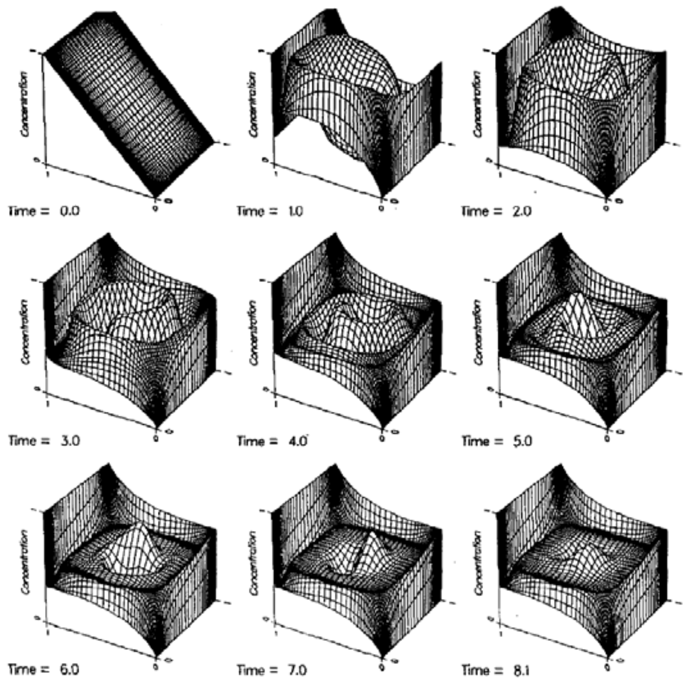

Figure 10 The spin-up of a passive tracer in a gyre circulation with Péclet number of 2.5×10^3, based on the basin scale and interior velocity (Musgrave 1985). The ridge of high values does not follow the streamlines but represents the winding up of the initial conditions. A weak diffusive spiral crossing ψ-lines remains in the steady state upon the homogenized plateau. The injected boundary values can be followed through the western-boundary current, but they are quickly assimilated by horizontal mixing. The large tracer flux through the system depends on thin boundary layers, which are treated with a stretched grid.